DETERMINING THE REGIONAL-SCALE DETRITAL ZIRCON PROVENANCE OF THE MIDDLE-LATE ORDOVICIAN KINNIKINIC (EUREKA) QUARTZITE, EAST-CENTRAL IDAHO, U.S.

By

ERIC EDWARD BAAR

A thesis submitted in partial fulfillment of
the requirements for the degree of

MASTER OF SCIENCE IN GEOLOGY

WASHINGTON STATE UNIVERSITY
School of Earth and Environmental Sciences

MAY 2009

To the Faculty of Washington State University:

The members of the Committee appointed to examine the thesis of

ERIC EDWARD BAAR find it satisfactory and recommend that it be accepted.

_____

Michael C. Pope, Ph.D., Chair

_____

David R. Gaylord, Ph.D.

_____

S. Andrew Dufrane, Ph.D.

ACKNOWLEDGEMENT

Foremost, I would like to thank my parents, Larry and Karen Baar, who have supported me in all my nonacademic and academic endeavors.

I would like to thank my committee members, Mike Pope, David Gaylord, and S. Andrew Dufrane for their criticisms, guidance and advice. I also like to thank Jeff Vervoort for his expertise and assistance with uranium-lead geochronology.

I would also like to thank Charles Knaack for assistance using the LA-ICP-MS at Washington State University, Bill McClelland for the use of the mineral separation laboratory at the University of Idaho, and Thomas Williams for help assistance with CL imaging at the University of Idaho.

I would like to thank Jennifer L. Manion for all of her support, patience, and understanding. I would like to thank James F. Glover III for all of his invaluable advice and assistance and Richard M. Gaschnig for many enlightening discussions about zircons and North American geology.

I express my gratitude to Dr. and Mrs. Praetorius, A to Z Inc., the Tobacco Root Geological Society, the WSU Graduate School, and the WSU School of Earth and Environmental Sciences for funding this research.

DETERMINING THE REGIONAL-SCALE DETRITAL ZIRCON PROVENANCE OF THE MIDDLE-LATE ORDOVICIAN KINNIKINIC (EUREKA) QUARTZITE, EAST-CENTRAL IDAHO, U.S.

Abstract

By Eric Edward Baar, M.S.
Washington State University
MAY 2009

Chair: Michael C. Pope

The Middle-Late Ordovician Kinnikinic Quartzite and its lateral equivalents in the western North American Cordillera extend from the Peace River Arch, British Columbia to northern Mexico. Deposited in a high energy, shallow-shelf marine environment, these quartzites represent a unique episode of mature siliciclastic deposition along an otherwise carbonate-dominated passive margin of western Laurentia. The Peace River Arch was suggested via U-Pb detrital zircon geochronology to be the sole source of sediment for the Ordovician quartzites, a model which requires longshore currents to transport sediment over 2000 km, precluding sediment input from underlying rocks and potentially exposed sources east of the passive margin. The Kinnikinic Quartzite differs from most of its coeval units along the Laurentian margin, in that many of its eastern exposures were deposited unconformably on Mesoproterozoic metasedimentary rocks or Ordovician plutons along the Lemhi Arch.

Laser ablation ICP-MS U-Pb geochronology of 1439 individual detrital zircon grains from eleven samples (four locations) of Kinnikinic Quartzite provides a distinct spectrum of ages: ~0.9-1.3 Ga, 1.8-2.0 Ga, ~2.0-2.2 Ga, and ~2.4-2.9 Ga. This age spectrum suggests

provenance links to sources east of the Paleozoic passive margin, rather than to the north. It is hypothesized that the Trans-Hudson Arch (and Saskatchewan craton), adjacent Paleoproterozoic-Archean provinces (Wyoming, Hearne, and Rea), and possibly recycled underlying metasedimentary units (Mesoproterozoic Belt Supergroup and lateral equivalents) are major contributors of sediment. The detrital zircon populations of all samples of Kinnikinic Quartzite are similar, but slight changes in populations occur. Changes in detrital zircon populations occur spatially between sample locations and temporally within sample locations. Measures of overlap and similarity calculated for each sample of Kinnikinic Quartzite against each other provide a numerical evaluation of the spatial and temporal provenance variation. The average overlap is 0.665, and average similarity is 0.823. Spatial and temporal variations in provenance are suggested to be a result of long-term sea level fluctuations systems tracts, which are capable of covering (TST, HST), or uncovering (LST, FSST) broad areas of potential source rocks.

TABLE OF CONTENTS

Page

APPENDIX

LIST OF TABLES

LIST OF FIGURES

CHAPTER 1

INTRODUCTION

The Middle-Late Ordovician Kinnikinic Quartzite and its equivalents represent a unique episode of siliciclastic deposition (Figure 1) along an otherwise carbonate-dominated Laurentian passive margin (Webb, 1958; Ketner, 1968). This isolated episode of siliciclastic deposition also is distinct because of its extreme textural and compositional maturity (Ross, 1937, 1947, 1961). These two characteristics have made the Kinnikinic Quartzite a focus of several sedimentological studies (e.g., Ketner, 1966, 1968; Hobbs et al., 1968; James and Oaks, 1977; Oaks and James, 1980). The provenance of the Kinnikinic Quartzite's equivalents was previously studied via detrital zircon geochronology (Gehrels et al, 1995; Gehrels and Dickinson, 1995; Gehrels, 2000). Previous detrital zircon ages of Ordovician miogeoclinal quartzites included four samples that were analyzed using thermal ionization mass spectrometry (TIMS), and were comprised on average of >30 grains per sample (Gehrels et al, 1995; Gehrels and Dickinson, 1995; Gehrels, 2000). Additionally, George Gehrels has provided unpublished analyses of 90+ grains analyzed via laser ablation inductively coupled mass spectrometry (LA-ICP-MS) from the same samples used for the TIMS analyses (Gehrels et al., 1995).

The Kinnikinic Quartzite of east-central Idaho is significantly different from most of its coeval units along the Laurentian margin, because many of its eastern exposures (Figure 1) are deposited unconformably on Mesoproterozoic metasedimentary rocks (Belt Supergroup and equivalents) or Ordovician plutons along the Lemhi Arch (Sloss, 1954; Ruppel, 1986; Evans and Zartman, 1988; Thomas, 2007), both of which could have been local contributors of siliciclastic detritus during the Ordovician (Webb, 1958). The remainder of Middle-Late Ordovician siliciclastic units along this passive margin accumulated on a thick succession of Cambro-

Ordovician carbonate and mixed carbonate-siliciclastic strata. These carbonate and mixed carbonate-siliciclastic strata were not likely sources of abundant siliciclastic detritus during the Middle-Late Ordovician. The unique setting of the Kinnikinic Quartzite in east-central Idaho makes it a superb candidate for a detrital zircon provenance study, which explores not only provenance, but also spatial and temporal changes in provenance.

U-Pb detrital zircon geochronology is a valuable tool in unraveling questions of provenance in the sedimentary record (e.g., Fedo et al., 2003 and references therein). Detrital zircon age distributions from siliciclastic strata can provide critical information on sediment provenance, basin evolution, tectonic history, and sediment transport and dispersal (e.g. Ross and Bowring, 1990; Rainbird et al., 1992, 1997; Gehrels, 2000, and references therein; DeGraaff-Surpless et al. 2002, 2003). The identification of a spectrum of ages that coincide with an age distribution of rocks within a source region, can allow a detrital zircon study to define sediment provenance and characterize spatial and temporal variations in provenance of a clastic sedimentary unit (DeGraaff-Surpless et al., 2003).

Spatial and temporal variations in provenance may be related to long-term sea level fluctuations. Long-term sea level rises and falls can cover and uncover substantial areas of source rocks, causing dramatic changes in sediment supply (Figure 2). Changes in sediment supply should be reflected in the detrital zircon populations within a single sedimentary unit. Spatial and temporal variations in provenance may be recorded in lateral and vertical changes in the detrital zircon populations. Long-term sea level changes are best characterized by sequence stratigraphic systems tracts. Lowstand Systems Tracts (LST) would potentially source uncovered areas of proximal and remote source regions supplying sediment into the siliciclastic system. Transgressive Systems Tracts (TST) however, would cover or partially cover proximal

source rocks leaving remote source regions as the main contributors of sediment. As sea level begins to fall during the Highstand Systems Tracts and Falling Stage Systems Tracts (HST, FSST), sediment from proximal sources may reenter the siliciclastic system along with sediment from remote source regions. As a result the detrital zircon population of an LST and HST/FSST will likely reflect both proximal and remote source regions, while a TST would reflect mainly remote source regions.

The goal of this study is to determine the high-resolution depositional history of the Kinnikinic Quartzite, and use its detrital zircon populations to determine the provenance of the Kinnikinic Quartzite in east-central Idaho. This thesis uses sequence stratigraphy to provide a framework for a high-resolution provenance study to test if local and/or distant sediment sources provided detritus for the Kinnikinic Quartzite.

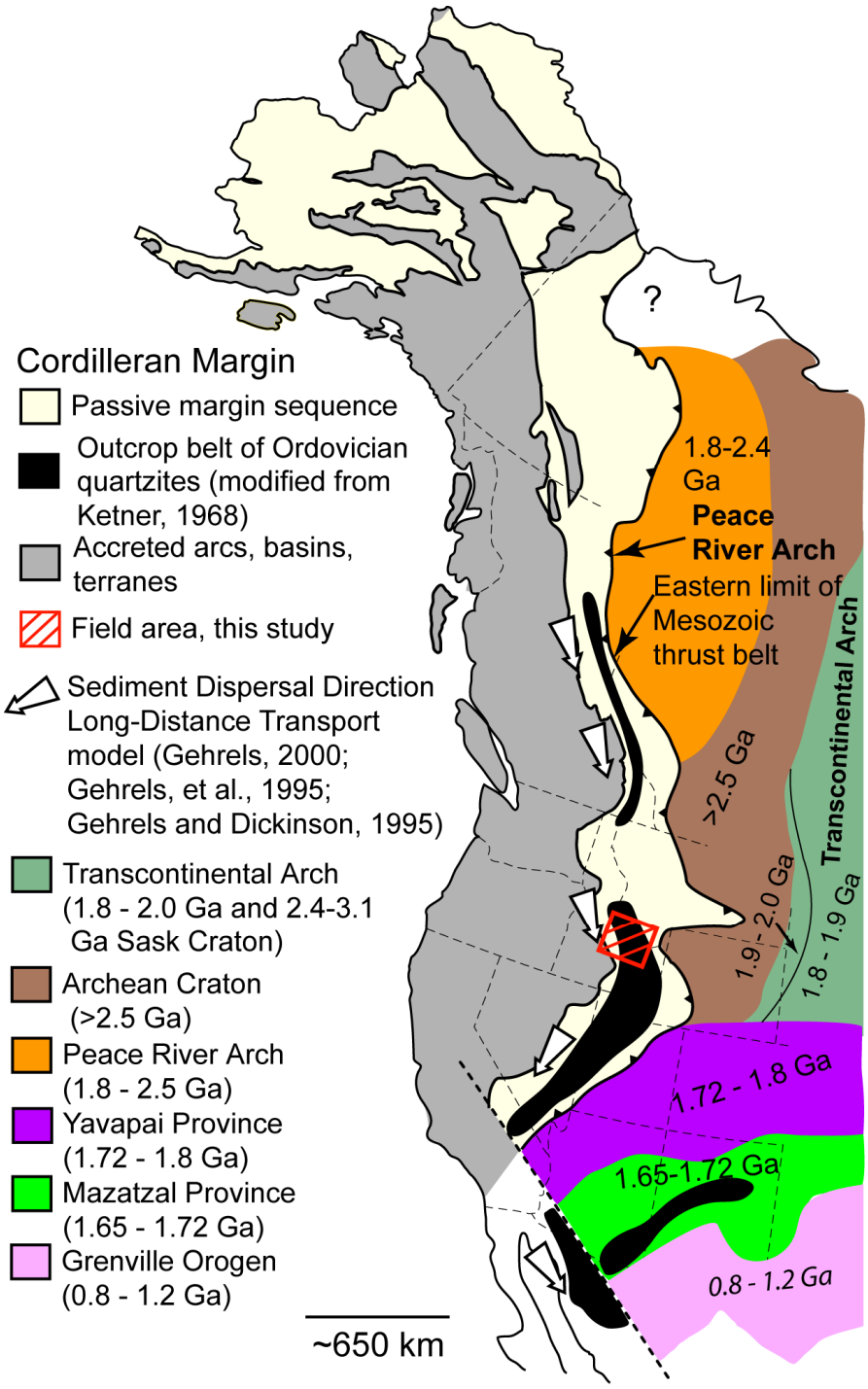

Figure 1: Generalized Geologic Map of the Western North American Cordillera. Map shows major age provinces, spatial extent of Ordovician Siliciclastics, field area of this study, and sediment transport direction of the Long-Distance Transport model (modified from McClelland unpublished).

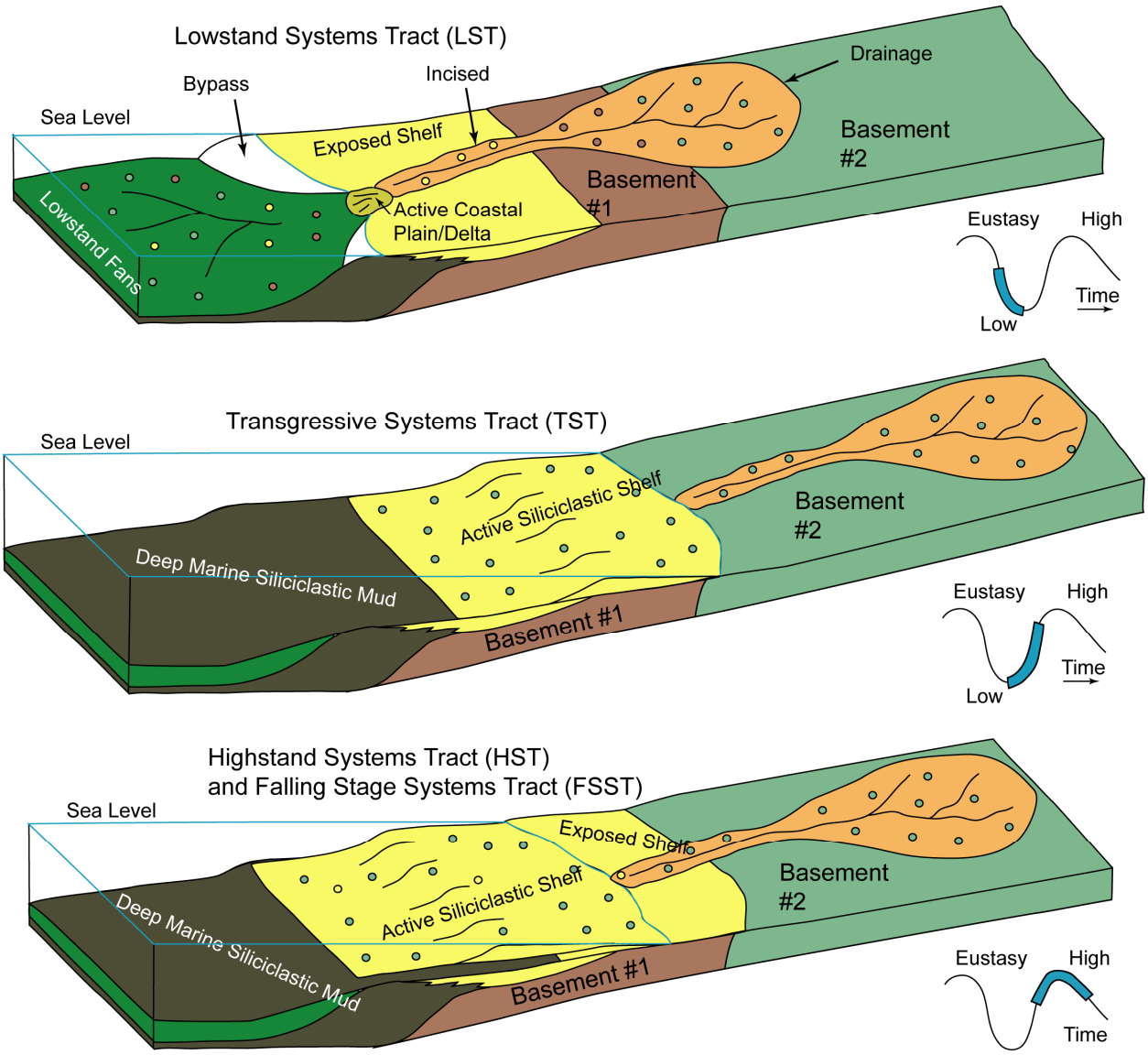

Figure 2: Provenance Change and Systems Tracts. The colored dots represent different sediment sources: yellow-siliciclastic shelf, brown-basement #1, and green-basement #2. During the LST (top) when the sea level is low, both basement sources and the exposed siliciclastic shelf will be subaerially exposed and eroded to supply sediment for coastal plains, deltas, or lowstand fans. During the TST (middle) when the sea level is rising, the siliciclastic shelf and local basement rocks will be covered by sediment from remote basement rocks. During the HST or FSST (bottom) when sea level begins to fall, sediment from the previously constructed siliciclastic shelf and remote basement rocks will prograde into the basin.

CHAPTER 2

GEOLOGIC SETTING

The western margin of the North American Cordillera formed following Neoproterozoic-Early Cambrian rifting from Russia, Australia, Antarctica, or China (e.g. Moores, 1991; Dalziel, 1991; Karlstrom et al., 1999; Sears and Price, 1999). A passive margin stretching from present-day Alaska to Mexico (Figure 1) developed following rifting and persisted until the Late Devonian Antler Orogeny. Initial deposits following rifting were Neoproterozoic to Early Cambrian immature siliciclastics (e.g. Fedo and Cooper, 1990, 2001). A thick succession of predominantly carbonate Cambrian to Devonian rocks were deposited in close proximity to the equator and overlie the initial siliciclastic sedimentary units (Sloss, 1988). During the Middle-Late Ordovician a unique, texturally and compositionally mature sandstone, the Kinnikinic Quartzite and its lateral equivalents, were deposited on this passive margin, from the Peace River Arch, British Columbia to Mexico (Figure 1). The Middle-Late Ordovician Kinnikinic Quartzite, was originally ascribed to a prolonged sea level lowstand (Webb, 1958); however, it was recently suggested that at least part of this unit formed as a result of the initial lowering of sea level associated with long-term Late Ordovician Gondwanan glaciation (Saltzman and Young, 2004).

The Kinnikinic Quartzite in east-central Idaho is a silica cemented, fine-to-medium grained, moderately-to-well sorted orthoquartzite, ranging from 0 to ~500 m in thickness in (Ross, 1937; Ketner, 1966, 1968; James and Oaks, 1977; Oaks and James, 1980). This unit was deposited in a subtidal, shallow-shelf marine environment, (Ketner, 1966, 1968; James and Oaks, 1977; Oaks and James, 1980). The Kinnikinic Quartzite is grey to white, thin to medium bedded, very fine to fine grained, and well sorted. Whereas this unit is generally massive,

parallel and wavy laminations, horizontal and vertical burrows (*Skolithos*), low-angle planar cross-stratification, and hummocky cross-stratification all occur in outcrop.

The Kinnikinic Quartzite, where conformable, overlies a thick succession of predominantly Cambrian to Ordovician carbonate strata (Biek, 1999). Along the Lemhi and Salmon River Arches the Kinnikinic Quartzite unconformably overlies Mesoproterozoic siliciclastic rocks (Armstrong, 1975; Ruppel, 1975; Hobbs, 1980) and Ordovician plutons (Scholten and Ramspott, 1968; Evans and Zartman, 1988). The Lemhi (Salmon River) Arch was prolonged topographic positive elements during the Late Proterozoic and Early Paleozoic (Sloss, 1954; Armstrong, 1975; Ruppel, 1984; Thomas, 2007). The Kinnikinic Quartzite is commonly overlain by the transgressive Late Ordovician Fish Haven Dolomite (Measures, 1992) and its equivalents.

Conodont biostratigraphy indicates the Kinnikinic Quartzite was deposited during the Whiterockian to Mohawkian (Hobbs et al., 1968; Ross C.P., 1947; Ross R.J., 1959, 1961). However, macrofossil biostratigraphy in western Kinnikinic Quartzite facies north of the Snake River Plain, Idaho is nearly equivalent to biostratigraphy of the Late Ordovician Saturday Mountain Formation (Zimmerman and Cooper, 1989; Sweet, 2000) indicating the upper portions of the Kinnikinic Quartzite were deposited during the Cincinnatian (Figure 3).

The Peace River Arch, British Columbia is suggested to be the sole source of siliciclastic sediment in the Eureka Quartzite and its equivalents based on southward grain size reduction and increased sorting (Ketner, 1968). A depositional model invoking southerly longshore currents to carry sediment from the Peace River Arch (PRA), over 2,000 km with little or no sediment input from other sources. Previous detrital zircon provenance also studies attribute the PRA as the sole source of sediment for the Kinnikinic Quartzite (Gehrels, 2000;

Gehrels et al, 1995; Gehrels and Dickinson, 1995). This model is referred to as the single-source long-distance transport model (LDT), which precludes the possibility of locally derived sediment from potentially exposed source areas such as the Archean Wyoming craton, the Trans-Hudson Arch (THA) east of the passive margin, as well as Mesoproterozoic quartzites and Ordovician plutons which locally unconformably underlie the Kinnikinic Quartzite.

Potential Detrital Zircon Sources

As previously stated, the LDT precludes other potential sources. Underlying sources include the Mesoproterozoic Belt Supergroup, which is known to contain a large population of ~1.6-1.8 Ga grains as well as smaller populations of ~1.4-1.5 Ga and Archean grains (Lewis et al., 2007; Link et al., 2007; Ross and Villeneuve, 2003). To the east and northeast of the Kinnikinic Quartzite lie the Archean Wyoming craton and other Paleoproterozoic-Archean provinces. Rocks of the Wyoming craton are predominantly ~2.4-3.4 Ga in age, but span from ~2.0 to 3.4+ Ga in age (see Chamberlain et al., 2003). Adjacent to the Wyoming craton (north) are the Hearne and Rae provinces, which contain rocks ~1.8-2.7 Ga and ~2.0-2.6 Ga in age respectively (Hoffman, 1988, 1989; Bickford et al., 1990). The Saskatchewan craton (within the THA) contains ~2.4-3.1 Ga rocks (Chiarenzelli et al., 1998; Bickford et al., 2005). East of the Paleoproterozoic-Archean provinces lies the THA, which contains rocks predominantly ~1.8-2.0 Ga in age (Bickford et al., 1990; Ansdell et al., 1995; Chiarenzelli et al., 1998). A narrow ~1.9-2.0 Ga fold and thrust belt lies on southwestern edge of the ~1.8-1.9 Ga magmatic arc of the THA (Ross and Villeneuve, 2003). To the south and southeast of the Kinnikinic Quartzite lie the Mazatzal, Yavapai, and Grenville provinces, which contain rocks ~1.72-1.8 Ga, ~1.65-1.72 Ga,

and ~0.8-1.2 Ga in age respectively (Hoffman, 1989). These potential source areas and their proximities to the Kinnikinic Quartzite in east-central Idaho are shown in Figure 1.

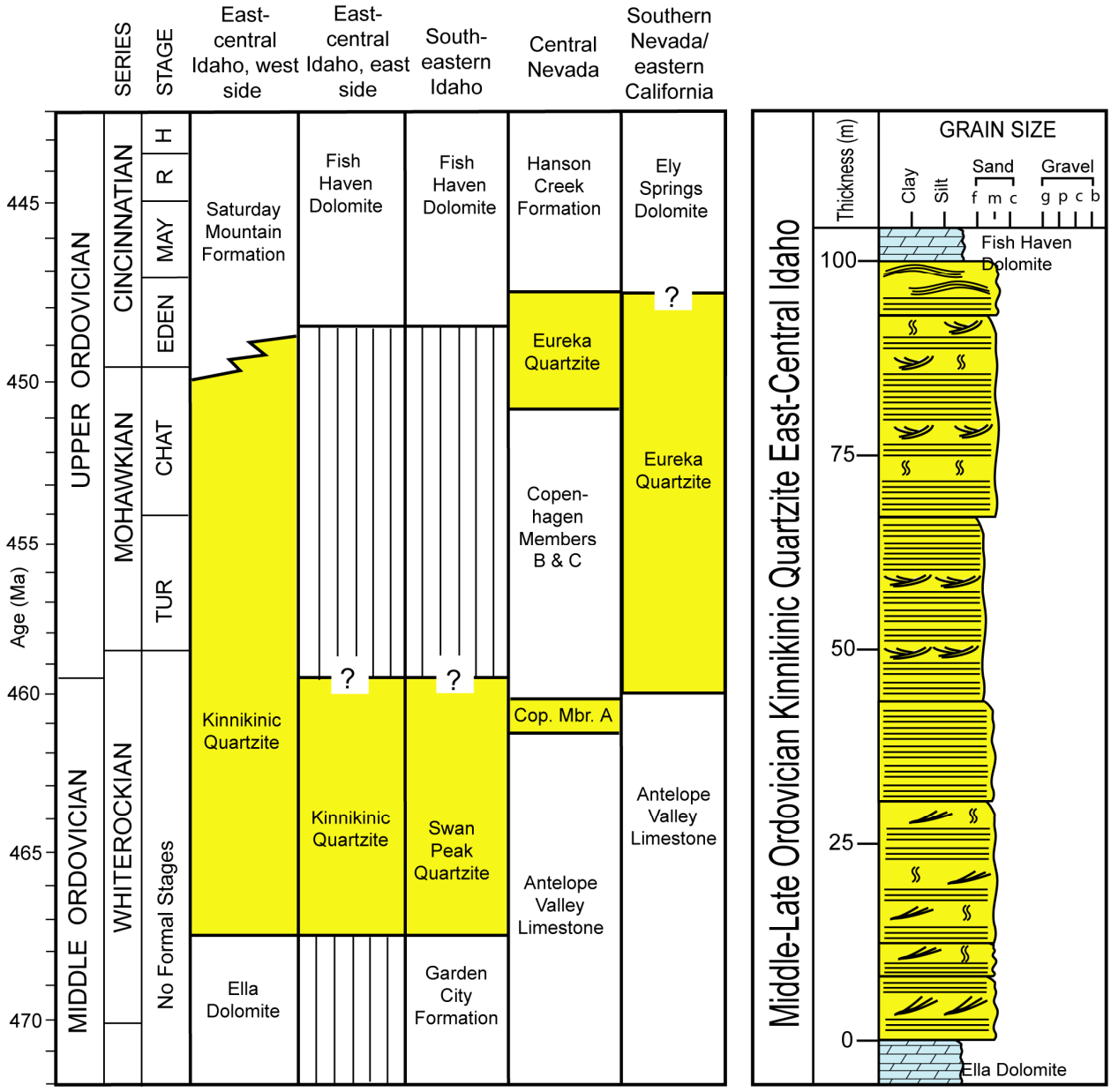

Figure 3: Biostratigraphy of Middle-Late Ordovician Quartzites and generalized stratigraphic column of the Middle-Late Ordovician Kinnikinic Quartzite in east-central Idaho. Biostratigraphic correlation chart for the Middle-Late Ordovician sandstones (yellow) of Idaho, central and southern Nevada, and eastern California (modified from James and Oaks, 1977; Churkin, 1962; Hobbs et al., 1968; Biek, 1999; Saltzman and Young, 2004).

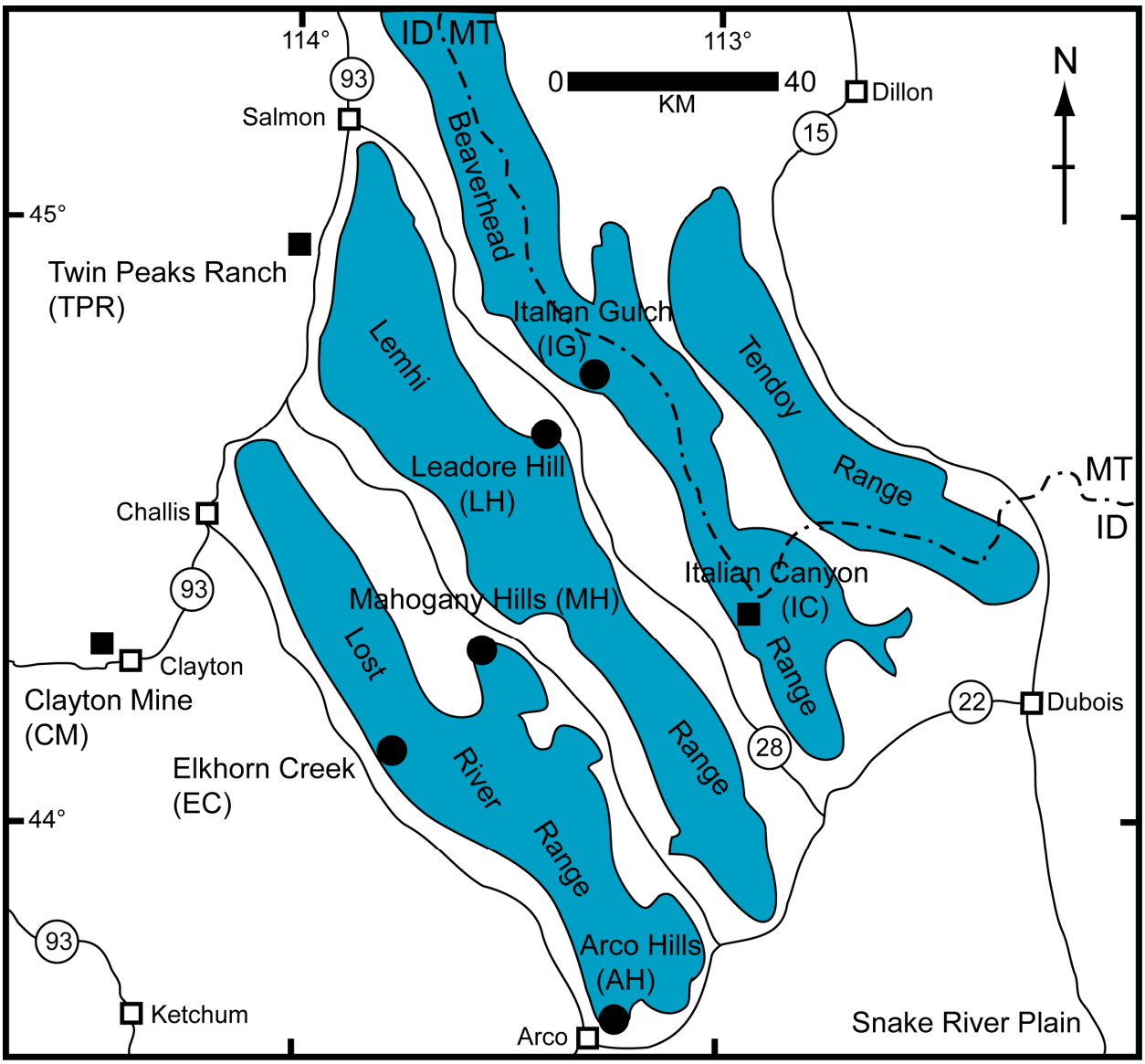

Figure 4: Map of east-central Idaho and southwestern Montana, showing outlines of mountain ranges containing outcrops of Paleozoic rocks, and locations of measured sections (squares) and other outcrops (circles) visited during this study.

CHAPTER 3

METHODS

Field Methods

Sampling Strategy

To study the regional spatial and temporal variance in provenance of the Kinnikinic Quartzite in east-central Idaho, a high-resolution 3-dimensional data set was developed. This data set includes measured sections of Kinnikinic Quartzite along its paleodepositional strike and dip from outcrops located 10's of km apart, in east-central Idaho (Figure 4). Detailed measuring and sampling of the base, middle, and tops of outcrops along a strike and dip transect for detrital zircons provide this high-resolution, 3-dimensional data set.

Stratigraphic sections of Kinnikinic Quartzite were measured using a Jacob's staff, level, and a Brunton compass. Unit thickness, grain size, sorting, and sedimentary structures were recorded. Detrital zircon samples were systematically collected from the basal, middle, and upper portions of each measured stratigraphic section to ensure stratigraphic position of detrital zircon samples. Samples collected from basal and upper contacts of the Kinnikinic Quartzite were taken within 5 m or less from their contacts.

Site Locations and Samples

An east to west (with some north-south variability) down paleodip transect was constructed by sampling the Kinnikinic Quartzite locations from Italian Canyon (southern Beaverhead Range) and Italian Gulch (near Leadore, Idaho), Twin Peaks Ranch (near Salmon, Idaho), and Clayton Mine (near Clayton, Idaho) (Figure 4). In all, twelve detrital zircon samples were collected, eleven from the Kinnikinic Quartzite and one from the Precambrian Wilbert

Formation (quartzite). Four samples were collected from Italian Canyon, including: IC3 (upper), IC2 (middle), IC5 (basal), and ICWF (underlying Precambrian Wilber Formation). Four samples were collected from Twin Peaks Ranch, including: TPR2 (upper), TPR4 (upper middle), TPR3 (lower middle), and TPR5 (basal). The remaining three samples were collected from Clayton Mine, and include: CM3 (upper), CM2 (middle), and CM1 (basal). One sample was taken from Italian Gulch near the basal contact with an Ordovician granitic pluton, IG1. See Appendix A for UTM coordinates of each section.

Sample Collection

Sample locations were chosen by stratigraphic position. Samples were collected along the basal and upper contact with underlying and overlying units, as well as near the middle of each stratigraphic section. Known stratigraphic position provides a context for the detrital zircon data. Samples were collected from each outcrop by using a geologic hammer or a sledge hammer and wedge. The hammers and wedge were cleaned with a wire brush after each sample was collected to prevent contamination. A ~3-5 kg sample was taken to assure there was a sufficient number of detrital zircons for analysis. Each sample was stored in a separate sample bag to avoid contamination.

Analytical Methods

Sample Preparation

Sample preparation was completed at the University of Idaho and Washington State University under guidelines established by Dr. William McClelland. The quartzite samples were crushed into chips using a Jaw Crusher and subsequently milled into sand-sized particles with a

Disc Mill. High density mineral fractions were separated from the milled sample using a Gemini^{TM} gold table. During this procedure the "light" fraction (mostly quartz and feldspar) was separated and discarded. The remaining dense fraction was washed three times with acetone and allowed to dry. The dense fraction was sieved to remove grains greater than 350 µm (leaving fine sand-sized and smaller grains). All grains less than 350 µm were processed with magnetic techinques. The sample was passed through a free-fall Frantz magnetic separator (with a maximum setting of 2.0 amps) or swept with a hand magnet. Once the highly magnetic portion (containing iron fillings and magnetite) of the sample was separated, the sample was further processed on a Frantz side-slope magnetic barrier separator. The magnetic separator had a set front slope of 10° and a side slope of 20° (setting notation of 10/20). Three passes were made with increasing magnetic strengths, M = 0.3, 0.5, 0.7 Amps (setting notation of 0.3M10/20, 0.5M10/20, and 0.7M10/20). The resulting magnetic fraction from each of these settings was labeled and stored. The nonmagnetic portion from the highest magnetic setting was processed using the heavy liquid Methylene Iodide (MI, $\rho = 3.32$ g/cm^3). In a fume hood, a funnel and filter paper were placed above a flask (with stopcock), which in turn was placed above a large funnel and filter paper in a Buchner beaker. MI was poured into the flask via the funnel and filter paper. The sample was poured directly into the flask containing MI and the sample was stirred with a plastic stirring rod to allow the dense minerals to settle to the bottom of the flask. The stopcock was opened briefly to release the dense minerals into the collection filter paper. This preceding procedure was repeated three times. The sample was then washed with acetone nine times (three filter papers, three washes per filter paper). The less dense portion of the sample was washed in the same manner and allowed to dry. Once dry, the less dense portion of the sample was stored in a plastic bag or container. The remaining heavy mineral fraction

containing the zircons was re-processed with the Frantz side-slope magnetic barrier separator, this time with settings of 1.0M10/20, 1.5M10/20, 1.8M10/20, 1.8M5/15, and 1.8M1/15. This final magnetic separation produced a remnant sample of nearly pure zircon.

A small fraction of the detrital zircons was placed into a Petri dish with alcohol and examined under a binocular microscope. A metal dental tool was used to remove any non-zircon grains. The zircons were then extracted from the Petri dish using a disposable plastic pipette and placed onto weighing paper to dry. Double sided tape was placed onto a glass plate. A thin rectangular strip of backing was removed with a small knife to expose the tape's adhesive. A subset of zircons were poured onto the exposed adhesive, pressed with the dental tool into the adhesive and covered with a new strip of backing. The remaining sample was labeled and stored. Commonly three to five zircon samples were adhered to the glass in the above manner. Once all of the samples were added to the glass, grains of FC-1 and Peixe U-Pb zircon reference materials were added to the tape using a dental tool. Large, flat grains were sought to provide a surface that could accommodate multiple laser ablation analyses. A hand drawn sample map made during this procedure was used to keep track of sample locations on the grain mount.

Once all of the samples and standards were in place, the backing was removed from the adhesive tape and a plastic ring was placed around the samples. The plastic ring was filled with an epoxy having a 5:1 ratio of resin and hardener and allowed to harden overnight. The resulting grain mount (containing multiple samples) was removed from the glass plate and tape. The grain mount was then coarsely polished using 1200 grit on a glass plate and then fine polished using 3 µm and 1 µm diamond grit on a polishing plate to expose the zircon grain surfaces. The finely polished mount was then carbon coated in the GeoAnalytical lab at Washington State University.

Cathodoluminescence (CL) images of the sample were acquired on a scanning electron microscope (SEM) housed at the University of Idaho. The CL images (Figure 5) were used to record spot locations and to avoid ablating undesirable locations on the zircon grains, such as compositional zoning, inclusions, and fractures which could result in faulty analyses.

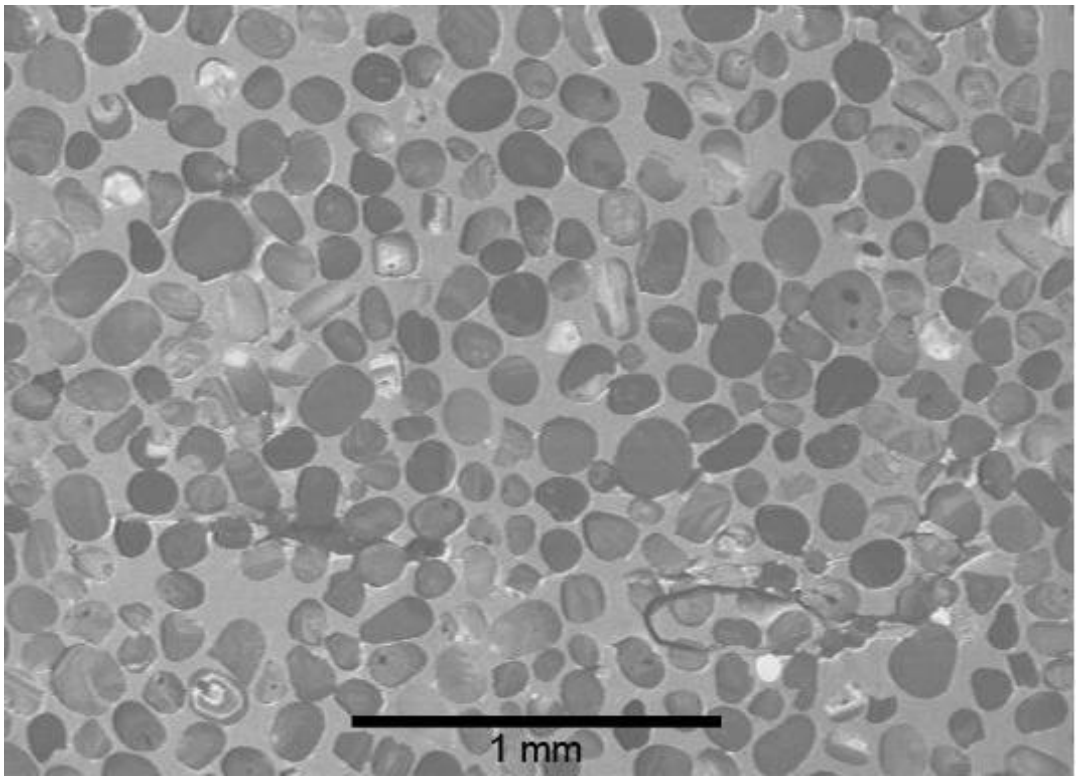

Figure 5: Cathodoluminescence images of detrital zircons (TPR2) by SEM. Note the high degree of roundness and sphericity of the zircon grains.

Sample Size

A minimum of 117 detrital zircon grains were analyzed for each sample (except CM1). This minimum number was analyzed to statistically ensure that all populations representing at least 5% of the total zircon population of a sample were represented in the analysis (Vermeesch, 2004). The number of actual analyses for each sample is listed in Appendix B.

Analytical Equipment and Analysis

U-Pb analysis was preformed with a New Wave^{TM} UP-213 (Nd-YAG 213 nm) laser ablation system coupled to a Thermo-Finnigan Element 2 ^{TM}, a high-resolution inductively coupled plasma mass spectrometer (HR-ICP-MS), housed at the Washington State University GeoAnalytical Laboratory. The laser was operated at a fluence of 10-12 J/cm^2, 10 Hz frequency, and a 30 µm beam diameter. The analysis sequence consisted of a 30 second background measurement, followed by an 8 second laser warm-up (with the shutter closed). Then the zircon was ablated for 8 seconds prior to data collection to account for sample transport time to the plasma and to achieve signal stability. Data was collected for ~46 seconds consisting of 300 scans of the masses ^{202}Hg, ^{204}(Pb+Hg), ^{206}Pb, ^{207}Pb, ^{208}Pb, ^{232}Th, ^{235}U and ^{238}U.

At the beginning of an analytical session, zircon U-Pb reference materials Peixe and FC-1 were analyzed until age variations were <1% 1 standard deviation (typically 5 to 7 anaylses). After instrument stability was achieved, 2-3 analyses of Peixe and FC-1 were analyzed between every 10-15 unknown analyses. For some zircon mounts, Peixe was either plucked or polished off the grain mount, so only analysis of FC-1 was possible (IC3, ICWF(4) TPR3, and TPR2). The location of the spot analyses were recored on the CL images of the grain mounts.

Data Reduction

Raw data from the LA-ICP-MS was reduced offline in a Microsoft Excel^{TM} spreadsheet (Chang et al., 2006). The data were filtered by removing sweeps outside of 98% confidence. Each individual analysis was corrected for mass bias using fractionation factors derived from analyses of FC-1 and Peixe zircon references that bracketed the unknowns. Since the U-Pb reference Peixe was not available for all unknown analyses, only fractionation factors derived

from FC-1 were used for consistency. The $^{206}Pb/^{238}U$ intercept and standard error were calculated using the Excel™ function Linest. The in-run error for the $^{207}Pb/^{206}Pb$ ratio is the standard error as calculated on the mean of the $^{207}Pb/^{206}Pb$ measurements. Fractionation factors were determined from the ratio of the "true" $^{206}Pb/^{238}U$, $^{207}Pb/^{235}U$, and $^{207}Pb/^{206}Pb$ values for the standard and their measured values (FF = true ratio/measured ratio). These fractionation factors were used to correct each unknown analysis. The assigned errors in Appendix B are a quadratic combination of the variance in the fractionation factor values and the within run measurement error of the unknowns. Fractionation factors with their associated variance are tabulated in Appendix C. No correction for common Pb was made. Once all of the data was corrected, the reduced data ($^{207}Pb/^{206}Pb$ ages only) were plotted on Probability Density Plots and Wetherill Concordia diagrams using the Microsoft Excel™ addin Isoplot (Ludwig, 2001). Only analyses less than 10% discordant are reported in these diagrams.

CHAPTER 4

FIELD RESULTS

Field findings resulted from the measuring and describing of three outcrops of Kinnikinic Quartzite and the description of five other locations (Figure 4). Overall, the Kinnikinic Quartzite is grey to white, thin- to medium-bedded, very fine to fine grained, well sorted and silica cemented. The Kinnikinic Quartzite in east-central Idaho is generally massive and devoid of primary sedimentary structures; measured sections often contained many 10's of m of massive quartzite. However, several sedimentary structures occur locally including: parallel and wavy laminations, horizontal and vertical burrows (*Skolithos*), low-angle planar cross-stratification, and possible hummocky cross-stratification. Each measured section is described below, and location coordinates are given in Appendix A.

Measured Sections

Italian Canyon ~80 m (Figure 6):

The lower portion (~0-10 m) of the Italian Canyon section consists of thin- to medium-bedded, low-angle planar cross-stratified, very fine grained quartzite. The middle of the section (~10-40 m) is predominantly medium- to thin-bedded, massive, and fine grained quartzite, with minor low-angle planar cross-stratification and possible hummocky cross-stratification. The upper portion (~40-80 m) is thin- to medium-bedded, fine grained, with low-angle planar cross-stratification and vertical burrows (*Skolithos*). Six paleocurrent measurements were collected from the very upper reaches of the section (~1-5 meters below the contact with the overlying Devonian strata). Paleocurrent directions are as follows: south = 2 (~180°, ~175°), north = 1 (~0°), southwest = 3 (~240°, ~225°, ~209°). Overall the section is thin- to medium-bedded, fine

grained, well sorted, massive to cross-stratified and bioturbated. Samples for detrital zircons were taken at ~5 m (IC5), ~62 m (IC2), and ~78 m (IC3). The Kinnikinic Quartzite unconformably overlies the Precambrian Wilbert Formation with a slight angular discordance. The Wilbert Formation is a reddish purple, medium grained, moderately to poorly sorted quartzite, with thin parallel laminations and occasional cross-stratification. A sample for detrital zircons (ICWF) was collected from the Wilbert Formation several 10's of m below the contact with the Kinnikinic Quartzite. A bed of Devonian sandy (quartz), cross-stratified dolomite unconformably overlies the Kinnikinic Quartzite (James and Oaks, 1977).

Twin Peaks Ranch ~180 m (Figure 7):

The lower and middle portions (~0-160 m) of the Twin Peaks Ranch section are medium- to thick-bedded, fine grained, and massive. Occasional low-angle planar cross-stratification is present. The upper portion (~160-180 m) of this section is thin- to medium-bedded, fine grained, with minor low-angle planar cross-stratification. Overall the section is medium bedded, fine grained, well sorted, and massive. Samples for detrital zircons were collected at ~0 m (TPR5), ~45 m (TPR3), ~ 120 m (TPR4), and ~180 m (TPR2). The Kinnikinic Quartzite unconformably overlies the Precambrian Swauger Formation with slight angular discordance. The Swauger Formation consists of a fine to medium grained, cross-stratified quartzite with minor shale partings. Conformably overlying the Kinnikinic Quartzite at this location is the cross-stratified sandy dolomite of the Late Ordovician Fish Haven Formation (James and Oaks, 1977; Measures, 1992).

Clayton Mine ~125 m (Figure 8):

The Clayton Mine section of Kinnikinic Quartzite is subdivided into three parts: Lower Quartzite Member, Middle Member, and Upper Quartzite Member (Oaks and James, 1980). The Lower Quartzite Member is medium- to thin-bedded, very fine to fine grained quartzite with minor siltstone-shale partings. Horizontal burrows are common. The upper portion of the Lower Quartzite Member is slightly coarser grained than the lower portion. The Middle Member includes subequal thin interbeds of fine grained quartzite and siltstone-shale. Horizontal burrows are common in the quartzite beds. The Upper Quartzite Member is thin- to medium-bedded, fine grained quartzite. Wavy to planar laminations and possible hummocky cross-stratification occur throughout this member, with horizontal burrows in its lower portions. Near the top of the section the Kinnikinic Quartzite is medium grained and poorly sorted. Overall the section is a thin- to medium-bedded, fine grained, and well sorted, bioturbated quartzite with siltstone-shale partings. Samples for detrital zircons were taken at ~2 m (CM1), ~80 m (CM2), and ~125 m (CM1). The Kinnikinic Quartzite conformably overlies the Middle Ordovician Ella Dolomite (James and Oaks, 1977). Conformably overlying the Kinnikinic Quartzite is the Late Ordovician Saturday Mountain Formation, which is a thinly laminated, tan to brown shale containing abundant graptolites. This section was not measured during this study due to the structural complexity of the outcrop location.

Italian Gulch:

The Italian Gulch section was not measured in detail, but was described in reconnaissance fashion and sampled. The Kinnikinic Quartzite at this location is a fine grained, well sorted, and massive quartzite. The lower contact is mapped as conformable onto granite of

uncertain age (Ruppel, 1968), but in the field it appears to be faulted. The granite is pink, feldspar and quartz rich, and coarse grained. A sample for detrital zircons (IG1) was taken approximately 1 m above the contact between the quartzite and the granite, but the apparent fault contact makes the stratigraphic position of this sample uncertain. Overlying the Kinnikinic Quartzite is the Late Ordovician Saturday Mountain Formation, juxtaposed along a fault contact (Ruppel, 1968).

Other Locations:

Four other locations were visited during this study, but were not measured or sampled for detrital zircons. Outcrops of Kinnikinic Quartzite were present at Leadore Hill, Mahogany Hills, Arco Hills, and Elkhorn Creek. The massive, fine grained nature of the Kinnikinic Quartzite was observed at each of these locations; however, sedimentary structures observed in the measured sections, except for hummocky cross-stratification, were observed in these locations as well. The Kinnikinic Quartzite at Leadore Hill, Mahogany Hills, and Elkhorn Creek is medium-bedded, fine grained, with minor cross-stratification. Cross-stratification was restricted to the upper portions only of Mahogany Hills and Elkhorn Creek. The Kinnikinic Quartzite at Arco Hills is thin- to medium-bedded, fine grained, with abundant low-angle planar cross-stratification and burrows (vertical and horizontal).

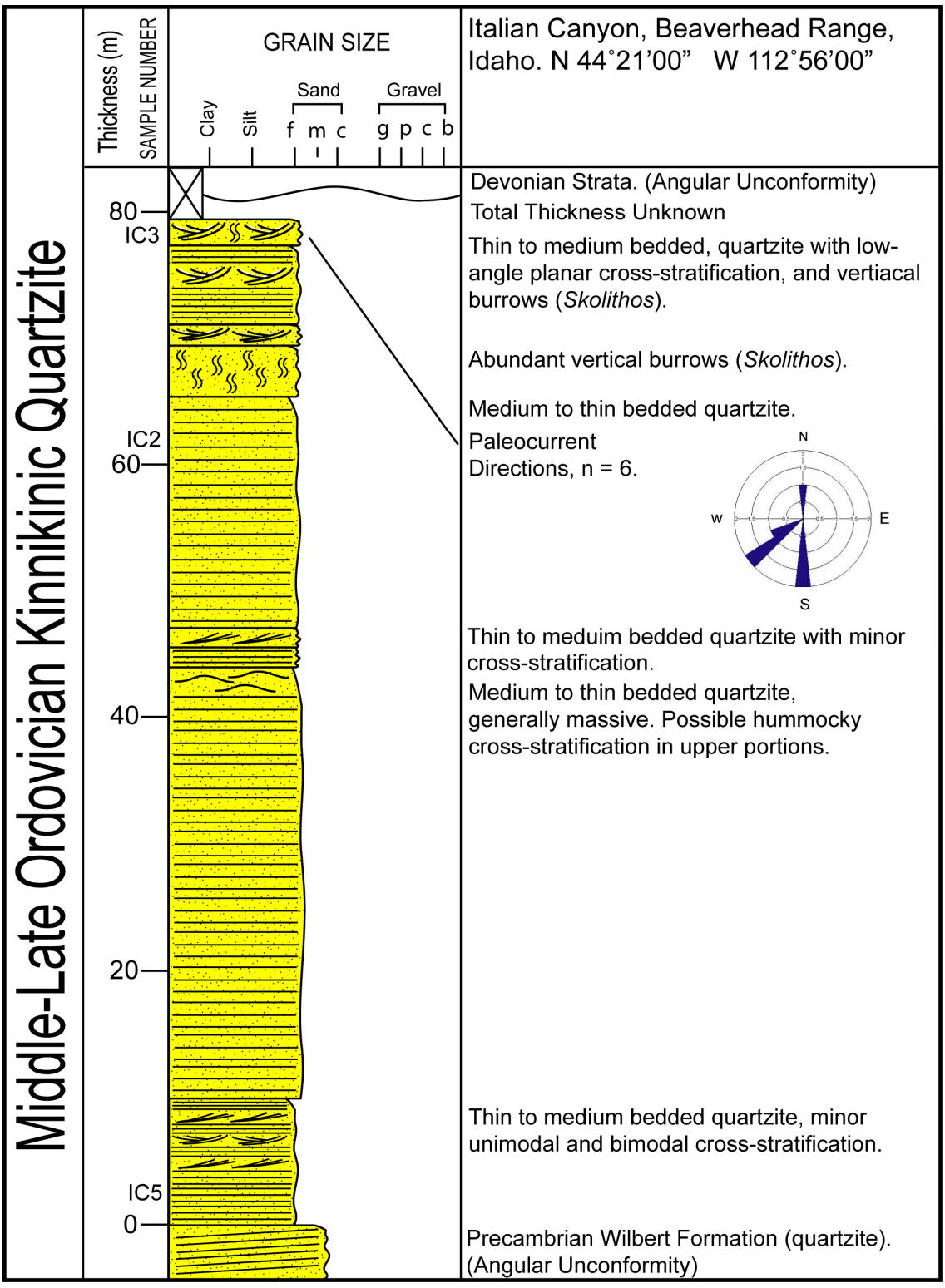

Figure 6: Stratigraphic Column of Italian Canyon.

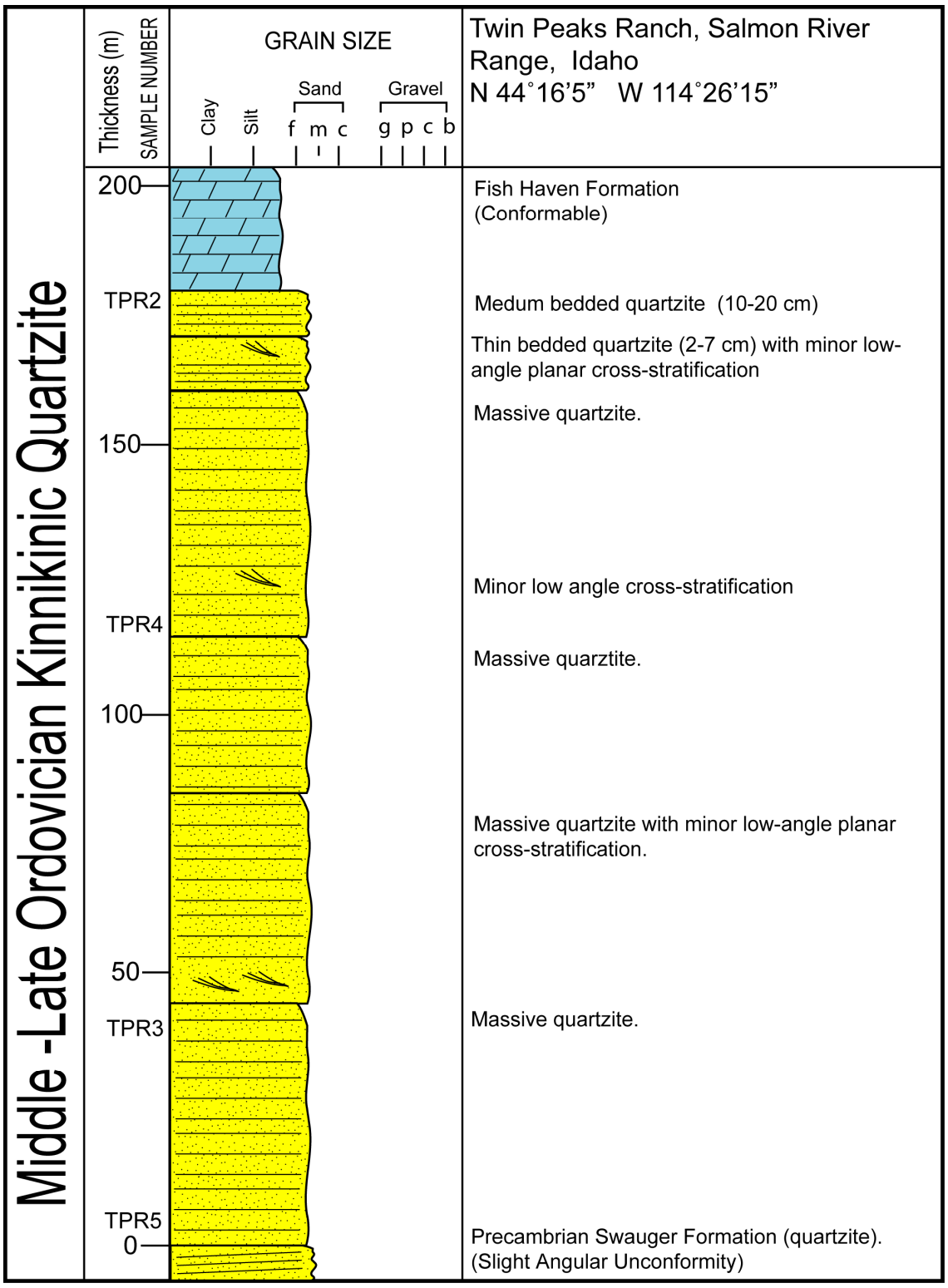

Figure 7: Stratigraphic Column of Twin Peaks Ranch.

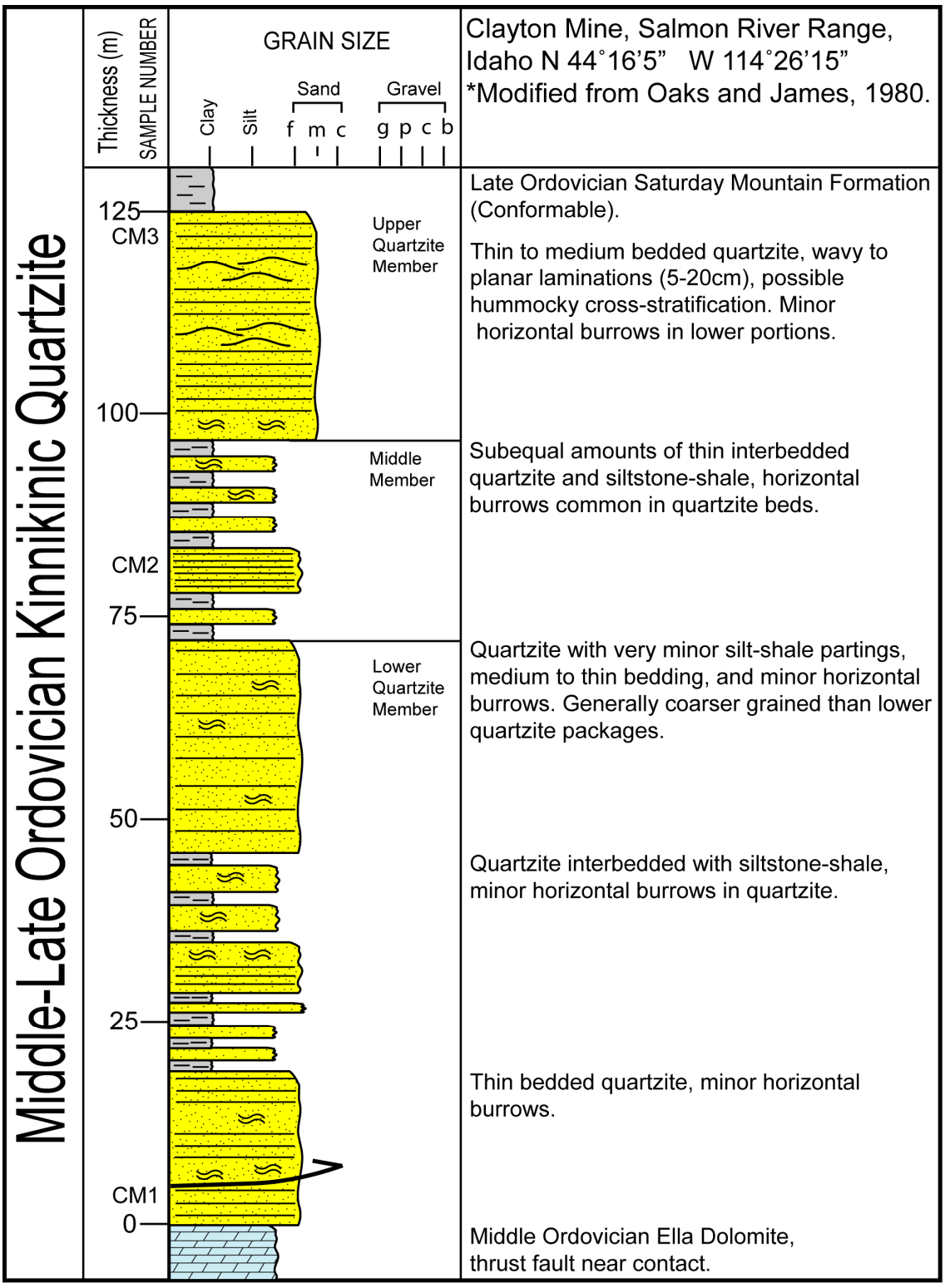

Figure 8: Stratigraphic Column of Clayton Mine, modified from Oaks and James, 1980.

Sedimentary Facies

Assessments of all the locations indicate six distinct sedimentary facies defined on the basis of texture and sedimentary structures. Each facies contains a unique set of characteristics. Facies identified are the: Massive Facies, Cross-Stratified Facies, Burrowed Facies, Laminated Facies, Interbedded Shale and Quartzite Facies, and Hummocky Cross-Stratified Facies. No complete section of these facies occurred in the field area. A description of each facies and locations where it occurs is provided below:

Interbedded Shale and Quartzite Facies (Figure 9, A) consists of thin bedded shale-siltstone and quartzite interbeds in subequal proportions. The quartzite in this facies is very fine grained and well sorted whereas the shale-siltstone layers are thinly laminated. This facies occurs only at Clayton Mine.

The Laminated Facies (Figure 9, B) is generally thin to medium bedded, fine grained, well sorted, and characterized by thin parallel to wavy laminations (2-5 mm thick). This facies occurs at Italian Canyon and Clayton Mine.

The Hummocky Cross-Stratified Facies (Figure 9, C) is generally medium bedded, fine grained and well sorted. It is marked by large (10-15 cm thick) wedge shaped beds interpreted to be hummocks. These possible hummocks occur at Italian Canyon and Clayton Mine.

The Cross-Stratified Facies (Figure 9, D) is generally thin to medium bedded, fine grained, and well sorted. It is characterized by low-angle planar cross-stratification. This facies occurs at Italian Canyon, Clayton Mine, and was rare at Twin Peaks Ranch. Vertical and horizontal burrows occur in this facies at Italian Canyon and Clayton Mine.

The Burrowed Facies (Figure 9, E) is generally medium bedded, fine grained, well sorted, and characterized by horizontal and vertical burrows (*Skolithos*). This facies occurs at Italian Canyon and Clayton Mine.

The Massive Facies (Figure 9, F) is generally medium bedded, very fine to fine grained, well sorted, and devoid of sedimentary structures. This facies occurs at Italian Canyon, Italian Gulch, Twin Peaks Ranch, and Clayton Mine. This facies may be widespread due to extensive bioturbation, subsequent silica flooding during diagenesis, or a lack of a sufficient amount of mafic sand grains to preserve sedimentary structures (James and Oaks, 1977).

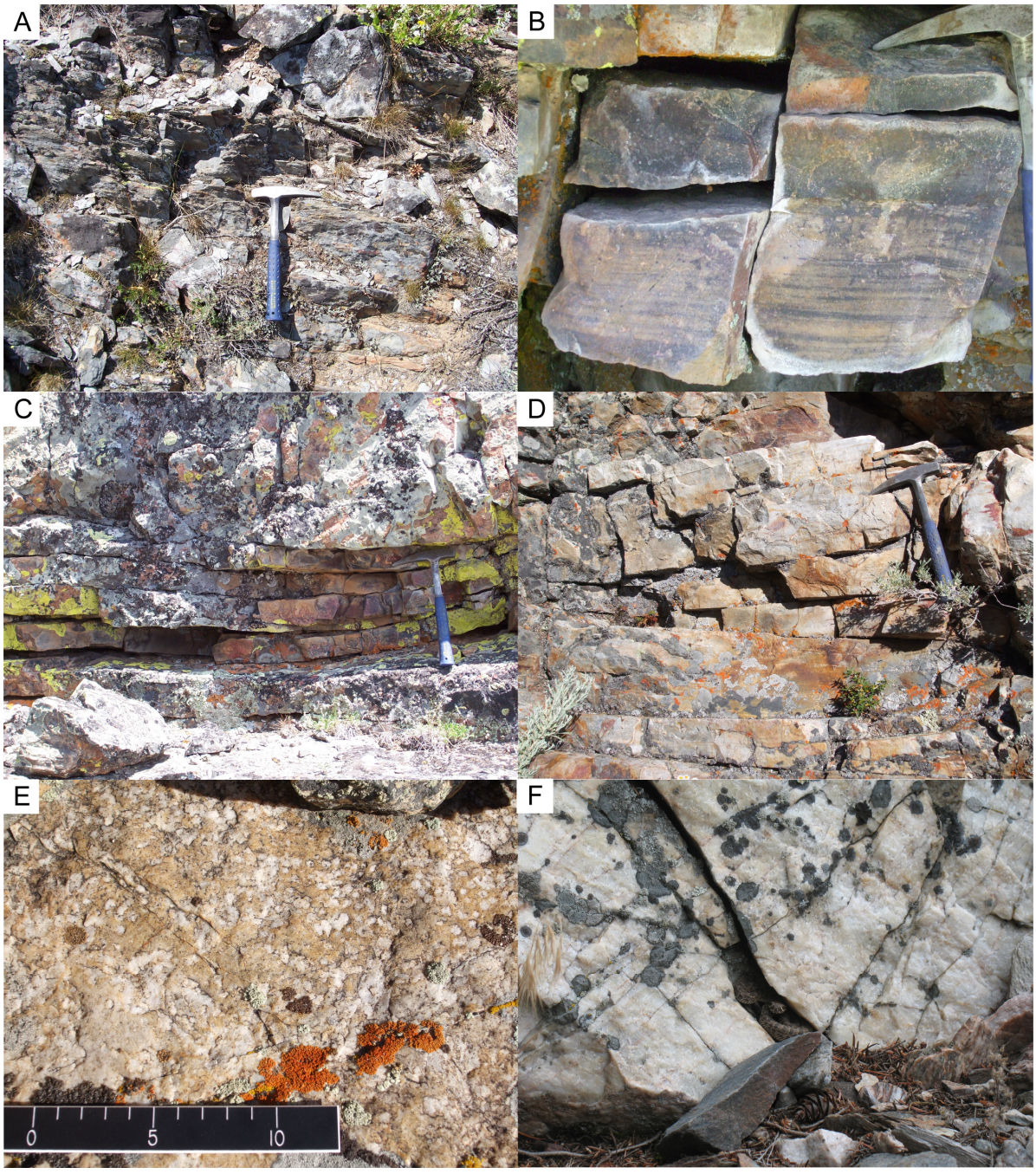

Figure 9: Photographs of sedimentary structures, which define the sedimentary facies: interbedded shale and quartzite (A), laminated (B), hummocky cross-stratified (C), cross-stratified (D), burrowed (E), and massive (F). Each photograph corresponds to the sedimentary structures and facies described in Chapter 4 and the interpreted shelf position (Figure 22) discussed in Chapter 6.

CHAPTER 5

DETRITAL ZIRCON RESULTS

Eleven detrital zircon samples of Kinnikinic Quartzite were collected from four locations (Italian Canyon, 3; Twin Peaks Ranch, 4; Clayton Mine, 3; and Italian Gulch, 1). One detrital zircon sample of Mesoproterozoic Wilbert Formation (ICWF) was collected from Italian Canyon for comparative purposes. A total of 1439 individual detrital zircon grains from the Kinnikinic Quartzite were analyzed for U-Pb ages, and a total of 125 were analyzed from the Wilbert Formation. Grains from all samples showed variations in color, shape, size, and zoning; though most grains were clear to pink, well rounded, 100 to 250 µm in diameter, and un-zoned. Grains for analysis were randomly selected regardless of variations in physical properties. During analysis it was noted that there did not seem to be a correlation between any physical property and age. Care was taken with grains that had internal zonation to make certain that analysis spots did not cross zone boundaries or between inherited cores and growth rims. Relative probability plots, histograms, and Wetherill Concordia diagrams are provided for each sample. Relative probability plots, which show the detrital zircon age spectrum, allow for efficient comparative analysis between samples, while histogram plots show specific age populations more clearly. The number of individual grains, the realative probability age spectum, and individual age populations for each sample are given below. Only grains 10% discordant or less are reported. An outline of major and minor age populations, their number of grains, and percentages of the total number of grains in each sample is given in Table 1. Data tables, including the standard fractionation factors and the specific age for each analysis set and analyses greater than 10% discordance are included in Appendix B. Wetherill diagrams for each sample, including error ellipses, showing concordance are included in Appendix D.

IC3: This sample, which includes 131 individual grain analyses, was collected near the upper contact of Kinnikinic Quartzite and overlying Devonian carbonate rocks at Italian Canyon. Nearly all of the grains analyzed were rounded to nearly spherical, clear to pink, with diameters between 100 to 250 µm. The detrital zircon signature of IC3 (Figure 10) has two major peaks at ~1850 Ma and ~1900 Ma. Two minor peaks occur at ~2050-2100 Ma and ~2650-2700 Ma. The histogram plot and data tables (Figure 10, Appendix B) have smaller populations and individual ages which are summarized in Table 1.

IC2: This sample, which includes 142 individual grain analyses, was collected from the middle portion of Kinnikinic Quartzite at Italian Canyon. Nearly all of the grains analyzed were rounded to nearly spherical, clear to pink, with diameters between 100 to 250 µm. The detrital zircon signature of IC2 (Figure 11) has three major peaks at ~1850 Ma, ~1900-1950 Ma, and ~2050-2100 Ma. A minor peak also occurs at ~2650-2700 Ma. The histogram plot and data tables (Figure 11, Appendix B) have small populations and individual ages which are summarized in Table 1.

IC5: This sample, which includes 136 individual grain analyses, was collected near the lower contact of the Kinnikinic Quartzite and the underlying Precambrian Wilbert Formation at Italian Canyon. Nearly all of the grains analyzed were rounded to nearly spherical, clear to pink, with diameters between 100 to 250 µm. The detrital zircon signature of IC5 (Figure 12) has one main peak at ~1850 Ma. Four minor peaks occur at ~~1900-1950 Ma, ~2050-2100 Ma, and a broad peak at ~2650-2750 Ma. The histogram plot and data tables (Figure 12, Appendix B) have small populations and individual ages which are summarized in Table 1.

TPR2: This sample, which includes 122 individual grain analyses, was collected at the upper contact of Kinnikinic Quartzite and the overlying Late Ordovician Fish Haven Dolomite at Twin Peaks Ranch. Nearly all of the grains were rounded to nearly spherical, clear to pink, with diameters between 100 to 250 µm. The detrital zircon signature of TPR2 (Figure 13) has two main peaks at ~1800-1900 Ma and ~2700-2750 Ma. Three minor peaks occur at ~1900 Ma, ~2050-2100 Ma, and ~2600-2700 Ma. The histogram plot and data tables (Figure 13, Appendix B) have small populations and individual ages which are summarized in Table 1.

TPR4: This sample, which includes 134 individual grain analyses, was collected from the upper-middle portions of Kinnikinic Quartzite at Twin Peaks Ranch. Nearly all of the grains analyzed were rounded to nearly spherical, clear to pink, with diameters between 100 to 250 µm. The detrital zircon signature of TPR4 (Figure 14) has three main peaks at ~1850 Ma, ~1900-1950 Ma, and ~2050-2100 Ma. The histogram plot and data tables (Figure 14, Appendix B) have small populations and individual ages which are summarized in Table 1.

TPR3: This sample, which includes 140 individual grain analyses, was collected from the lower-middle portion of Kinnikinic Quartzite at Twin Peaks Ranch. Nearly all of the grains analyzed were rounded to nearly spherical, clear to pink, with diameters between 100 to 250 µm. The detrital zircon signature of TPR3 (Figure 15) has two main peaks at ~1800-1850 Ma and ~1900-1950 Ma. A minor peak also occurs at ~2700 Ma. The histogram plot and data tables (Figure 15, Appendix B) have small populations and individual ages which are summarized in Table 1.

TPR5: This sample, which includes 127 individual grain analyses, was collected at the lower contact of Kinnikinic Quartzite and the underlying Precambrian Swauger Formation at Twin Peaks Ranch. Nearly all of the grains analyzed were rounded to nearly spherical, clear to pink, with diameters between 100 to 250 µm. The detrital zircon signature of TPR5 (Figure 16) has one main peak at ~1800-1900 Ma. Two minor peaks also occur at ~2050-2100 Ma and ~2650-2750 Ma. The histogram plot and data tables (Figure 16, Appendix B) have small and individual ages which are summarized in Table 1.

CM3: This sample, which includes 136 individual grain analyses, was collected at the upper contact of the Kinnikinic Quartzite and the overlying Late Ordovician Saturday Mountain Formation at Clayton Mine. Nearly all of the grains analyzed were rounded to nearly spherical, clear to pink, with diameters between 100 to 250 µm. The detrital zircon signature of CM3 (Figure 17) has two main peaks at ~1850 Ma and ~1900-1950 Ma. Two minor peaks occur at ~2050-2100 Ma and ~2650-2750 Ma. The histogram plot and data tables (Figure 17, Appendix B) have small populations and individual ages which are summarized in Table 1.

CM2: This sample, which includes 129 individual grain analyses, was collected from the middle portion of Kinnikinic Quartzite at Clayton Mine. Nearly all of the grains analyzed were rounded to nearly spherical, clear to pink, with diameters between 50 and 200 µm. The detrital zircon signature of CM2 (Figure 18) has two main peaks at ~1850 Ma and ~1900-1950 Ma. Two minor peaks occur at ~2050-2100 Ma and ~2650-2750 Ma. The histogram plot and data tables (Figure 18, Appendix B) have small populations and individual ages which are summarized in Table 1.

CM1: This sample, which includes 113 individual grain analyses, was collected at the lower contact of Kinnikinic Quartzite and the underlying Middle Ordovician Ella Dolomite. Nearly all of the grains analyzed were rounded to nearly spherical, clear to pink, with diameters between 20 and 40 µm. CM1 was the finest grained sample analyzed. The detrital zircon signature of CM1 (Figure 19) has one main broad peak at ~1800-2000 Ma and ~1900-1950 Ma. Three minor peaks occur at ~2100 Ma, ~2500-2600 Ma, and ~2600-2700 Ma. The histogram plot and data tables (Figure 19, Appendix B) have small populations and individual ages which are summarized in Table 1.

IG: This sample, which includes 129 individual grain analyses, was collected near the lower contact of Kinnikinic Quartzite and underlying Ordovician granite at Italian Gulch. Nearly all of the grains analyzed were rounded to nearly spherical, clear to pink, with diameters between 100 and 250 µm. The detrital zircon signature of IG (Figure 20) has two main peaks at ~1850Ma and ~1900-1950 Ma. Three minor peaks occur at ~2050-2100 Ma, ~2600 Ma, and ~2700 Ma. The histogram plot and data tables (Figure 20, Appendix B) have small populations and individual ages which are summarized in Table 1.

ICWF: This sample of Precambrian Wilbert Formation, which included 125 individual grain analyses, was collected below the contact between the Wilbert Formation and the overlying Kinnikinic Quartzite. Sample ICWF was taken for comparative analysis only, the age populations within this sample will be compared to the data of the Kinnikinic Quartzite to investigate sediment recycling of local underlying rocks. Nearly all of the grains analyzed were rounded to nearly spherical, clear to pink, with diameters between 100 and 250 µm. The detrital

zircon signature of ICWF (Figure 21) has one main peak at ~1650-1750 Ma, and one minor peak at ~2450 Ma. The histogram plot and data tables (Figure 21, Appendix B) have small populations and individual ages which are summarized in Table 1.

Sample	Major Populations (Ma)	Number	~%	Minor Populations (Ma)	Number	~%
IC3	1800-1900	53	40	2600-2700	9	7
131 Grains	1900-2000	29	23	1000-1400	8	6
	2000-2100	13	10	2300-2400	6	4.5
				1700-1800	3	1.5
				2100-2200	3	1.5
				2400-2500	2	1.5
				1625	1	>1
				2278	1	>1
				2536	1	>1
				2720	1	>1
				2845	1	>1
IC2	1800-1900	52	37	2600-2700	8	5.5
142 Grains	1900-2000	28	20	2200-2300	5	3.5
	2000-2100	26	18	1000-1200	4	3
				2300-2400	3	2
				2500-2600	3	2
				2700-2800	3	2
				1700-1800	2	1.5
				2400-2500	2	1.5
				2800-2900	2	1.5
				2100	1	>1
				2989	1	>1
				3238	1	>1
IC5	1800-1900	58	43	2700-2800	13	9.5
136 Grains	1900-2000	18	13	2600-2700	12	9
	2000-2100	17	13	1000-1400	3	2
				1700-1800	3	2
				2500-2600	3	2
				2900-3000	3	2
				2400-2500	2	1.5
				2800-2900	2	1.5
				3003	1	>1
TPR2	1800-1900	52	43	1900-2000	12	10
123 Grains	2700-2800	19	16	2000-2100	6	5
	2600-2700	13	11	1700-1800	4	3
				2800-2900	4	3
				900-1100	3	2.5
				2400-2500	3	2.5
				2900-3000	3	2.5
				2500-2600	2	1.5
				2209	1	>1

Table 1: Summary of detrital zircon age populations. Table is organized by sample and shows major and minor populations. Numbers and percentages of grains of each population are given.

Sample	Major Populations (Ma)	Number	~%	Minor Populations (Ma)	Number	~%
TPR4	1800-1900	48	36	2100-2200	4	3
134 Grains	1900-2000	39	29	2600-2700	4	3
	2000-2100	25	20	2800-2900	4	3
				2500-2600	3	2
				2200-2300	2	1.5
				1731	1	>1
				2413	1	>1
				2722	1	>1
				2953	1	>1
TPR3	1800-1900	57	41	1700-1800	7	5
140 Grains	1900-2000	32	23	2300-2400	7	5
				2700-2800	7	5
				2000-2100	6	4
				2500-2600	6	4
				2600-2700	5	3.5
				2100-2200	4	3
				1000-1100	3	2
				2200-2300	2	1.5
				2400-2500	2	1.5
				2800-2900	2	1.5
TPR5	1800-1900	61	48	2700-2800	12	9.5
127 Grains	2000-2100	16	13	2500-2600	5	4
	1900-2000	15	12	2800-2900	2	1.5
	2600-2700	14	11	2128	1	>1
				2973	1	>1
CM3	1800-1900	63	46	2600-2700	8	6
136 Grains	1900-2000	33	24	2700-2800	6	4.5
	2000-2100	16	12	1700-1800	2	1.5
				2100-2200	2	1.5
				2400-2500	2	1.5
				1033	1	>1
				2398	1	>1
				2510	1	>1
				2961	1	>1
CM2	1800-1900	50	39	2000-2100	12	9
129 Grains	1900-2000	34	26	2700-2800	11	8.5
				1700-1800	5	4
				2500-2600	5	4
				2600-2700	5	4
				900-1100	2	1.5
				2119	1	>1
				2297	1	>1
				2303	1	>1
				2846	1	>1
				3036	1	>1

Table 1 (continued).

Sample	Major Populations (Ma)	Number	~%	Minor Populations (Ma)	Number	~%
CM1	1800-1900	35	31	2000-2100	9	8
113 Grains	1900-2000	23	20	2100-2200	9	8
				2500-2600	9	8
				2600-2700	8	7
				2700-2800	7	6
				1000-1200	3	3
				2300-2400	3	3
				2400-2500	3	3
				1641	1	>1
				1745	1	>1
				2943	1	>1
				3084	1	>1
IG	1800-1900	44	34	2000-2100	9	7
128 Grains	1900-2000	40	31	2600-2700	7	5.5
				2700-2800	7	5.5
				2500-2600	6	4.5
				1000-1300	4	3
				1700-1800	4	3
				2800-2900	2	1.5
				2308	1	>1
				2986	1	>1
				3379	1	>1
ICWF	1700-1800	73	59	1400-1500	2	1.5
125 Grains	1600-1700	32	26	1504	1	>1
	2400-2500	13	11	1857	1	>1
				2594	1	>1
				2662	1	>1
				3127	1	>1

Table 1 (continued).

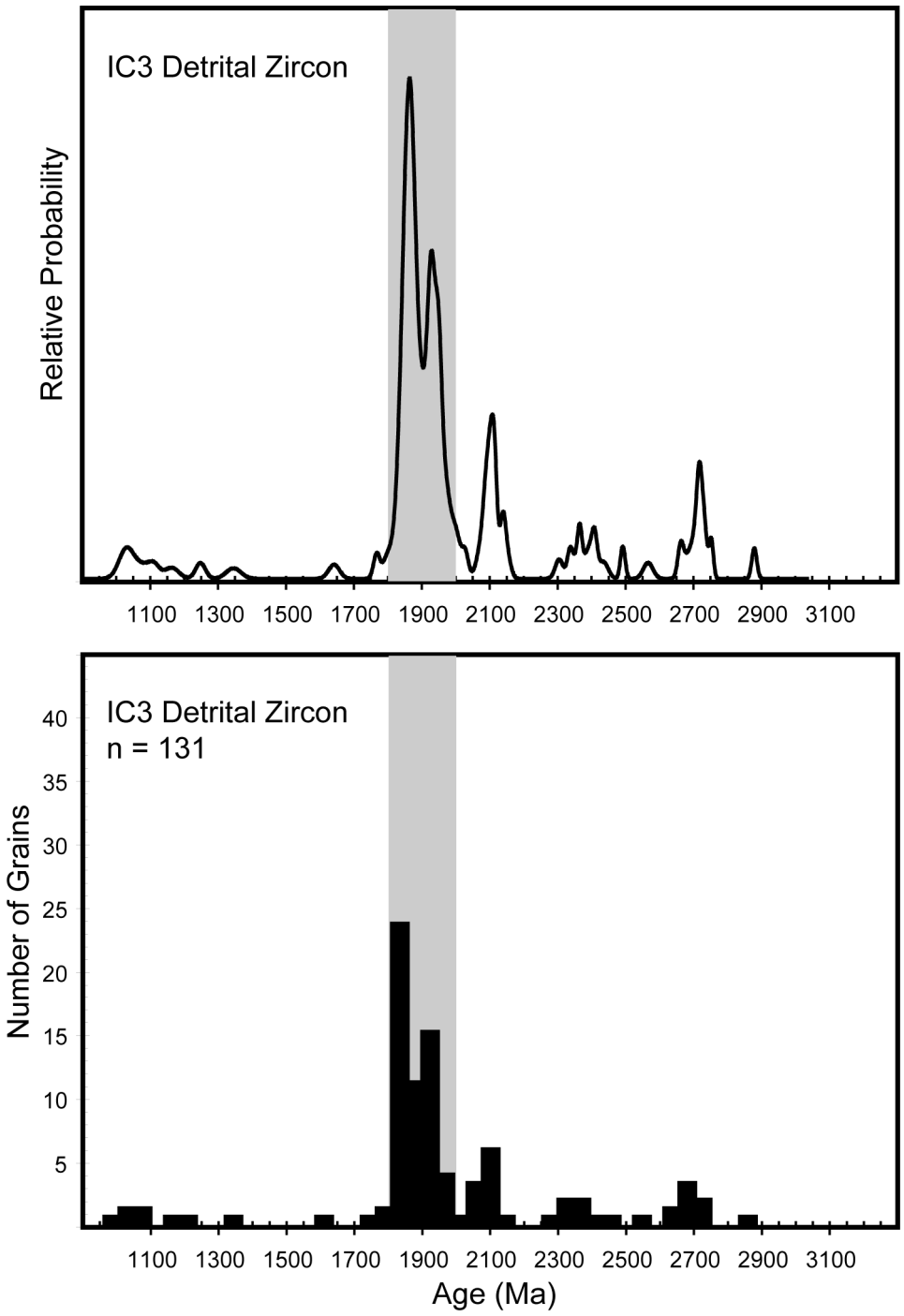

Figure 10: Italian Canyon upper (IC3) detrital zircon relative probability (top) and histogram (bottom). The gray bands correspond to the 1800-2000 Ma populations attributed to the Peace River Arch by the Long-Distance Transport model (Gehrels, 2000; Gehrels et al, 1995; Gehrels and Dickinson, 1995).

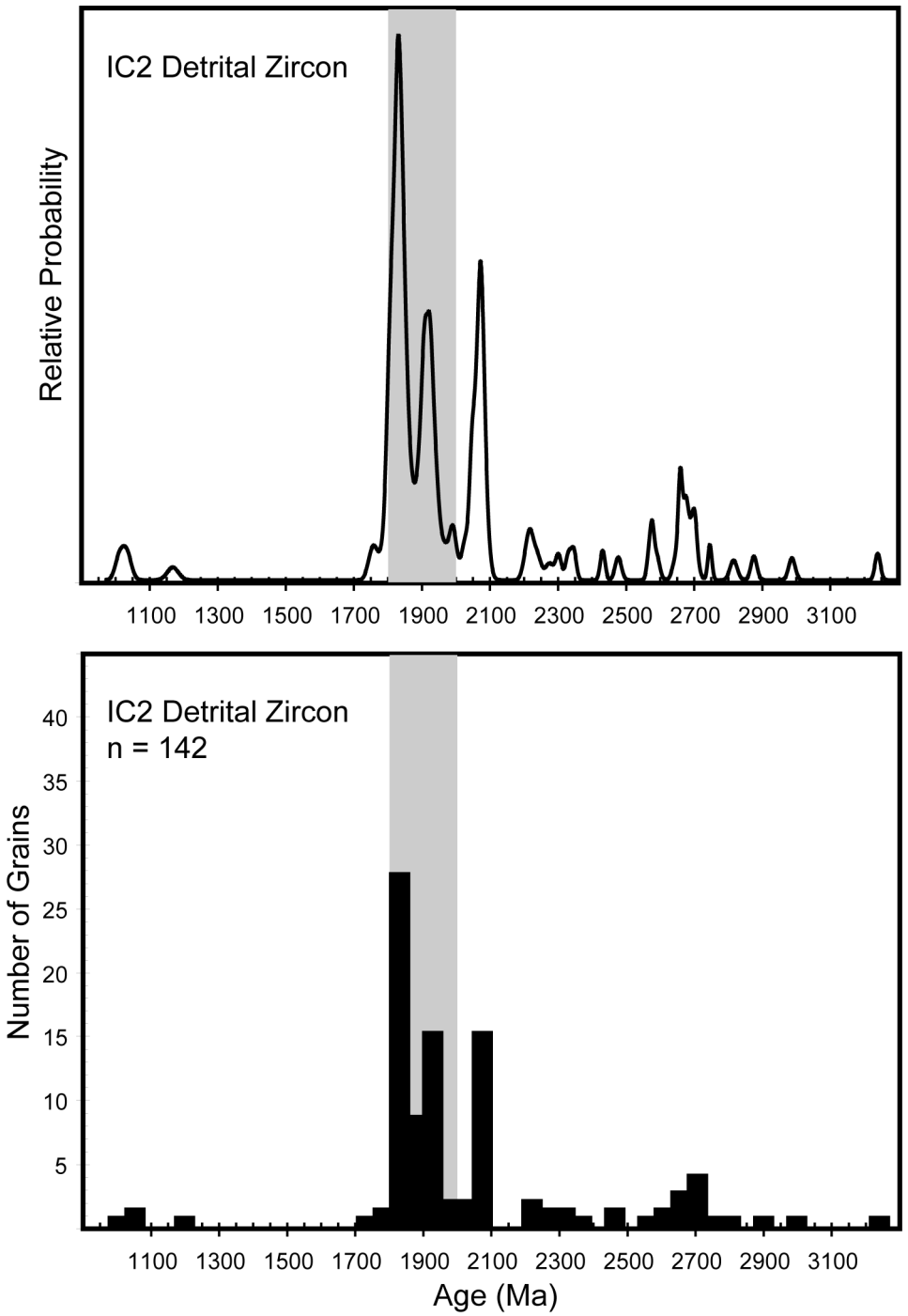

Figure 11: Italian Canyon middle (IC2) detrital zircon relative probability (top) and histogram (bottom). The gray bands correspond to the 1800-2000 Ma populations attributed to the Peace River Arch by the Long-Distance Transport model (Gehrels, 2000; Gehrels et al, 1995; Gehrels and Dickinson, 1995).

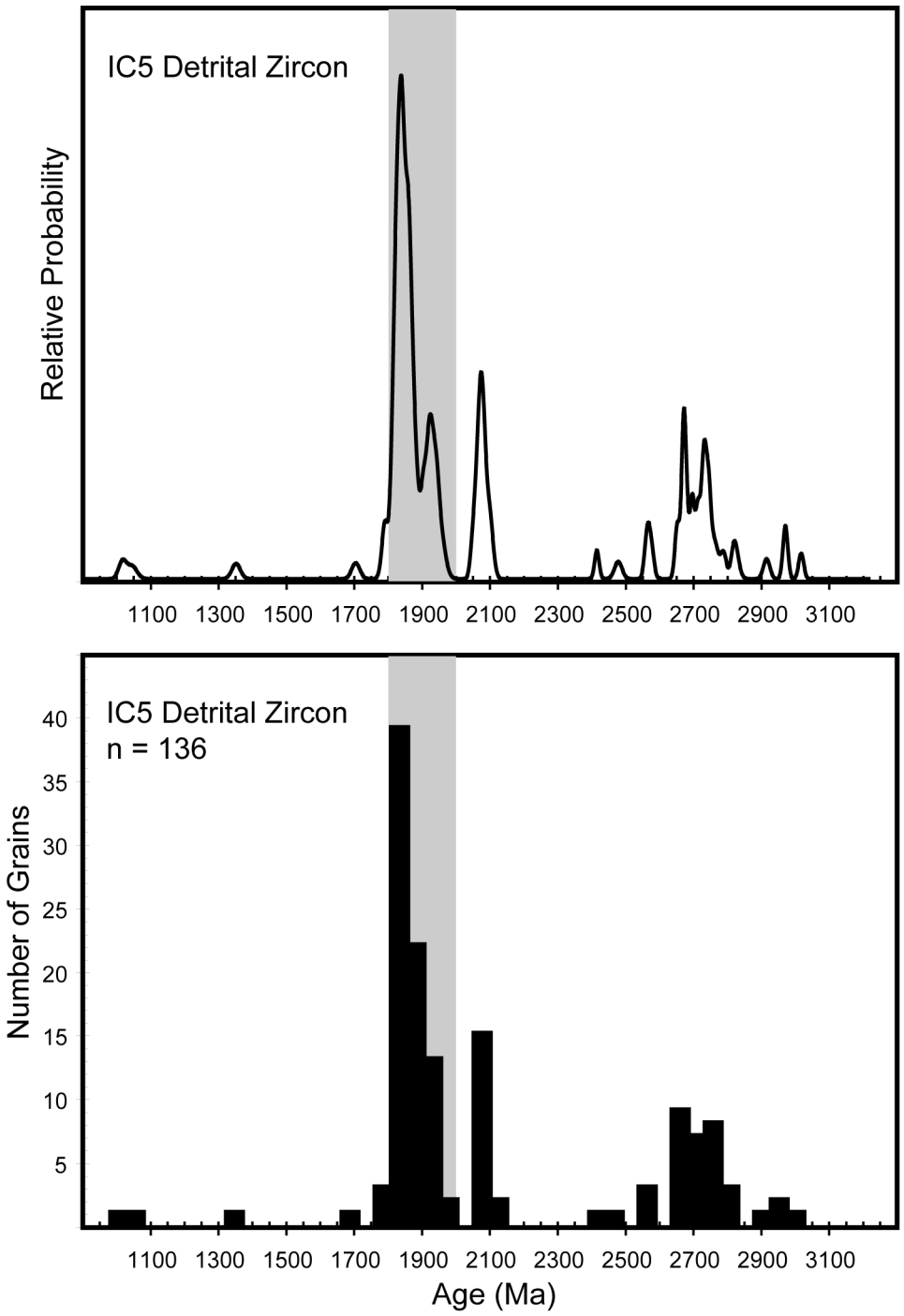

Figure 12: Italian Canyon basal (IC5) detrital zircon relative probability (top) and histogram (bottom). The gray bands correspond to the 1800-2000 Ma populations attributed to the Peace River Arch by the Long-Distance Transport model (Gehrels, 2000; Gehrels et al, 1995; Gehrels and Dickinson, 1995).

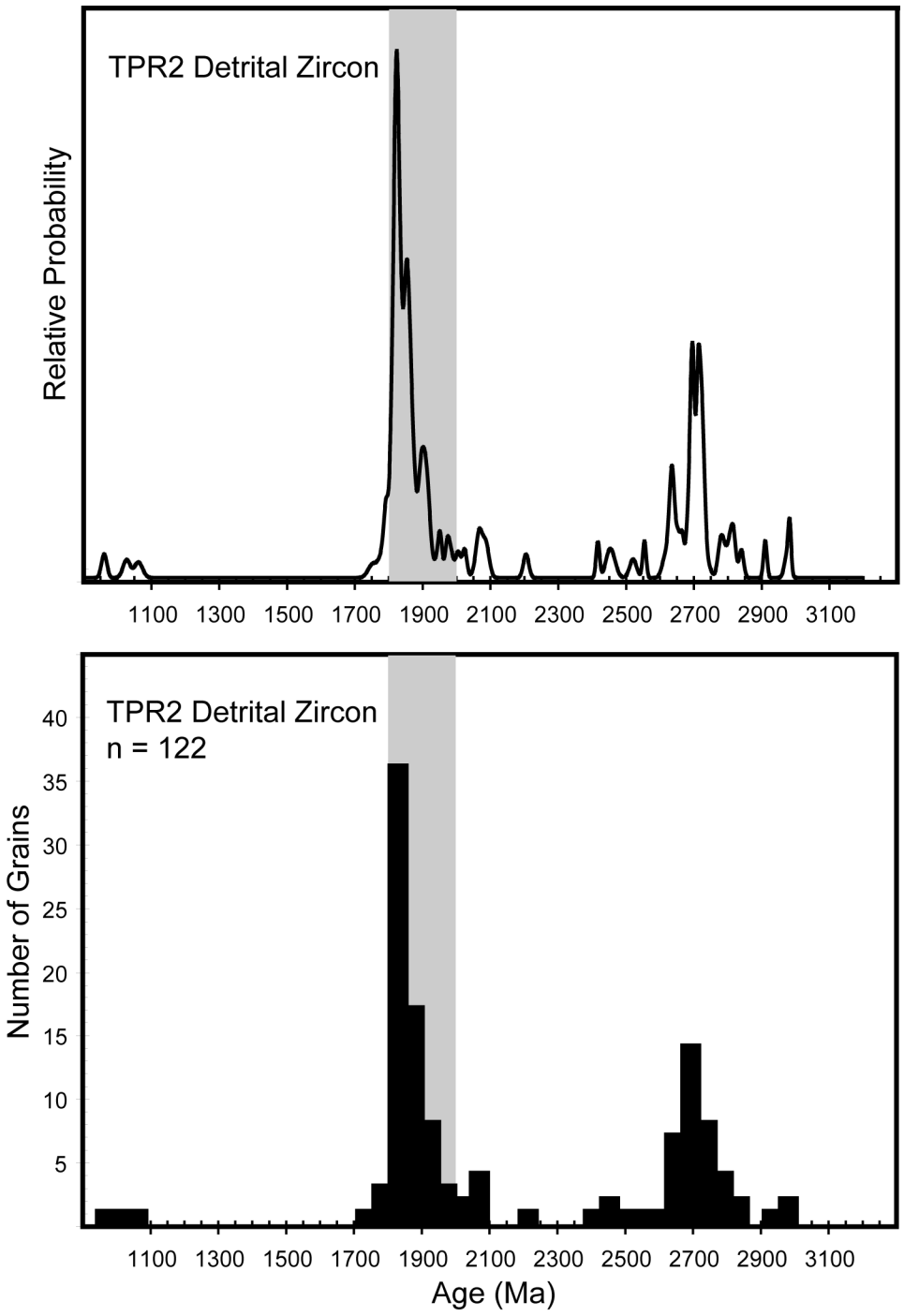

Figure 13: Twin Peaks Ranch upper (TPR2) detrital zircon relative probability (top) and histogram (bottom). The gray bands correspond to the 1800-2000 Ma populations attributed to the Peace River Arch by the Long-Distance Transport model (Gehrels, 2000; Gehrels et al, 1995; Gehrels and Dickinson, 1995).

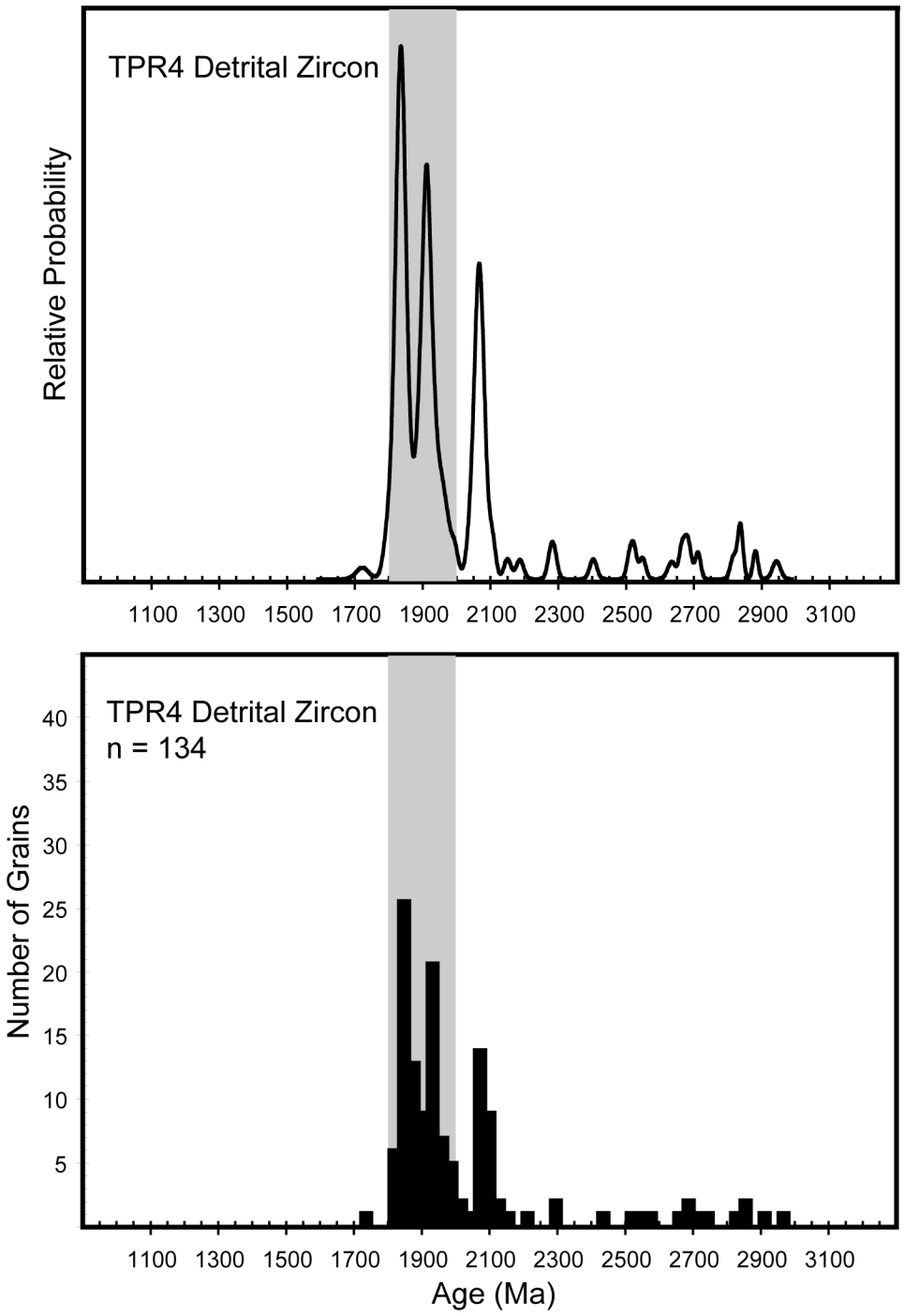

Figure 14: Twin Peaks Ranch upper-middle (TPR4) detrital zircon relative probability (top) and histogram (bottom). The gray bands correspond to the 1800-2000 Ma populations attributed to the Peace River Arch by the Long-Distance Transport model (Gehrels, 2000; Gehrels et al, 1995; Gehrels and Dickinson, 1995).

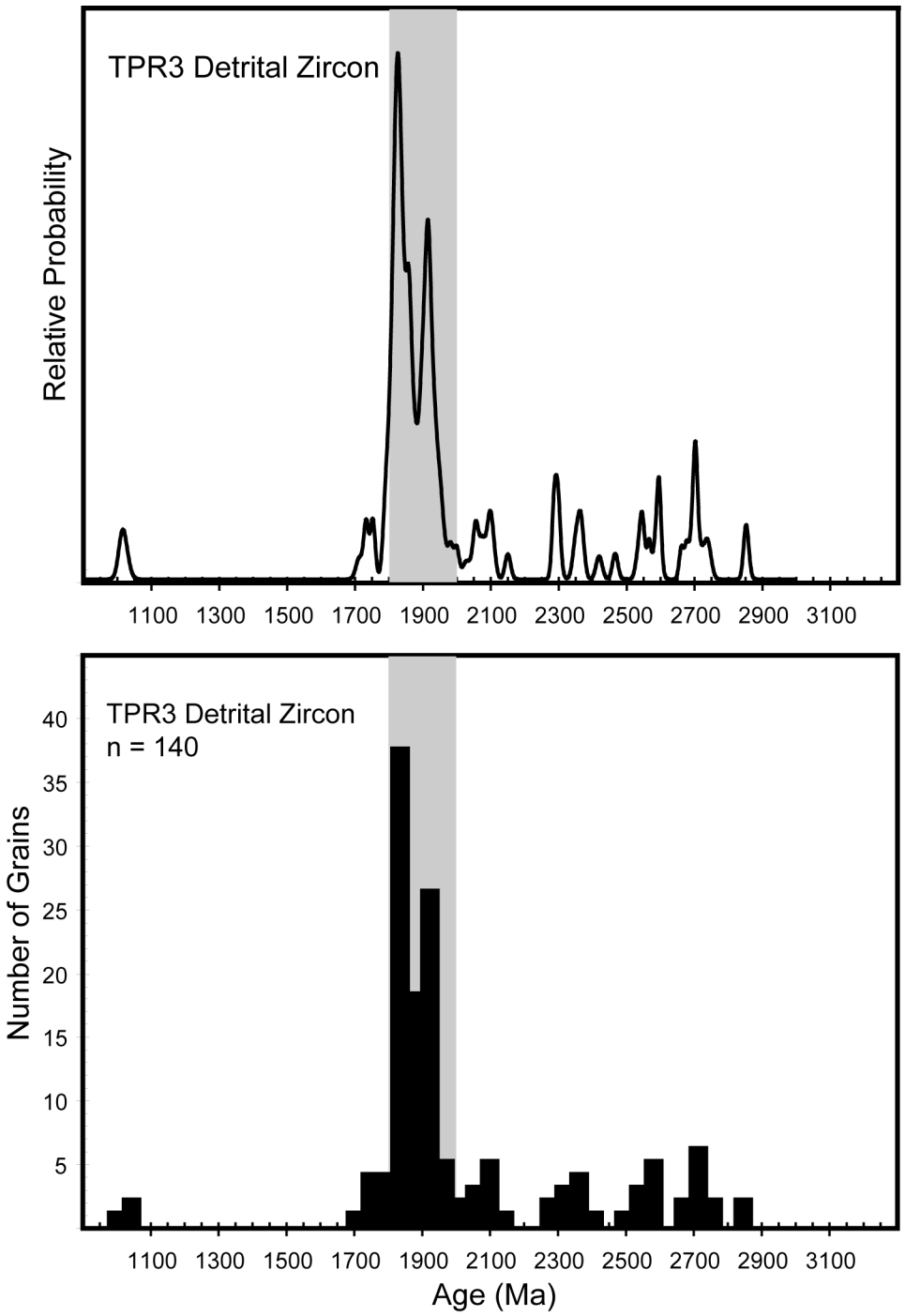

Figure 15: Twin Peaks Ranch lower-middle (TPR3) detrital zircon relative probability (top) and histogram (bottom). The gray bands correspond to the 1800-2000 Ma populations attributed to the Peace River Arch by the Long-Distance Transport model (Gehrels, 2000; Gehrels et al, 1995; Gehrels and Dickinson, 1995).

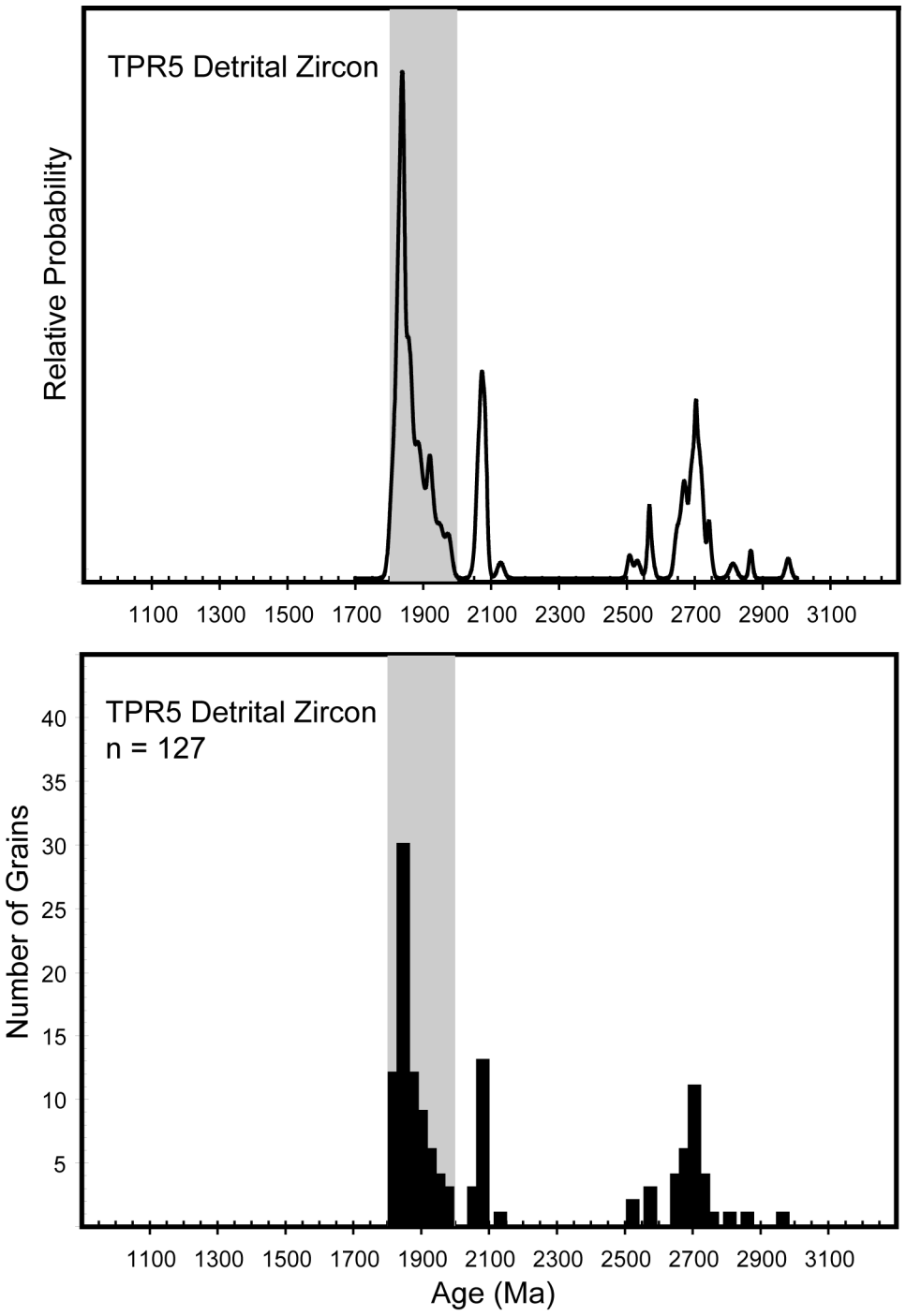

Figure 16: Twin Peaks Ranch basal (TPR5) detrital zircon relative probability (top) and histogram (bottom). The gray bands correspond to the 1800-2000 Ma populations attributed to the Peace River Arch by the Long-Distance Transport model (Gehrels, 2000; Gehrels et al, 1995; Gehrels and Dickinson, 1995).

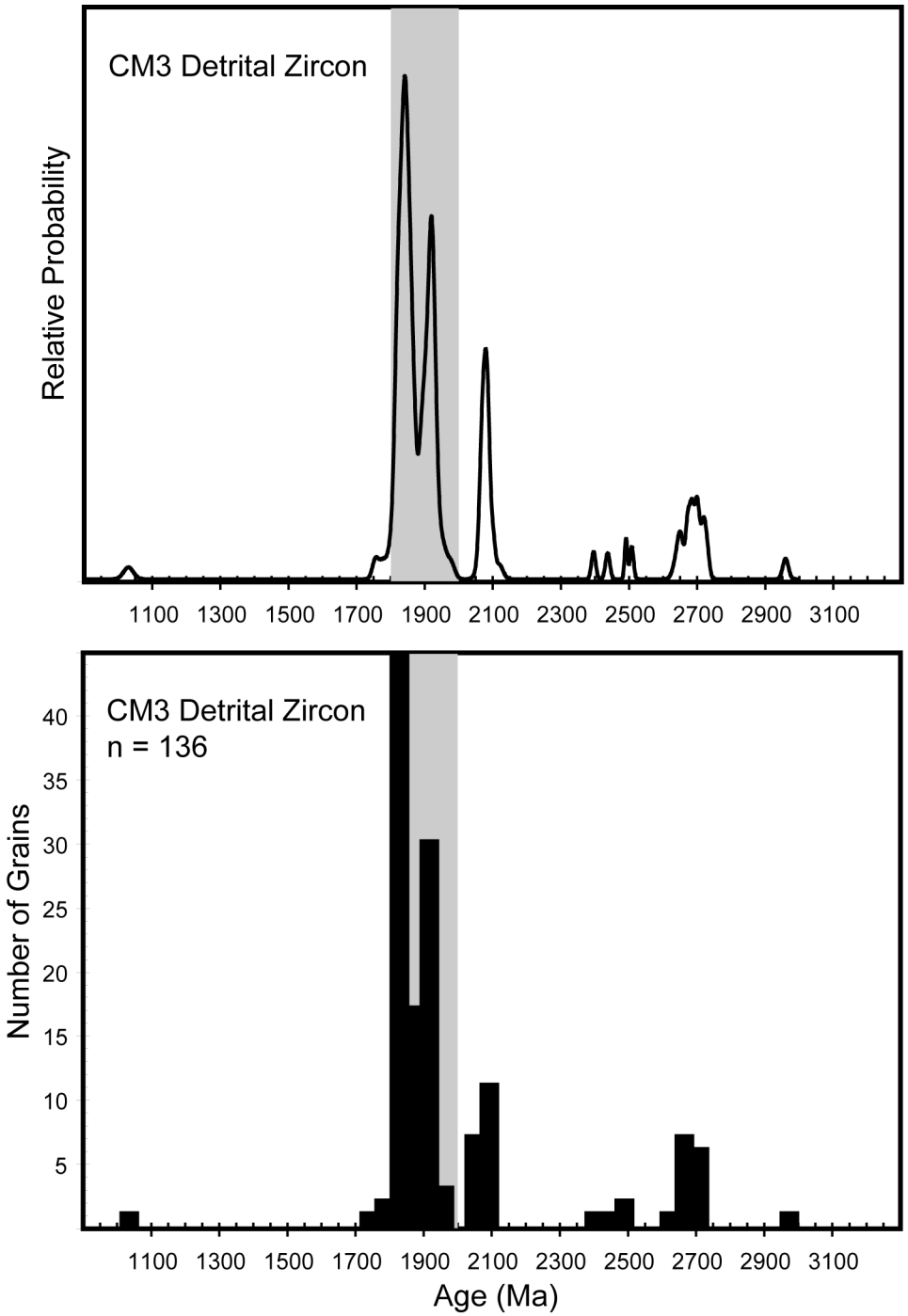

Figure 17: Clayton Mine upper (CM3) detrital zircon relative probability (top) and histogram (bottom). The gray bands correspond to the 1800-2000 Ma populations attributed to the Peace River Arch by the Long-Distance Transport model (Gehrels, 2000; Gehrels et al, 1995; Gehrels and Dickinson, 1995).

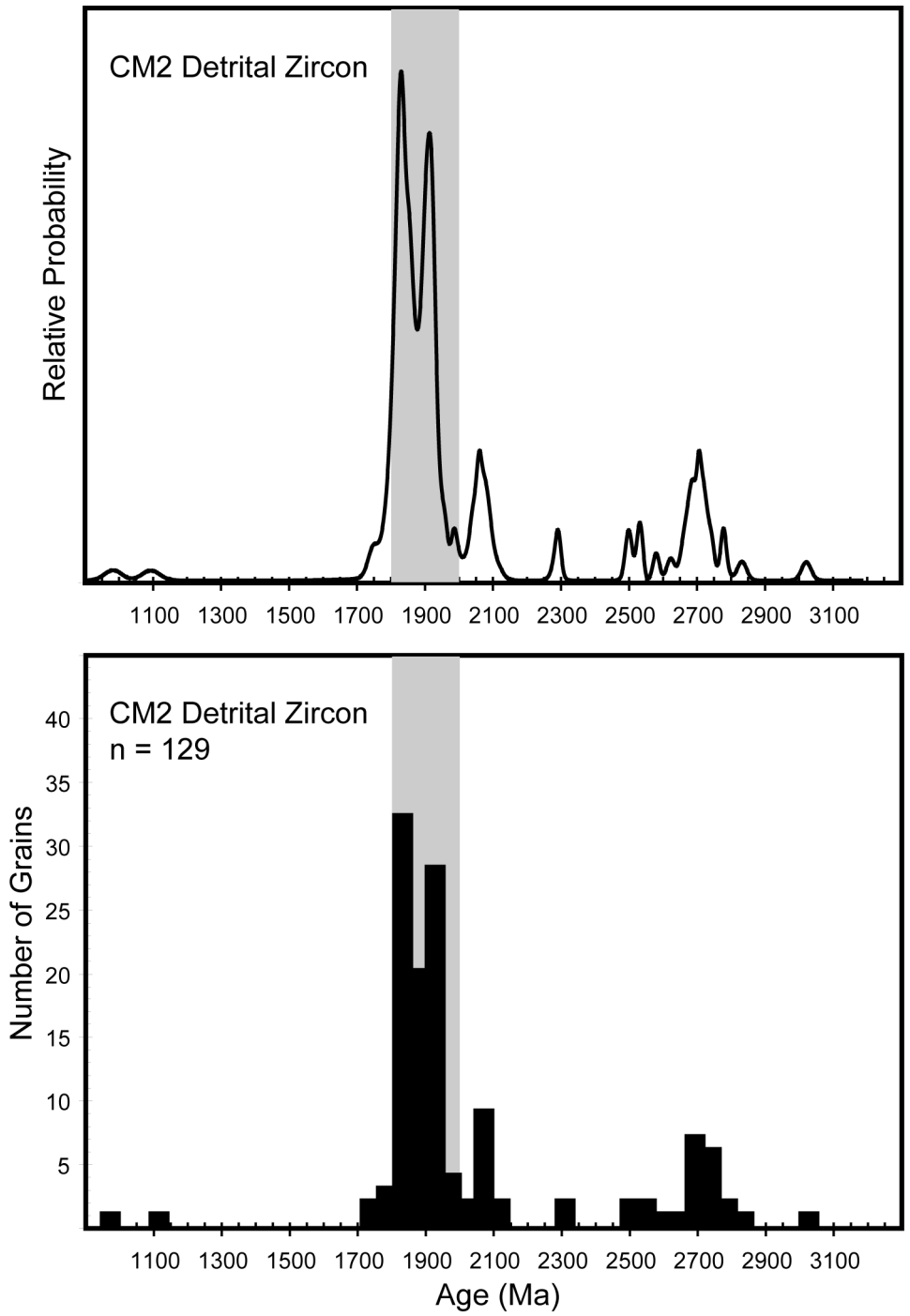

Figure 18: Clayton Mine middle (CM2) detrital zircon relative probability (top) and histogram (bottom). The gray bands correspond to the 1800-2000 Ma populations attributed to the Peace River Arch by the Long-Distance Transport model (Gehrels, 2000; Gehrels et al, 1995; Gehrels and Dickinson, 1995).

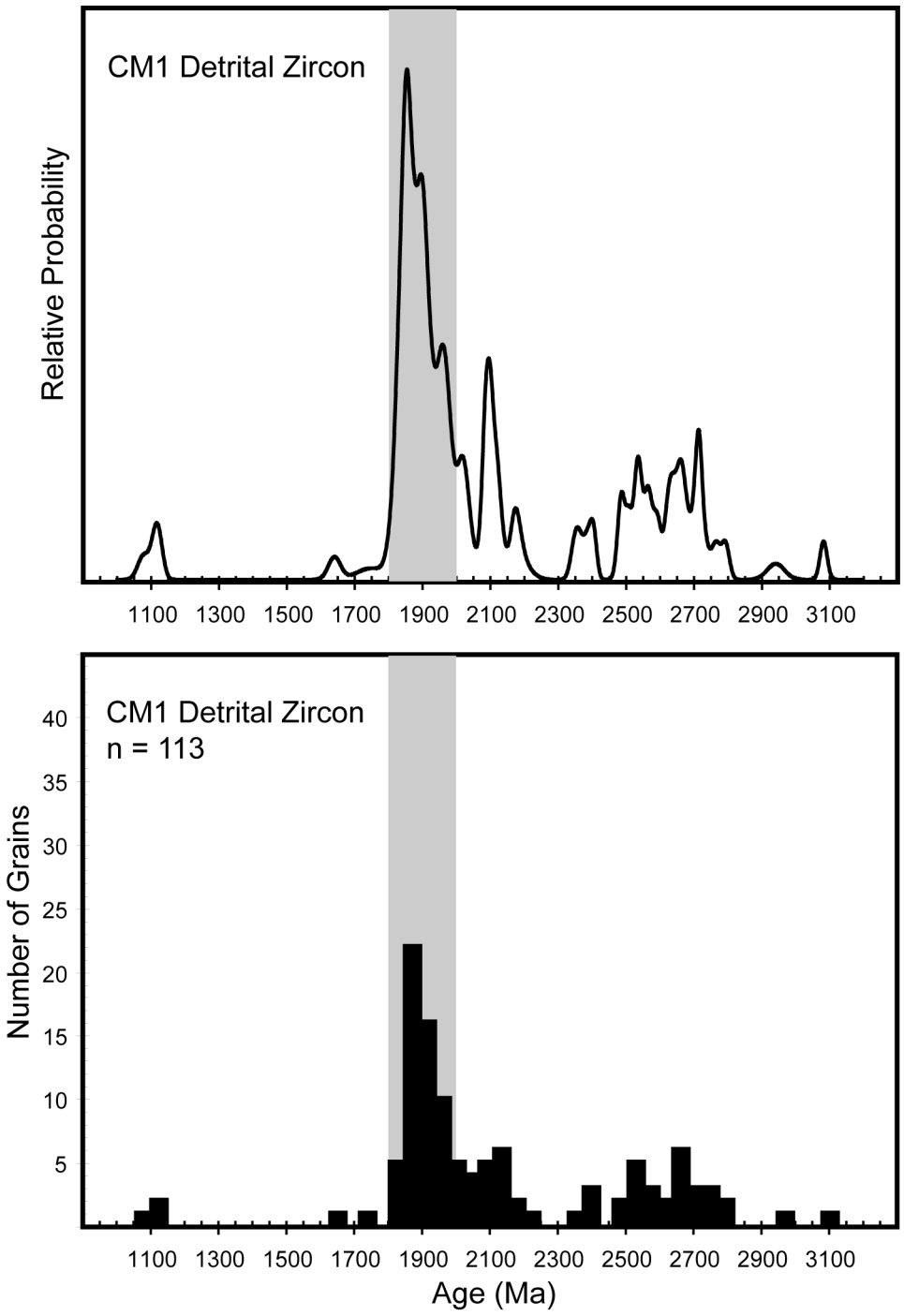

Figure 19: Clayton Mine basal (CM1) detrital zircon relative probability (top) and histogram (bottom). The gray bands correspond to the 1800-2000 Ma populations attributed to the Peace River Arch by the Long-Distance Transport model (Gehrels, 2000; Gehrels et al, 1995; Gehrels and Dickinson, 1995).

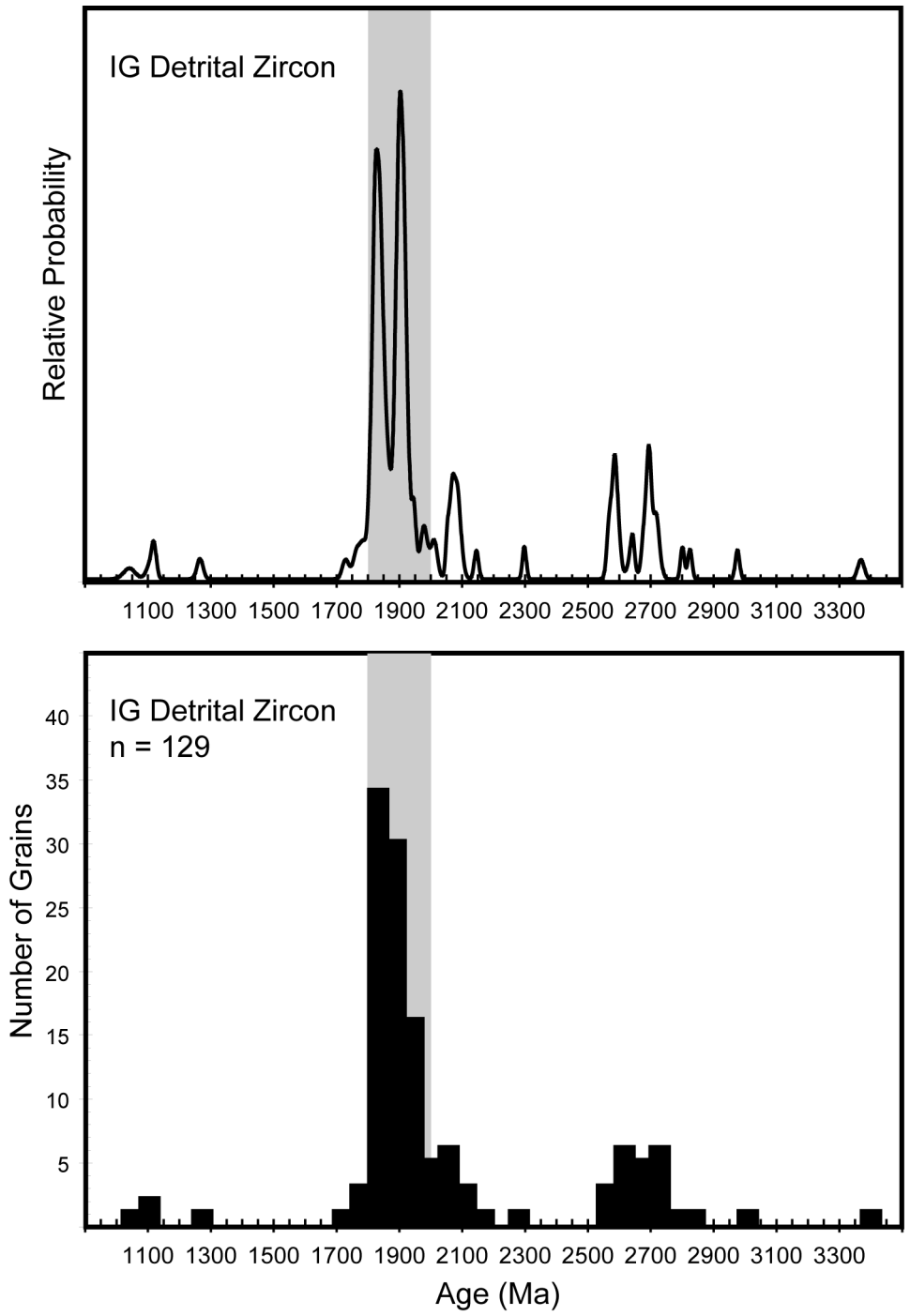

Figure 20: Italian Gulch (IG) detrital zircon relative probability (top) and histogram (bottom). The gray bands correspond to the 1800-2000 Ma populations attributed to the Peace River Arch by the Long-Distance Transport model (Gehrels, 2000; Gehrels et al, 1995; Gehrels and Dickinson, 1995). Note the change in the x-axis scale to accommodate a broader age range.

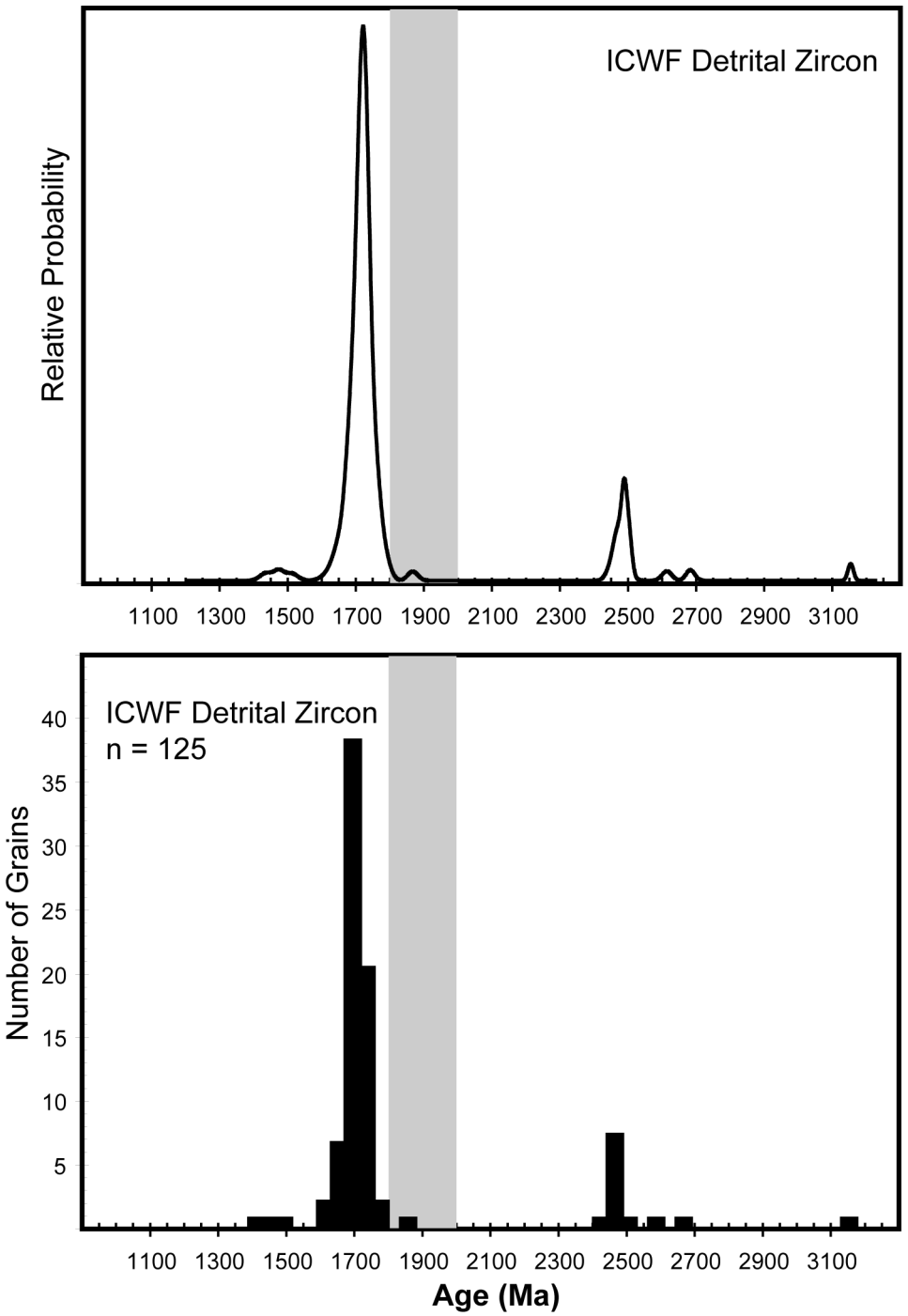

Figure 21: Wilbert Formation from Italian Canyon (ICWF) detrital zircon relative probability (top) and histogram (bottom). The gray bands correspond to the 1800-2000 Ma populations in the Kinnikinic Quartzite and lateral equivalents which are attributed to the Peace River Arch by the Long-Distance Transport model (Gehrels, 2000; Gehrels et al, 1995; Gehrels and Dickinson, 1995).

CHAPTER 6

DISCUSSION

Facies Interpretation

In general, the Kinnikinic Quartzite was deposited in shallow marine shelf settings (Ketner, 1968, 1966; Oaks and James, 1980; James and Oaks, 1977). However, each of the six sedimentary facies identified from outcrops in east-central Idaho likely represent a specific position on the shallow shelf (Figure 22). A summary of each facies' name, sedimentology, interpreted position, and locations they were observed is given in Table 2. The Laurentian passive margin setting formed a shallow, gently dipping shelf margin that was probably similar in geometry to the shelf margins of cratonic sheet sandstones described from the north-central interior of North America (e.g. Runkel et al., 2007; Runkel et al., 1998). Thus, the shallow marine depositional environments on this passive margin setting were likely similar to those of cratonic sandstones. Sedimentary structures of cratonic sheet sandstones such as trough and planar cross-stratification, laminations, and trace fossils were used to interpret depositional settings on a shallow, gently dipping shelf margin (Runkel et al., 2007). Although no complete section of these facies occurred in the field area, the shelf position of each facies is implied (Figure 22).

Interbedded shale and quartzite likely represents offshore interfingering with the Late Ordovician Saturday Mountain (Oaks and James, 1980) indicating a transition zone between inner shelf and outer shelf deposits (Oaks and James, 1980; Reading, 1996; Runkel et al., 2007). Parallel and wavy laminations represent a depositional setting near or below stormweather wave base (Reading, 1996). The absence of shale in this facies likely indicates a shelf position landward of the interbedded shale and quartzites (James and Oaks, 1977; Runkel et al., 2007).

Hummocky cross-stratification is indicative of a relatively proximal offshore shelf setting (Hall, 1989; Runkel et al., 2007). Unlike parallel laminations, hummocks commonly form within stormweather wave base, the hummocky cross-stratified facies formed landward of the laminated facies (Reading, 1996; Runkel et al., 1998, 2007). Low-angle planar cross-stratification is typical of deposition at or above fairweather wave base in a foreshore to shoreface setting (Ketner, 1968; James and Oaks, 1977; Runkel et al., 1998, 2007) and formed landward of the stormweather wave base hummocky cross-stratification (Runkel et al., 2007). Vertical burrows (*Skolithos)* are largely an indicator of foreshore to shoreface settings (James and Oaks, 1977; Runkel et al., 1998, 2007) landward of the cross-stratified facies. The massive facies, which is dominant throughout the Kinnikinic Quartzite, is likely a result of extensive bioturbation, subsequent silica flooding during diagenesis, or a lack of sufficient mafic sand grains to result in sedimentary structures (James and Oaks, 1977). If massive beds are a result of extensive bioturbation then this facies coincide with the burrowed facies. However, if the massive facies is due to diagenesis or a lack of mafic grains, then its position on the shallow shelf margin is difficult to determine.

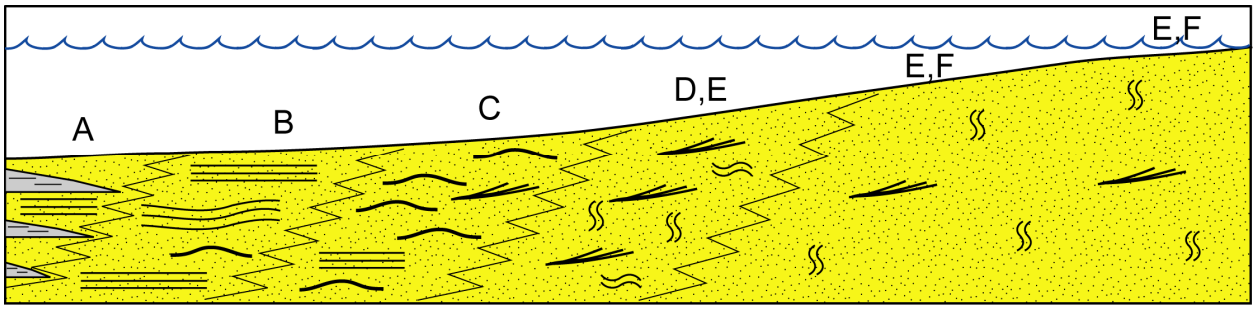

Figure 22: Sedimentary Facies Shelf Position. Diagram shows each sedimentary facies' interpreted shelf position (adapted from Runkel et al., 2007). Letters correspond to facies outlined in Table 2 and photographs in Figure 9.

Facies Name	Sedimentology	Interpretation of Shelf Position	Locations Observed
A Interbedded Shale and Quartzite	Thinly bedded shale and very find grained quartzite interbeds.	Outer Shelf – Represents interfingering of Kinnikinic Quartzite with the Saturday Mountain Formation (Oaks and James, 1980; Runkel et al., 2007).	Clayton Mine
B Laminated	Thin bedded, fine grained quartzite with parallel to wavy laminations.	Offshore to Offshore-Transition or Foreshore (James and Oakes, 1977; Runkel et al., 2007)	Italian Canyon Clayton Mine
C Hummocky Cross-Stratification	Thin to medium bedded, fine grained quartzite, with large wedge-shaped hummocks.	Offshore-Transition (Hall, 1989; Runkel et al., 2007)	Italian Canyon Clayton Mine
D Low-Angle Planar Cross-Stratification	Thin to medium bedded, fine grained quartzite, with large (20-40 cm) wedge-shaped to small (2-10 cm) low-angle planar cross-stratification.	Foreshore to Shoreface (Ketner, 1968; James and Oaks, 1977; Runkel et al., 2007)	Italian Canyon Twin Peaks Ranch Clayton Mine
E Horizontal and Vertical Burrows	Medium bedded, fine grained quartzite with horizontal and vertical burrows (*Skolithos*).	Foreshore to Shoreface (James and Oaks, 1977; Runkel et al., 2007)	Italian Canyon Clayton Mine
F Massive	Medium bedded, fine grained quartzite and internally structureless.	A lack of internal structures may indicate bioturbation, which would indicate Shoreface to Offshore-Transition, though this determination is difficult. (James and Oaks, 1977)	Italian Canyon Twin Peaks Ranch Clayton Mine

Table 2: Name, sedimentology, interpretation, and locations observed for the six sedimentary facies identified in outcrop.

Detrital Zircon Interpretation- Internal Variability: Spatial and Temporal Variance

As Table 1 demonstrates, each of the detrital zircon samples of the Kinnikinic Quartzite contain the same basic age populations, but with varying proportions. To address questions of spatial and temporal provenance variance, changes in the grain percentages of age populations of samples within and between locations are examined.

The detrital zircon histograms and relative probability plots were compiled for each measured section (Figures 23, 24 and 25) to see how detrital zircon populations evolved over time. While the Ordovician Quartzites have a very distinct detrital zircon signature from other

Paleozoic quartzites of the western Cordillera (Gehrels, 2000; Gehrels et al, 1995; Gehrels and Dickinson, 1995), spatial and temporal variations is readily noticeable. The significance of spatial and temporal provenance variations is debatable, but this study argues that even small changes in detrital zircon signatures and age populations are significant. Subtle changes of relative probability (relative abundance) plots between samples such as heights and shifts of peaks, and appearance and disappearance of peaks may indicate changes in source regions or sediment influx. If this is true, three major questions arise:

1. How do relative abundances of age populations change between samples within and between sections?
2. What do these changes signify in terms of provenance?
3. What causes these changes to occur?

Temporal Variability

Italian Canyon (Figure 23): The three samples from Italian Canyon all have very similar detrital zircon signatures. All three samples contain four prominent peaks: ~1800-1900 Ma, ~1900-1950 Ma, ~2000-2150 Ma, and ~2600-2750 Ma. The most prominent peak in the samples from Italian Canyon is the ~1800-1900 Ma peak. The ~1800-1900 Ma and ~2000-2150 Ma peaks have a constant relative probability in all samples. The ~1900-1950 Ma peak sharply increases up-section, while the ~2600-2750 Ma peak decreases up-section. Small but, notable peaks occur at ~1000-1100 Ma and ~2400-2500 Ma. Small peaks at ~2200-2400 Ma occur in the upper (IC3) and middle (IC2) samples.

Twin Peaks Ranch (Figure 24): The four samples from Twin Peaks Ranch have varying detrital zircon signatures, but a peak from ~1800-1900 Ma is the most dominant. Other dominant peaks include: ~1900-1950 Ma, ~2000-2150 Ma, and ~2600-2750 Ma. The ~1900-1950 Ma peak is dominant in the middle samples (TPR4 and TPR3), but is minor in the upper (TPR2) and basal (TPR5) samples. The ~2000-2150 Ma peak is prominent in the upper-middle (TPR4) and basal samples, but is minor in the upper and lower middle (TPR3) samples. The ~2600-2750 Ma peak decreases up-section until the upper sample, where it rises to being the second most prominent peak after the ~1800-1900 Ma peak. A small peak at ~1000-1100 Ma only occurs in the upper and lower-middle samples. Small peaks from ~2400-2500 Ma occur in all samples except the basal sample. A peak near ~2300 Ma only occurs in the middle samples.

Clayton Mine (Figure 25): The upper (CM3) and middle (CM2) samples from Clayton Mine have similar detrital zircon signatures, but the signature of the basal (CM1) sample is distinctly different. The most prominent peak in all three samples is the ~1800-1900 Ma peak, however this peak varies slightly within this section. The ~1800-1900 Ma peak in the basal sample is shifted slightly to the right, but the change in position is minor. Other main peaks include: ~1900-1950 Ma, ~2000-2150 Ma, ~2500-2550 Ma, and ~2650-2750 Ma. The ~1900-1950 Ma peak is dominant in the upper and middle samples, but is minor in the basal sample. The ~2000-2150 Ma sample varies slightly in relative probability, being more prominent in the upper and basal samples than the middle sample. The ~2500-2550 Ma and ~2650-2750 Ma peaks decrease up-section. A small peak at ~1000-1150 Ma occurs in all three samples. Small peaks near ~2350-2450 Ma occur in the upper and basal samples. A small peak at ~2150-2200 Ma is only present in the basal sample, and a peak at ~2300 Ma only occurs in the middle sample.

Italian Gulch (Figure 20): The detrital zircon signature of the sample taken from Italian Gulch (IG) is very similar to those of Italian Canyon, Twin Peaks, and Clayton Mine, but there are distinct differences. The most prominent peak in IG is the ~1900-1950 Ma peak, followed by the ~1800-1900 Ma peak. Three other prominent peaks occur at ~2050-2100 Ma, ~2550-2600 Ma, and ~2650-2750 Ma, which are all subequal in relative probability. Other notable peaks occur at ~1000-1150 Ma and ~2300 Ma.

Spatial Variability and Significance

The detrital zircon signatures of Kinnikinic Quartzite vary within and between, measured sections. The stacked relative probability plots of all the Kinnikinic Quartzite samples from each measured section are plotted in approximate stratigraphic position (Figure 26). The sample from Italian Gulch was taken near the basal contact, but there is some uncertainty regarding the nature of the contact. Thus comparison of IG with other samples with respect to stratigraphic position is unclear, so it was omitted from the regional synthesis (Figure 26).

Several distinct patterns occur in the detrital zircon populations of the Kinnikinic Quartzite. The most apparent patterns are the increase in abundance of the ~1.9-1.95 Ga population up-section and up-section decrease in abundance of the ~2.6-2.75 Ga population (excluding TPR2). These patterns indicate that at the onset of deposition the provenance consisted of predominantly from ~1.8-1.9 Ga rocks, but over time as sea level rose onto the continent a higher percentage of ~1.9-1.95 Ga rocks were eroded and a lower percentage of ~1.8-1.9 Ga rocks were being sourced. Conversely, at the onset of deposition ~2.6-2.75 Ga rocks were a major contributor of sediment, but over time this source area was probably partially covered by rising sea level.

The ~2000-2150 Ma populations is similar in all of the basal samples, but changes up-section. Landward (Italian Canyon), the ~2000-2150 Ma population increases (IC2) and then subsides at the top of the section up-section (IC3). Distally (Clayton Mine and Twin Peaks Ranch), this population decreases (CM2, TPR3) and then increases at the top of the section (CM3, TPR3), except for the sharp decrease at the top of Twin Peaks Ranch (TPR2).

The 900-1300 Ma zircon population appears in eight of the ten samples and is proportionally small in each (6% in one sample, but generally <3%). Landward this population increase up-section, but distally it decreases up-section. The 900-1300 Ma population it is absent in the basal and upper-middle samples from Twin Peaks Ranch, but occurs in the lower-middle and upper samples. Since this population is typically < 3%, the relative abundance may not be as significant as the presence of the population. Thus, its presence in the majority of the samples indicates that the source of this population, possibly extensive river systems and isolated ~1030 and ~1050 Ma plutons in northern Canada, were actively supplying sediment throughout deposition (Cook et al., 1992).

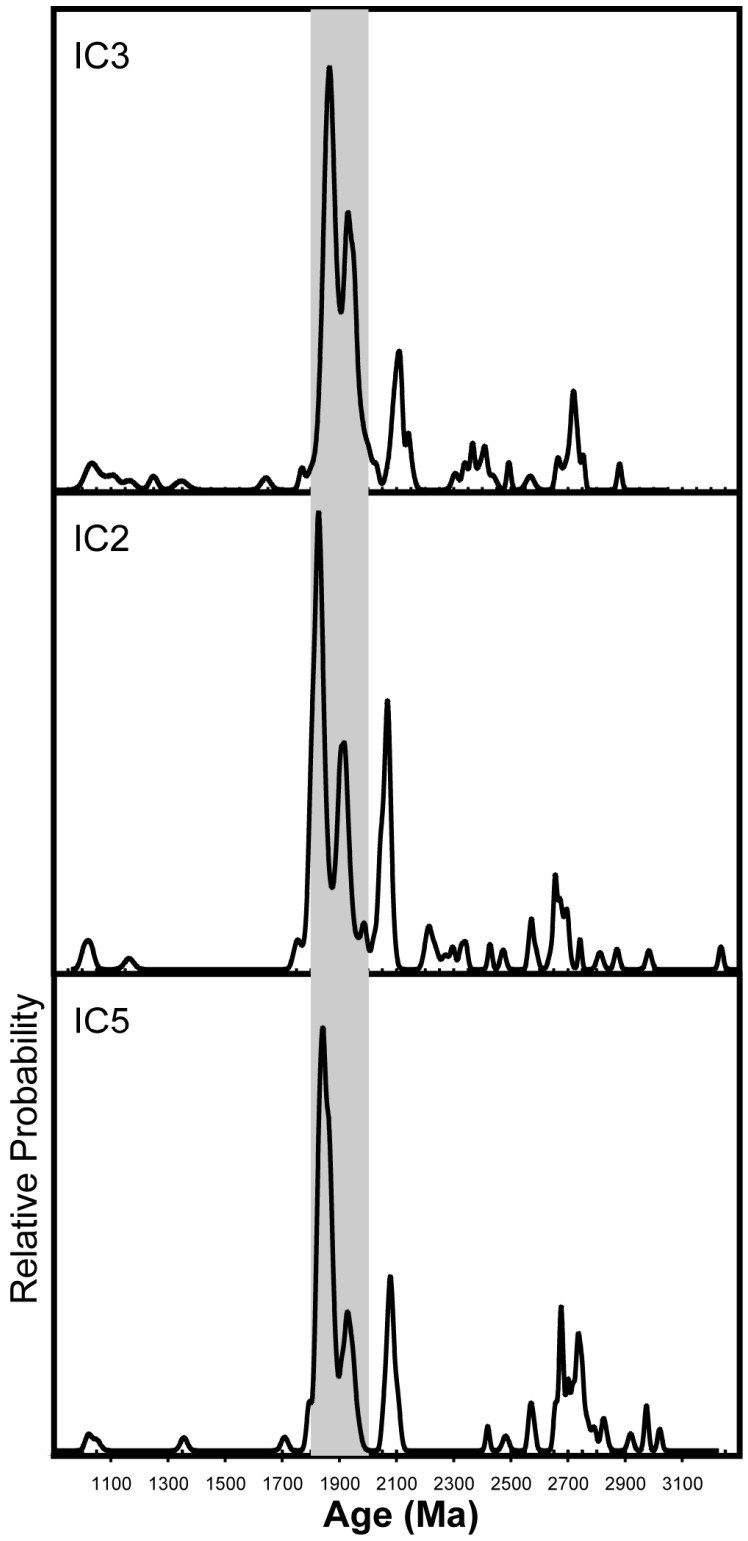

Figure 23: Stacked Relative Probability Plots from Italian Canyon. Plots are stacked in stratigraphic order (oldest to youngest).

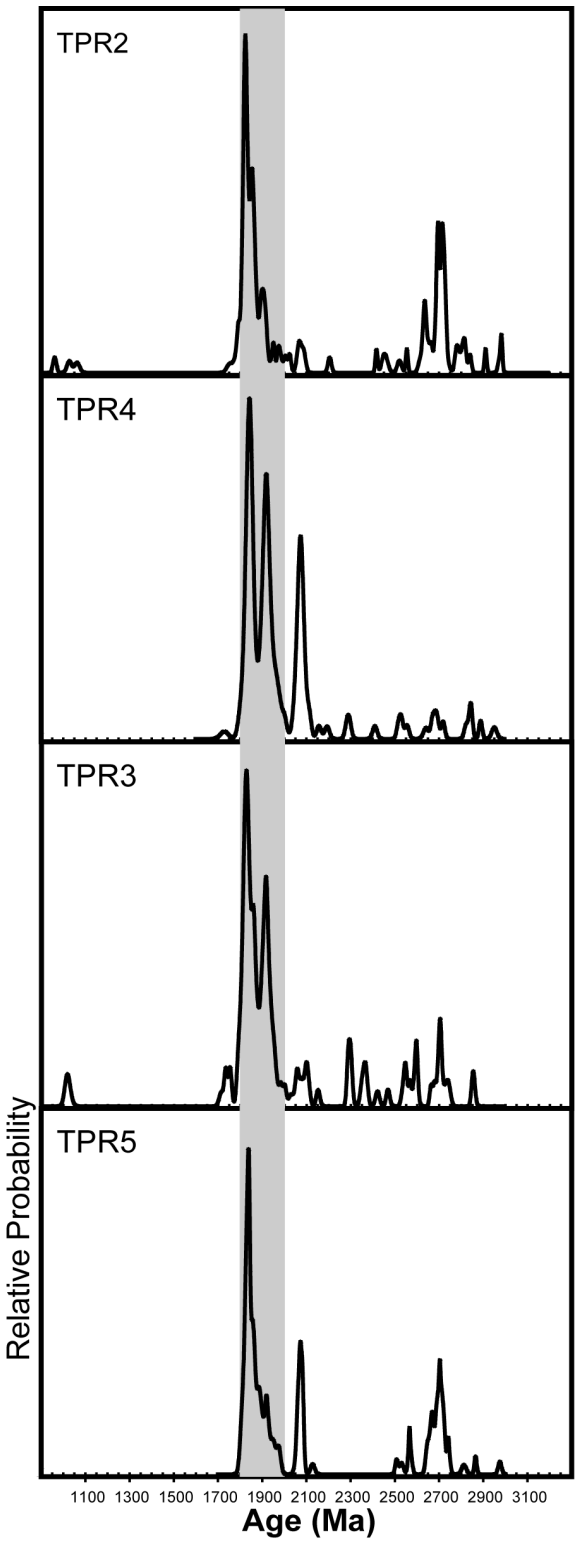

Figure 24: Stacked Relative Probability Plots from Twin Peaks Ranch. Plots are stacked in stratigraphic order (oldest to youngest).

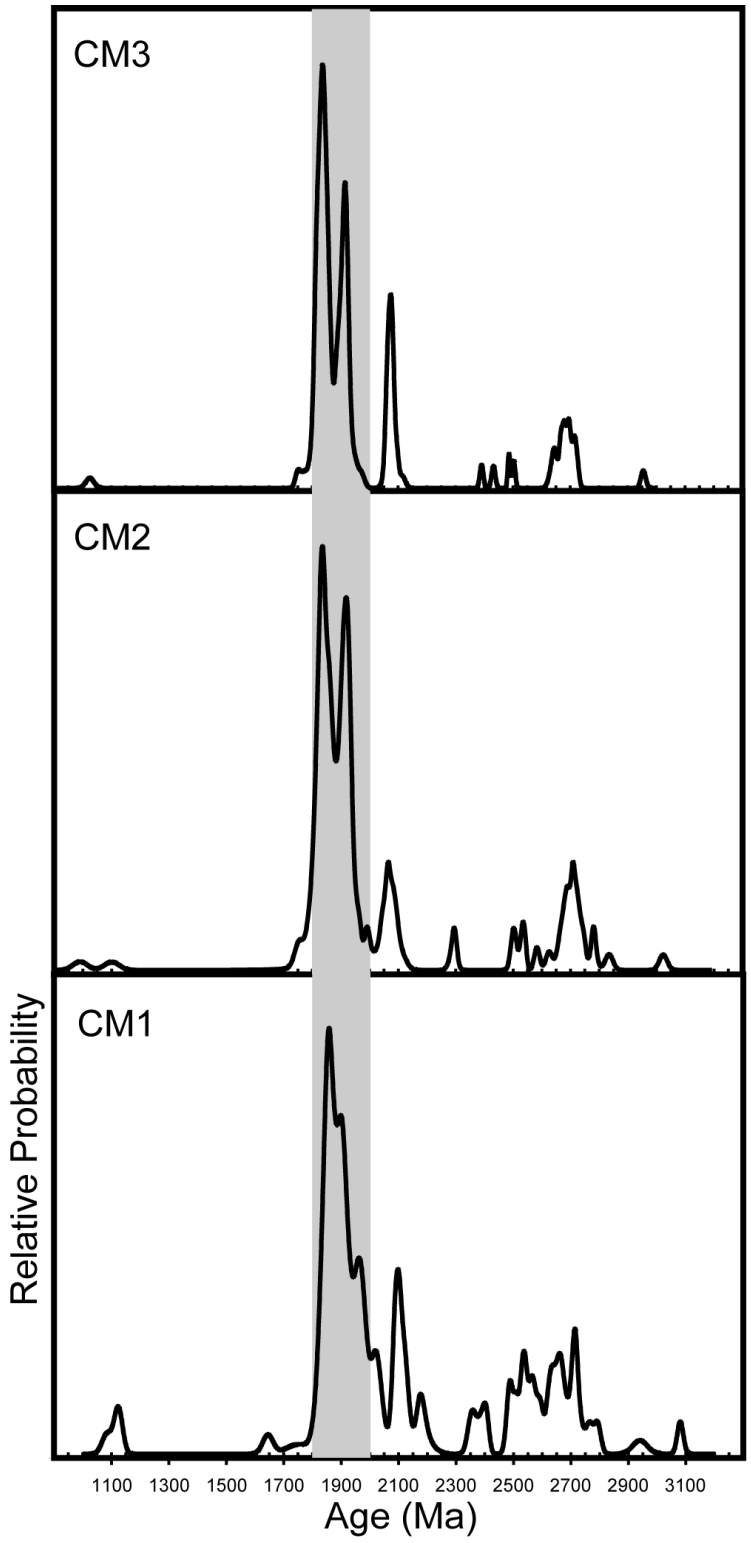

Figure 25: Stacked Relative Probability Plots from Clayton Mine. Plots are stacked in stratigraphic order (oldest to youngest).

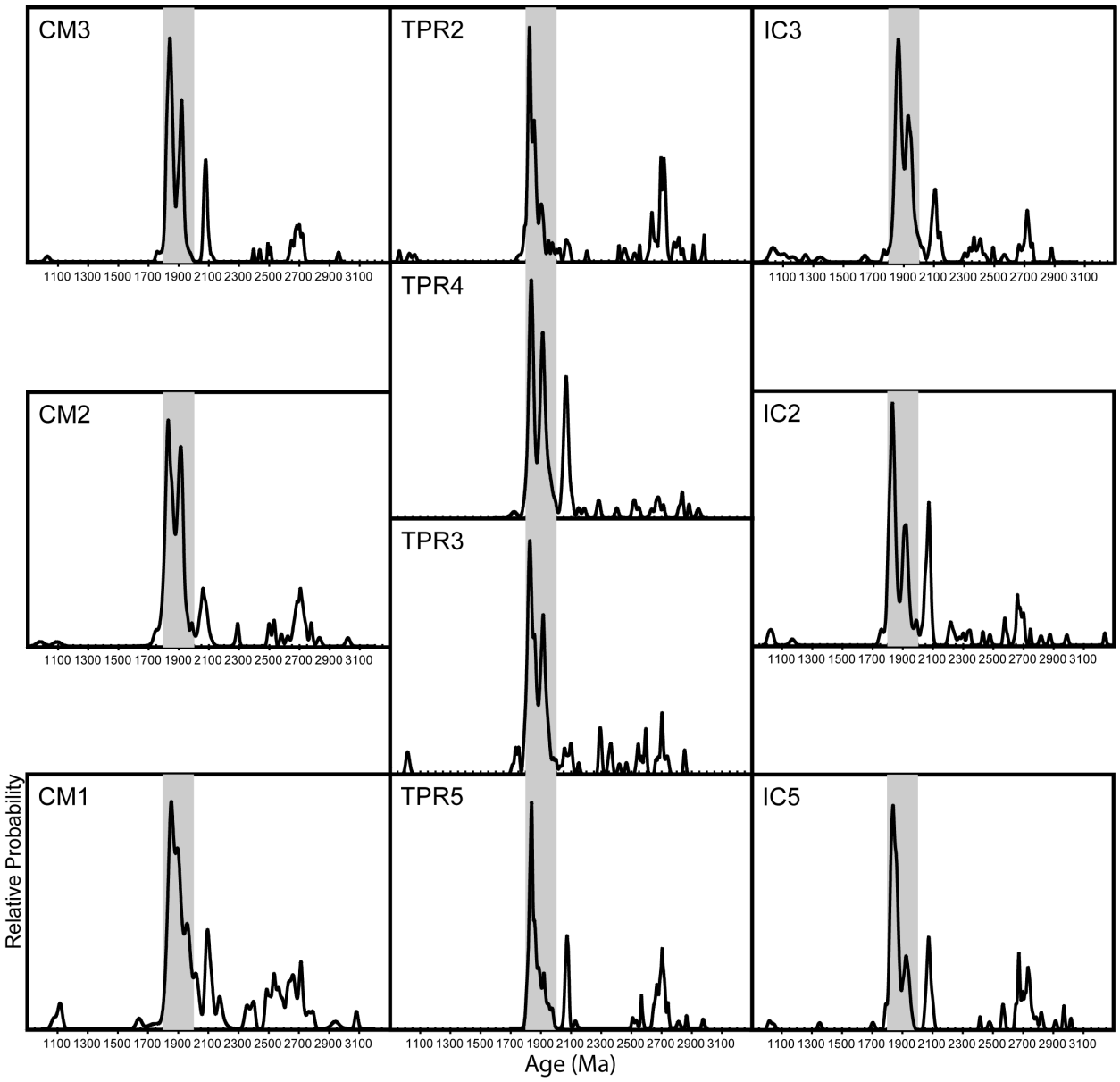

Figure 26: Stacked relative probability plots for all samples of Kinnikinic Quartzite (excluding sample IG due to stratigraphic uncertainty). Plots are arranged in stratigraphic order (oldest to youngest).

Provenance Change and Sequence Stratigraphy

Long-term sea-level fluctuations offer the most convincing explanation for changes in detrital zircon populations.. Long-term sea level rises and falls can cover and uncover substantial source areas, causing dramatic changes in sediment supply. These long-term sea level changes are best characterized by sequence stratigraphic systems tracts (Figure 2). During a Lowstand Systems Tract (LST) when there is a prolonged sea level low, the previously constructed siliciclastic shelf, deposited during the Transgressive Systems Tract (TST) and Highstand Systems Tract (HST), will be subaerially exposed and incised valley erosion will supply a local source of sediment. Large portions of basement #1 (Figure 2) and basement #2 (Figure 2) rocks will also be subaerially exposed and eroded, supplying much of the sediment for coastal plains, deltas, or lowstand fans. During the a relative sea level rise of the subsequent TST, the underlying shelf and basement #1 rocks will be covered by sediment predominantly derived from the rocks of basement #2 farther inland. This does not necessarily mean that the nearby basement rocks will be completely unavailable to contribute sediment, but their spatial extent may be considerably reduced. As sea level begins to fall during the HST or Falling Stage Systems Tract (FSST), sediment from basement #2 rocks and recycled shelf deposits will provide the majority of the sediment prograding HST and FSST units. Since the Kinnikinic Quartzite of east-central Idaho was generally devoid of sedimentary structures, the establishment of a detailed sequence stratigraphic framework was difficult. Instead a generalized sequence stratigraphic framework is established.

Potential Sources and Provenance

Although previous provenance studies have attributed detrital zircon age populations of the Ordovician quartzarenites to the Peace River Arch (PRA) (Gehrels, 2000; Gehrels et al., 1995; Gehrels and Dickinson, 1995), the model presents two main quandaries:

1. The long-distance transport model does not allow sediment input of weathered igneous and metamorphic provinces with similar age distributions elsewhere along the Cordillera to be significant and local contributors of sediment. Many such provinces may have been subaerially exposed and subject to intense weathering and erosion by equatorial conditions (Sloss, 1954; Armstrong, 1975; Ruppel, 1984; Thomas, 2007).
2. The LDT model also does not allow sediment input from the recycling of underlying, local, or remote sediments; which also may have been subaerially exposed and subject to intense equatorial weathering and erosion.

The purpose of this research is to investigate other igneous, metamorphic, and sedimentary provinces with similar age distributions for the Kinnikinic Quartzite. Each major population of Kinnikinic Quartzite detrital zircons is grouped and its possible provenance will be discussed below; the percentage of each population with respect to the total number of detrital zircon grains from all samples is included.

Previous provenance studies of the Ordovician quartzites have all suggested the PRA is the source of sediment for these widespread units. The PRA is a tectonic arch in northern British Columbian and Alberta, composed of Precambrian basement rocks as well as Precambrian – Early Paleozoic sedimentary rocks (O'Connell et al., 1990). A general range of ages of the

Precambrian basement rocks of the PRA is 1.9-2.32 Ga (Ross, 1990). As seen by the relative probability plots and histograms, the range of detrital zircon ages from the Kinnikinic Quartzite is much broader than 1.9-2.32 Ga and several ages within this range are only minor populations. Additionally, sediment transport from the PRA into directly adjacent siliciclastic units was very restricted in direction and spatial extent. Middle Ordovician siliciclastic units adjacent to the PRA thin drastically to the south and Late Ordovician siliciclastic deposition was restricted to the west and northwest, making sediment transport from the PRA long distances to the south unlikely (Norford, 1990). The unlikely hood of sediment being transported south is supported by previous detrital zircon studies of the Kinnikinic Quartzite's lateral equivalents (e.g. Eureka Quartzite), which indicate detrital zircon signatures of Ordovician strata in northern British Columbia are very similar to that of Cambrian strata; however, farther south from southern British Columbia to northwestern Mexico, the detrital zircon signatures of Ordovician and Cambrian strata become very dissimilar (Gehrels, 2000). The dissimilarity of detrital zircon populations between Ordovician and Cambrian strata away from the PRA indicates that the recycling of Cambrian siliciclastics from the PRA into the Kinnikinic Quartzite of east-central Idaho is very unlikely.

Aside from the PRA, described above, several other possible source regions for the Kinnikinic Quartzite occur nearby. Some of these include: the underlying Precambrian quartzites such as the Mesoproterozoic Belt Supergroup and lateral equivalents, the nearby Paleoproterozoic-Archean basement rocks of the Wyoming province, and the Paleoproterozoic Trans-Hudson Arch and Archean Saskatchewan craton that would have been exposed along the Transcontinental Arch during the Ordovician. While these three major source regions may not account for all of the detrital zircon ages contained in the Kinnikinic Quartzite, they cover a wide

spectrum of ages and offer an alternative to a solely PRA source. The possibility that these and other source regions provided sediment to the Kinnikinic Quartzite is addressed below.

~900-1300 Ma (~2% of total): This is a small, but significant population (31grains) of grains within the Kinnikinic Quartzite. Of all of the age populations, this is perhaps the most intriguing due to a lack of recognized magmatic activity along the western North American Cordilleran during this time. These "Grenville" age grains may be recycled grains that were originally transported from the Grenville province of eastern Laurentia to the Cordilleran margin during the Middle to Late Proterozoic by extensive river systems (Rainbird et al., 1992, 1997). It is also possible that "Grenville" age magmatic activity along the Cordilleran margin included rocks which may have been accessible during the Ordovician (Ross, 1991; Cook et al., 1992). Previous provenance studies (Gehrels and Ross, 1998; Smith and Gehrels, 1994; Gehrels and Ross, 1995; Gehrels et al, 1995, 1999) have attributed ~1030 and ~1050 Ma grains to plutons along the Cordilleran margin that coincide to the orogenic activity recognized by Cook et al. (1992). But, the spread of ages which are designated as "Grenville" is much greater than ~1030 and ~1050 Ma (~964-1360 Ma). Thus, it is suggested that grains of these ages may be tied to both transport by large river systems across the continent and recycled and/or possible orogenic activity along the Cordilleran margin.

~1600-1800 Ma (~2% of Total): This population is most likely a result of the recycling of regional, possibly underlying, Mesoproterozoic Belt Supergroup quartzites. A sample from the underlying Mesoproterozoic Wilbert Formation (ICWF) contained a large number of detrital zircon grains of this population, suggesting the Precambrian Wilbert Formation or other

Precambrian quartzites are possible minor contributors. These other Precambrian quartzites are most likely members of the Mesoproterozoic Belt Super Group (BSG). Previous detrital zircon studies of the BSG have reported abundant ages of ~1600-1800 Ma (Lewis et al., 2007; Link et al., 2007; Ross and Villeneuve, 2003). Approximately 1600-1800 Ma grains are most common in the Revett, Wallace, Garnet Range and Pritchard formations (Ross and Villeneuve, 2003; Link et al., 2007). The suspected BSG equivalent Swauger Formation, which underlies the Kinnikinic Quartzite at Twin Peaks Ranch, and the probable post-BSG Yellowjacket Formation also contain ~1600-1800 Ma grains (Link et al., 2007) and may also have been available to contribute sediment. The samples from the Kinnikinic Quartzite contained relatively few grains of this population, suggesting that the source of this population, if recycled sediments, predominantly contained ~1700-1800 Ma grains with relatively few ~1600-1700 Ma grains, which would include the Niehart, Mount Nelson, Mount Shields, and Bonner Formations (Ross and Villeneuve, 2003). An alternative to the recycling of Precambrian sediments is the Trans-Hudson arch, which beyond its general ~1.8-2.0 Ga igneous activity also has reported ages of 1.79-1.76 Ga (Bickford et al., 1990; Chiarenzelli et al., 1998). The rarity and narrow age of this population within the Trans-Hudson Arch and the Kinnikinic Quartzite makes correlation between the two probable.

~ 1800-2000 Ma (~61% of total): This subset occurs in all Kinnikinic Quartzite samples and is the largest population in each sample. Due to the prominence of this population, it is exceptionally important that its source rocks are identified. This population is suspected to have derived from the Trans-Hudson Orogen (THO), because it was likely exposed during the Ordovician (Witzke, 1980). In general, igneous activity of the THO occurred approximately

from 2000-1800 Ma (Bickford et al., 1990; Gordon et al., 1990; Ansdell et al., 1995; Ansdell et al., 1999; Chiarenzelli et al., 1998; Hollings and Ansdell, 2002); however, specific ages have been reported throughout the literature, which are reflected in the detrital zircon age populations of the Kinnikinic Quartzite. An incomplete list of these rocks include: ~1810-1860 Ma plutons (Bickford et al., 1990; Gordon et al., 1990; Meyer et al., 1992; David et al., 1996; Hollings and Ansdell, 2002), and ~1830-1920 Ma volcanics (Bickford et al., 1990; Chiarenzelli et al., 1998; Ansdell et al., 1999). The Wyoming province may include rocks of this age population, ~1885-1975 Ma, but they are relatively few (Redden et al., 1990).

~2000-2200 Ma (~13% of total): This population, while generally small in most samples, is persistent peak in most samples (Figures 23, 24 and 25). This population is hypothesized to have originated from the interior of the continent and is most likely derived from Paleoproterozoic - Archean provinces amalgamated by the THO. These provinces include the Hearne, Rae and Wyoming provinces. The Hearne province contains rocks ~2075 Ma in age (Ansdell et al., 2000), whereas the Rea province contains rocks ~2.0-2.1 Ga in age (Bickford et al., 1990). While the Wyoming province includes predominantly much older rocks (~2.5+ Ga), it does contain a few rocks ~2010-2095 Ma in age (Premo and Van Schmus, 1989; Snyder et al., 1995; Cox et al., 2000).

~2200-2400 Ma (~2% of total): It appears that the post-Archean history of the western North American craton was relatively free from ~2.1-2.4 Ga magmatic and volcanic activity (O'Neill and Lopez, 1985; Dahl et al., 1999; Mueller et al., 2002, 2004, 2005; Mueller and Frost, 2006).

A leucogranite with a Sm-Nd whole rock age of ~2.3 Ga was identified near the THO-Wyoming province suture zone (Sims et al., 1990).

~2400-3400+ Ma (~19% of total): This age population is most likely derived from the Wyoming and Saskatchewan cratons. The position of the Wyoming craton, directly adjacent to Paleozoic passive margin rocks, makes it the much more probable sediment contributor to the Kinnikinic Quartzite. It is also likely because it contains rocks of ages that span the entire population since ~2400-3500 Ma igneous and metamorphic rocks measured via U-Pb geochronology occur throughout this craton (see Chamberlain et al., 2003). The Saskatchewan craton (northern Manitoba) contains ~2400-3100 Ma rocks and was uplifted by the THO and was likely available for erosion during the Ordovician (Chiarenzelli et al., 1998; Bickford et al., 2005). While the Wyoming and Saskatchewan cratons both contain similar age rocks, the much larger extent of the Wyoming craton and its more proximal location makes it the more likely source area.

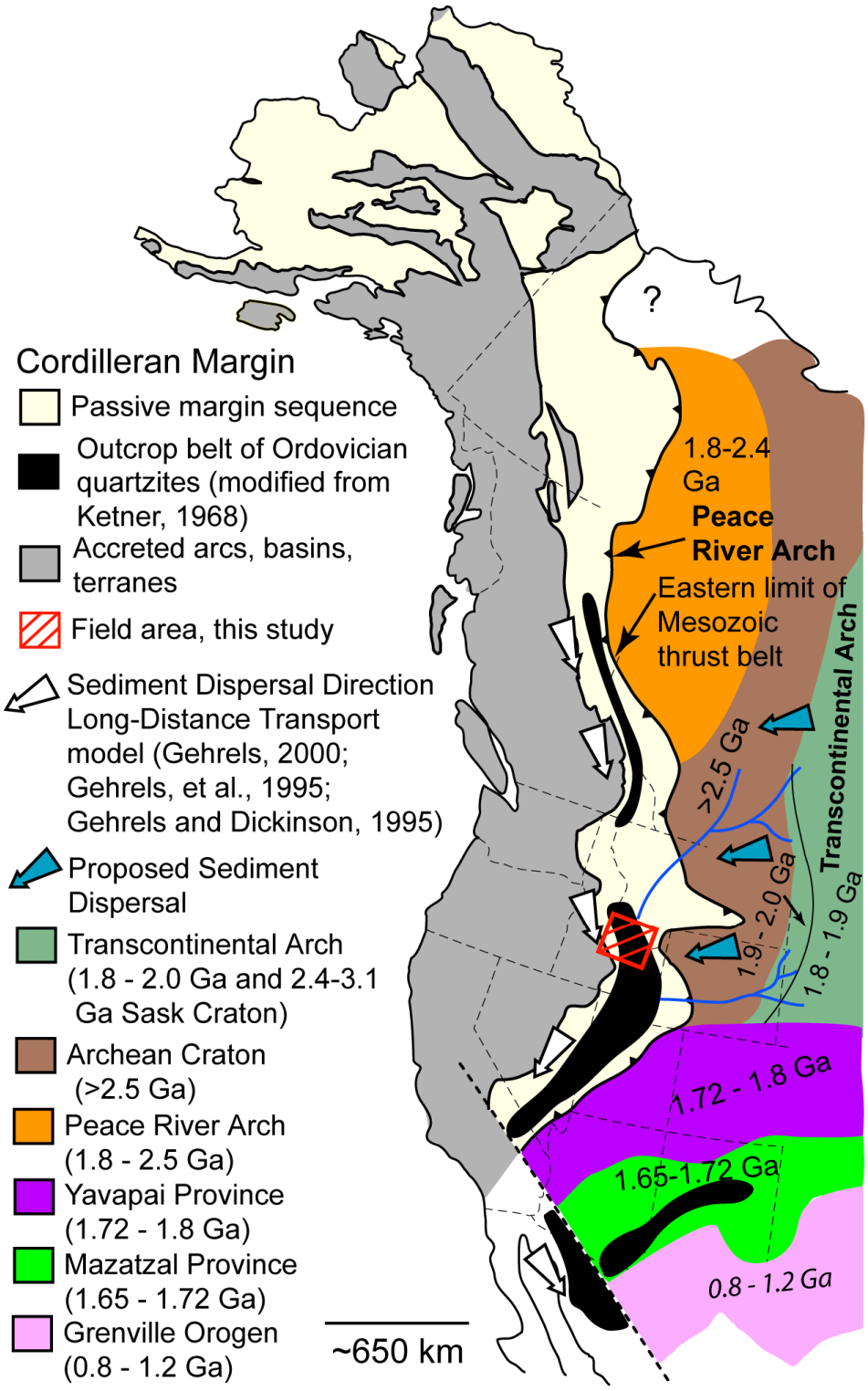

Figure 27: Generalized geologic map of the western North American Cordillera showing major age provinces, spatial extent of Ordovician Siliciclastics, field area of this study, and proposed sediment transport direction.

Sea Level

As previously stated, long-term changes in sea level are able to cover and uncover large areas of source rocks. If this is accurate then a detrital zircon sample from the LST of the Kinnikinic Quartzite would have a wide spread of ages, including: recycled underlying Belt Supergroup derived sediment (~1.6-1.8 Ga), Paleoproterozoic and Archean cratons (~2.0- 3.4+ Ga) and the Trans Hudson Arch (~1.8-2.0 Ga and Saskatchewan craton ~2.4-3.1 Ga). A sample from the TST also may have a wide range of ages, but local sources would likely be absent or their abundances decreased because they would be covered by the rising sea level. These ages would include Paleoproterozoic and Archean cratons (~2.0- 3.4+ Ga) and the THA (~1.8-2.0 Ga and ~2.4-3.1 Ga). A sample from the HST or FSST would have a similar age range to the TST, but perhaps an enhanced THA (~1.8-2.0 Ga) component due to the recycling of THA sediment from the previously constructed siliciclastic shelf (along with Paleoproterozoic and Archean craton sediment) and the introduction of new THA sediment.

Detrital zircon samples from the Kinnikinic Quartzite may show this progression of changing provenance with systems tracts. The basal samples, which have a fairly broad spread of ages, include a substantial population from Paleoproterozoic and Archean cratons (~2.0- 3.4+ Ga), correspond with a LST or TST sequence stratigraphic position. The up-section decrease of the ~2.0- 3.4+ Ga population in the middle samples and the upper samples from Clayton Mine and Italian Canyon, may be a response to a relative sea level rise. The upper sample from Twin Peaks Ranch, which resembles the basal samples, has a substantial ~2.0- 3.4+ Ga population. This resurgence of the ~2.0- 3.4+ Ga population may indicate sea level lowering and recycling of the previously constructed siliciclastic shelf late in the HST. This model works well for the

change in the ~2.0- 3.4+ Ga population, but does not fully address the change in the ~1.9-1.95 Ga population.

It is proposed that sediment was transported from the THA across the Wyoming province to the passive margin via extensive river systems during the Ordovician (Figure 27). The cause for change in the ~1.9-1.95 Ga population may be attributed to changing drainage patterns from the THA during the sea level rise of the TST to include this population. Another cause for the increase in ~1.9-1.95 Ga grains could be a multiple source model. A relative sea level rise directly east of the Kinnikinic Quartzite may denote a relative sea level lowering to the north. Thus, during a TST the Paleoproterozoic and Archean sources directly to the east and northeast would have been covered and the PRA to the north and east partiallyuncovered and supplying an increasing number of ~1.9-1.95 Ga grains.

Overlap and Similarity

Another way of objectively comparing detrital zircon populations is to measure the degree of overlap and the similarity of ages (Gehrels, 2000). Overlap is the degree to which grain ages overlap between samples, in which a value of 1.0 indicates a perfect match of ages and 0.0 indicates that no ages match (Gehrels, 2000). Similarity measures whether the proportions of overlapping ages are similar, in which a value of 1.0 indicates signatures that have similar proportions of perfectly overlapping ages and 0.0 indicates signatures do not overlap or have very different proportions of overlapping ages (Gehrels, 2000). For this study overlap and similarity were calculated using an Excel program written by George Gehrels that is available from the Arizona LaserChron Center (http://www.geo.arizona.edu/alc/). Measures of overlap and similarity were calculated for each sample of Kinnikinic Quartzite against each other and

against a composite reference set of detrital zircon data for the Ordovician miogeocline (Table 3) (Monkman, Mount Wilson, Eureka, and Lopez Quartzites; Gehrels, personal communication). Values were also calculated for each sample of Kinnikinic Quartzite plotted against individual samples of the Ordovician miogeocline (Monkman, Mount Wilson, Eureka, and Lopez Quartzites).

Overlap values for the Kinnikinic Quartzite samples plotted against each other (ex. IC3 vs. IC2, IC3 vs. TPR2) show the ages generally overlap, but some variance is evident (Table 3). The average overlap is 0.665, but ranges from a high value of 0.743 (CM1 vs. CM2) and low value of 0.514 (IC3 vs.TPR5). Similarity values for the Kinnikinic Quartzite samples plotted against each other show overall proportions of overlapping age are similar, but as with overlap there is some variance. The average similarity value is 0.823, and ranges from 0.879 to 0.754.

Overlap values of individual samples of Kinnikinic Quartzite plotted against miogeoclinal data generally show less overlap than for the Kinnikinic Quartzite plotted against itself. The average overlap value is 0.599, with a range of 0.750 to 0.446. Similarity values show that proportions of overlapping ages are relatively similar. The average similarity value is 0.847, with a range of 0.898 to 0.811.

Overlap and similarity values were also calculated for each Kinnikinic Quartzite sample plotted against individual samples from the Ordovician miogeocline data (Mount Wilson, Monkman, Eureka, and Lopez Quartzites; Gehrels, personal communication). Overlap values for the Kinnikinic Quartzite plotted against the individual samples the Ordovician miogeocline data are as follows: the Mount Wilson Quartzite averaged 0.719, with a range of 0.837 to 0.577; the Monkman Quartzite averaged 0.725, with a range of 0.840 to 0.597; the Eureka Quartzite averaged 0.638, with a range of 0.79 to 0.474; and the Lopez Quartzite averaged 0.661, with a

range of 0.799 to 0.554. Similarity values for the Kinnikinic Quartzite plotted against the individual samples the Ordovician miogeocline data are as follows: the Mount Wilson Quartzite averaged 0.842, with a range of 0.897 to 0.795; the Monkman Quartzite averaged 0.822, with a range of 0.867 to 0.752; the Eureka Quartzite averaged 0.843, with a range of 0.890 to 0.779; and the Lopez Quartzite averaged 0.773, with a range of 0.839 to 0.719. Overlap values show that the Kinnikinic Quartzite's age populations overlap the most with the Monkman Quartzite to the north, but overlap the least with the Eureka Quartzite to the south; however, similarity values show that the Kinnikinic Quartzite's age populations are most similar to the Mount Wilson Quartzite, and least similar to the Lopez Quartzite.

The overlap and similarity values presented in Table 3 illustrate the regional and continental-scale variability in provenance of the Ordovician quartzites. The values offer further evidence that the provenance of the Ordovician quartzites is heterogeneous at broad-scale, and varies spatially and temporally at a local-scale.

Overlap	IC3									
IC2	0.651	IC2								
IC5	0.572	0.635	IC5							
TPR2	0.647	0.716	0.736	TPR2						
TPR4	0.641	0.634	0.647	0.696	TPR4					
TPR3	0.697	0.708	0.643	0.716	0.739	TPR3				
TPR5	0.514	0.599	0.662	0.680	0.710	0.631	TPR5			
CM3	0.610	0.627	0.662	0.691	0.692	0.663	0.716	CM3		
CM2	0.718	0.631	0.627	0.715	0.672	0.705	0.598	0.590	CM2	
CM1	0.666	0.646	0.673	0.714	0.714	0.688	0.602	0.594	0.743	CM1
IG	0.646	0.703	0.635	0.721	0.667	0.709	0.632	0.650	0.725	0.670

Similarity	IC3									
IC2	0.844	IC2								
IC5	0.808	0.825	IC5							
TPR2	0.778	0.766	0.843	TPR2						
TPR4	0.859	0.845	0.825	0.754	TPR4					
TPR3	0.851	0.824	0.795	0.776	0.830	TPR3				
TPR5	0.804	0.809	0.879	0.837	0.834	0.791	TPR5			
CM3	0.865	0.846	0.863	0.805	0.870	0.813	0.874	CM3		
CM2	0.865	0.834	0.840	0.829	0.870	0.875	0.847	0.867	CM2	
CM1	0.813	0.778	0.766	0.762	0.800	0.788	0.762	0.769	0.830	CM1
IG	0.826	0.834	0.793	0.800	0.831	0.846	0.802	0.845	0.872	0.795

Overlap	Mt.Wil.	Monk.	Eureka	Lopez
IC3	0.720	0.728	0.669	0.599
IC2	0.725	0.769	0.651	0.573
IC5	0.636	0.632	0.564	0.677
TPR2	0.726	0.730	0.635	0.675
TPR4	0.732	0.740	0.630	0.741
TPR3	0.760	0.840	0.654	0.621
TPR5	0.588	0.597	0.474	0.608
CM3	0.577	0.678	0.491	0.554
CM2	0.837	0.736	0.724	0.706
CM1	0.822	0.787	0.774	0.799
IG	0.680	0.684	0.607	0.601
AllOk	0.831	0.781	0.790	0.780

Similarity	Mt.Wil.	Monk.	Eureka	Lopez
IC3	0.859	0.856	0.849	0.719
IC2	0.850	0.842	0.826	0.719
IC5	0.807	0.752	0.794	0.832
TPR2	0.801	0.754	0.807	0.839
TPR4	0.843	0.834	0.837	0.721
TPR3	0.868	0.852	0.855	0.739
TPR5	0.795	0.759	0.779	0.801
CM3	0.814	0.798	0.803	0.760
CM2	0.890	0.862	0.890	0.803
CM1	0.853	0.860	0.857	0.758
IG	0.828	0.831	0.818	0.747
AllOk	0.897	0.867	0.889	0.833

Overlap	OrdMio
IC3	0.655
IC2	0.615
IC5	0.576
TPR2	0.608
TPR4	0.594
TPR3	0.591
TPR5	0.446
CM3	0.459
CM2	0.707
CM1	0.750
IG	0.583
All Ok	0.827

Similarity	OrdMio
IC3	0.857
IC2	0.846
IC5	0.830
TPR2	0.840
TPR4	0.841
TPR3	0.862
TPR5	0.811
CM3	0.818
CM2	0.898
CM1	0.877
IG	0.840
All Ok	0.914

Table 3: Overlap and similarity values of detrital zircon data from the Kinnikinic Quartzite compared to the ~400 grains from samples of Ordovician Miogeocline (Gehrels, personal communication) collected from the four localities of Gehrels et al. (1995). An overlap value of 1 indicates a perfect match of ages and 0 indicates no ages match. A similarity value of 1 indicates signatures have similar proportions of perfectly overlapping ages and 0 indicates signatures do not overlap.

CHA PTER 7

CONCLUSIONS

The results of this research offer new insights into the provenance of the Kinnikinic Quartzite in east-central Idaho. A coarse regional sequence stratigraphy is established that provides a framework to better understand temporal and spatial variations of Kinnikinic Quartzite provenance. The detrital zircon populations of the Kinnikinic Quartzite in east-central Idaho indicate distinct provenance links to sources from the interior of North America, as opposed to the northern margin of the western North American Cordillera as its sole source. The various relative abundances and distributions of these populations from spatially and temporally separated samples provide insight into sediment dispersal along the Ordovician passive margin.

1) The Kinnikinic Quartzite of east-central Idaho is comprised of six sedimentary facies, each with its own distinct characteristics. Each facies represents a specific position on a shallow, gently dipping siliciclastic shelf. The facies (landward to basinward) are the burrowed, massive, cross-stratified, hummocky cross-stratified, laminated, and interbedded shale and quartzite facies. The identification of sedimentary facies is crucial to the construction of a detailed sequence stratigraphic framework. However, the Kinnikinic Quartzite outcrops in east-central Idaho contain few sedimentary structures because of subsequent silica flooding, which made establishment of the detailed sequence stratigraphic framework difficult. Instead a generalized sequence stratigraphic framework was established.

2) U-Pb geochronology of 1439 individual detrital zircon grains from eleven samples of Kinnikinic Quartzite reveals a distinct spectrum of ages. This age spectrum has direct

provenance links to sources east of the Paleozoic passive margin, rather than to the north as indicated by the long-distance transport model (LDT) (Gehrels, 2000; Gehrels et al, 1995; Gehrels and Dickinson, 1995). Major contributors of sediment to the Kinnikinic Quartzite of east-central Idaho are the Trans-Hudson Arch, adjacent Paleoproterozoic-Archean provinces (Wyoming, Hearne, Rea and Saskatchewan), and recycled underlying sediments (Mesoproterozoic Belt Supergroup and lateral equivalents). An alternative to the LDT model is that sediment was transported from the interior of North America and transported via extensive river systems off the Trans-Hudson Arch and across the Wyoming craton.

3) Detrital zircon populations of all Kinnikinic Quartzite samples are similar; however, considerable variability of populations occurs within the unit. This variability indicates that sediment provenance was not homogeneous. Slight, yet significant, changes in provenance occur spatially (between measured section locations) and temporally (vertically or stratigraphically through measured sections). These changes in provenance occur within a small area, indicating dynamic sediment dispersal changes along the Ordovician passive margin. While these changes may be subtle, their implications are significant. Slight changes in peak height indicate changes in sediment influx from source regions, and changes in peak widths indicate changes in source regions.

4) Changes in provenance, major and minor, are a product of prolonged sea level fluctuations producing characteristic systems tracts. Systems tracts are capable of covering (TST, HST), or uncovering (LST, FSST) broad areas of potential source rocks. During the LST and TST a steady flux of sediment was derived from the THA (THO and Saskatchewan craton), but during

the TST sediment influx from local basement rocks (Wyoming, Hearne, and Rea provinces; and underlying sediments) decreased.

5) The sampling strategy used in this study provides insight into spatial and temporal provenance variations; however, it is suggested that a detailed sequence stratigraphic framework be in place before samples for detrital zircons are collected. Samples taken from a known sequence stratigraphic position would provide a better understanding of how sediment provenance changes during prolonged sea level fluctuations.

REFERENCES

Anderson, T., 2005, Detrital Zircons as Tracers of Sedimentary Provenance: Limiting Conditions from Statistics and Numerical Simulation: Chemical Geology 216, p. 249-270.

Ansdell, K.M., MacNeil, A., Delaney, G.D., and Hamilton, M.A., 2000, Rifting and development of the Hearne craton passive margin: Age constraint from the Cook Lake area, Wollaston domain, Trans-Hudson orogen, Saskatchewan: Geological Society of Canada Conference Abstracts, v. 25.

Ansdell, K.M., Connors, K.A., Stern, R.A., and Lucas, S.B., 1999, Coeval sedimentation, magmatism, and fold-thrust belt development in the Trans-Hudson Orogen: geochronological evidence from the Wekusko Lake area, Manitoba, Canada: Canadian Journal of Earth Sciences, v. 36, p. 293-312.

Ansdell, K.M., Lucas, S.B., Connors, K.A., and Stern K.A., 1995, Kisseynew metasedimentary gneiss belt, Trans-Hudson orogen (Canada); back-arc origin and collisional inversion: Geology, v. 23, p. 1039-1043.

Armstrong, R.L., 1975, Precambrian (1500 million years old) rocks of central Idaho – the Salmon River arch and its role in Cordilleran sedimentation and tectonics: American Journal of Science, v. 275-A, p.437-467.

Beus, S.S., 1968, Paleozoic Stratigraphy of Samaria Mountain, Idaho-Utah: American Association of Petroleum Geologists Bulletin, v. 52, no. 5, p. 782-808.

Bickford, M.E., Mock, T.D., Collerson, K.D., Lewry, J.F., Steinhart III, W.E., 2005, Origin of the Archean Saskatchewan craton and its extent within the Trans-Hudson orogen: evidence from Pb and Nd isotopic compositions of basement rocks and post-orogenic intrusions: Canadian Journal of Earth Sciences, v. 42, n. 4, p. 659-684.

Bickford, M.E., Collerson, K.D., Lewry, J.F., Van Schmus, W.R., and Chiarenzelli, J.R., 1990, Proterozoic collisional tectonism in the Trans-Hudson orogen, Saskatchewan: Geology, v. 18, p. 14-18.

Biek, R.F., 1999, Geology of the Clarkston Mountain (Southern Malad Range) Box Elder and Cache Counties, Utah: Utah Geological Association Publication 27, p. 27-43.

Chamberlain, K.R., Frost, C.D., and Frost, B.R., 2003, Early Archean to Mesoproterozoic evolution of the Wyoming Province: Archean origins to modern lithospheric architecture: Canadian Journal of Earth Science, v. 40, p. 1357-1374.

Chang, Z., Vervoort, J.D., McClelland, W.C., and Knaack, C., 2006, LA-ICP-MS U-Pb Dating of zircon: Geochemistry, Geophysics, Geosystems.

Chiarenzelli, J., Aspler, L., Villeneuve, M., and Lewry, J., 1998, Early Proterozoic Evolution of the Saskatchewan Craton and its Allochthonous Cover, Trans-Hudson Orogen: Journal of Geology, v. 106, p. 247-267.

Cook, F.A., Dredge, M., and Clark, E.A., 1992, The Proterozoic Fort Simpson structural trend in northwestern Canada: Geological Society of America Bulletin, v. 104, p. 1121-1137.

Cox, D.M., Frost, C.D., and Chamberlain, K.R., 2000, 2.01 Ga Kennedy dike swarm, southeastern Wyoming: record of a rifted margin along the southern Wyoming province: Rocky Mountain Geology, v. 35, p.7-30.

Dahl, P.S., Holm, D.K., Gardner, E.T., Hubacher, F.A., and Foland, K.A., 1999, New constraints on the timing of Early Proterozoic tectonism in the Black Hills (South Dakota), with implications for docking of the Wyoming province with Laurentia: Geological Society of America Bulletin, v. 111, p. 1335-1349.

David, J., Bailes, A.H., and Machado, N, 1996, Evolution of the Snow Lake portion of the Paleoproterozoic Flin Flon and Kisseynew belts, Trans-Hudson Orogen, Manitoba, Canada: Precambrian Research, v. 80, p. 107-124.

Dalziel, I.W.D., 1991, Pacific margins of Laurentia and East-Antarctic-Australia as a conjugate pair; evidence and implications for an Eocambrian supercontinent: Geology, v. 19, p. 598-601.

DeGraff-Surpless, K., Graham, S.A., Wooden, J.L., and McWilliams, M.O., 2002, Detrital zircon provenance of the Great Valley Group, California: Evolution of an arc-forearc system: Geological Society of America Bulletin, v. 114, p. 1564-1580.

DeGraff-Surpless, K., Mahoney, J.B., Wooden, J.L., and McWilliams, M.O., 2003, Lithofacies control in detrital zircon provenance studies: Insights from the Cretaceous Methow basin, southern Canadian Cordillera: Geological Society of America Bulletin, v. 115, n. 8, p. 899-915.

Evans, K.V., and Zartman, R.E., 1988, Early Paleozoic Alkalic Plutonism in East-Central Idaho: Geological Society of America Bulletin, v. 100, p. 1981-1987.

Fedo, C.M., Sircombe, K.N., and Rainbird, R.H., 2003, Detrital zircon analysis of the sedimentary record: in Hanchar, J.M., and Hoskin, P.W.O., eds., Zircon, Reviews in Mineralogy and Geochemistry, v. 53, p. 277-303.

Fedo, C.M., and Cooper, J.D., 2001, Sedimentology and Sequence Stratigraphy of Neoproterozoic and Cambrian units across a craton –margin hinge zone, southeastern California, and implications for the early evolution of the Cordilleran margin: Sedimentary Geology 141-142, p. 501-522.

Fedo, C.M., and Cooper, J.D., 1990, Braided fluvial to marine transition: the basal Lower Cambrian Wood Canyon Formation, southern Marble Mountains, Mojave Desert, California: Journal of Sedimentary Petrology, v. 60, p. 220-234.

Gehrels, G.E., 2000, Introduction to detrital zircon studies of Paleozoic and Triassic strata in western Nevada and northern California. In Soregham, M.J., and Howell, D.G., eds., Paleozoic and Triassic paleogeography and tectonics of western Nevada and northern California: Geological Society of America Special Paper 347.

Gehrels , G.E., Dickinson, W. R., Ross, G.M., Stewart, J.H., and Howell, D.G., 1995, Detrital zircon reference for Cambrian to Triassic miogeoclinal strata of western North America: Geology: v.23, p. 831-834.

Gehrels, G.E., and Dickinson, W. R., 1995, Detrital Zircon Provenance of Cambrian to Triassic Miogeoclinal and Eugeoclinal Strata in Nevada: American Journal of Science, v. 295, p. 18-48.

Gehrels, G.E., and Ross, G.M., 1998, Detrital Zircon Geochronology of Neoproterozoic to Permian Miogeoclinal Strata in British Columbia and Alberta: Canadian Journal of Earth Sciences, 35:1380-1401.

Gordon, T.M., Hunt, P.A., Bailes, A.H., and Syme, E.C., 1990, U-Pb ages from the Flin Flon and Kisseynew belts, Manitoba: Chronology of crust formation at an Early Proterozoic accretionary margin: in Lewry, J.F., and Stauffer, M.R., eds., The Early Proterozoic Trans-Hudson orogen of North America: Geological Association of Canada Special Paper 37, p. 177-199.

Hall, C.D., 1989, Storm bedding in the Middle Ordovician Kinnikinic Quartzite, Beaverhead Range, east central Idaho: Geological Society of America Abstracts with Programs, v. 69, p. 414-433.

Hajnal, Z., Ansdell, K.M., and Ashton, K.N., 2005, Introduction to special issue of Canadian Journal of Earth Sciences: The Trans-Hudson Orogen Transect of Lithoprobe: Canadian Journal of Earth Sciences, v. 42, p. 379-383.

Hobbs, S.W., Hays, W.H., and Ross, R.J., Jr., 1968, the Kinnikinic Quartzite of central Idaho – redefinition and subdivision: U.S. Geological Survey Bulletin 1254-J, p. 22.

Hoffman, P.F., 1988, United Plates of America, the Birth of a craton: Early Proterozoic assembly and growth of Laurentia: Annual Review of Earth and Planetary Sciences, v. 16, p. 543-603.

Hoffman, P.F., 1989, Precambrian geology and tectonic history of North America: in Bally, A.W., and Palmer, A.R., eds., The geology of North America-An overview, Geological Society of America, Geology of America, v. A, p. 447-512.

Hollings, P., and Ansdell, K., 2002, Paleoproterozoic arc magmatism imposed on an older backarc basin: Implications for the tectonic evolution of the Trans-Hudson orogen, Canada: Geological Society of America Bulletin, v. 114, no. 2, p. 153-168.

James, W.C., and Oaks, R.Q., 1977, Petrology of the Kinnikinic Quartzite (Middle Ordovician), east-central Idaho: Journal of Sedimentary Petrology, v. 47, no. 4, p. 1491-1511.

Johnson, C.M., and Winter, B.L., 1999, Provenance Analysis of Lower Paleozoic Cratonic Quartz Arenites of the North American Midcontinent Region: U-Pb and Sm-Nd Isotope Geochemistry: Geological Society of America Bulletin, v. 111, no. 11, p, 1723-1738.

Karlstrom, K.E., Harlan, S.S., Williams, M.L., McLelland, J., Geissman, J.W., and Ahall, K.I., 1999, Refining Rodinia; geologic evidence for the Australia-western U.S. connection in the Proterozoic: GSA Today, v. 9, p. 1-7.

Karlstrom, K.E., and Bowring, S.A., 1988, Early Proterozoic assembly of tectonostratigraphic terranes in southwestern North America: Journal of Geology, v. 96, p. 561-576.

Ketner, K.B., 1968, Origin of Ordovician Quartzite in the Cordilleran Moigeosyncline: United States Geological Survey Professional Paper 600-B, p.B169-B177.

Ketner, K.B., 1966, Comparison of Ordovician Eugeosynclinal and Miogeosynclinal Quartzites of the Cordilleran Geosyncline: U.S. Geol Survey Prof. Paper 550-C, p. C54 – C60.

Lewis, R.S., Vervoort, J.D., Burmester, R.F., McClelland, W.C., and Chang, Z., 2007, Geochronological Constraints on Mesoproterozoic and Neoproterozoic(?) High-Grade Metasedimentary Rocks of North-Central Idaho, U.S.A.: Paleozoic Geology of Western North America and Siberia, SEPM Special Publication no. 86, p. 37-53.

Link, P.K., Fanning, C.M., Lund, K.I., and Alenikoff, J.N., 2007, Detrital-Zircon Populations of Mesoproterozoic Strata of East-Central Idaho, U.S.A.: Correlation with Belt-Supergroup of Southwest Montana: Proterozoic Geology of Western North America and Siberia, SEPM Special Publication no. 86, p. 101-128.

Measures, E.A., 1992, Stratigraphy, carbonate lithologies, and depositional environments of Upper Ordovician Fish Haven Dolomite and Saturday Mountain Formation, east-central and central Idaho, and implications for platform development and margin tectonics: Unpublished Ph.D. Dissertation, University of Idaho, Moscow, Idaho, 535 p.

Meyer, M.T., Bickford, M.E., and Lewry, J.F., 1992, The Wathaman batholith: An Early Proterozoic continental arc in the Trans-Hudson orogenic belt, Canada: Geological Society of America Bulletin, v. 104, p. 1073-1085.

Moecher, D.P., and Samson, S.D., 2006, Differential Zircon Fertility of Source Terranes and Natural Bias in the Detrital Zircon Record: Implications for Sedimentary Provenance Analysis: Earth and Planetary Science Letters 247, p. 252-266.

Moores, E.M., 1991, Southwest U.S.-East Antarctic (SWEAT) connection; a hypothesis: Geology, v. 19, p. 425-428.

Mueller, P.A., and Frost, C.D., 2006, The Wyoming Province: a distinctive Archean craton in Laurentian North America: Canadian Journal of Earth Sciences, v. 43, p. 1391-1397.

Mueller, P.A., Heatherington, A.L., Kelly, D.M., Wooden, J.L., and Mogk, D.W., 2002, Paleoproterozoic crust within the Great Falls tectonic zone: Implications for the assembly of southern Laurentia. Geology, v. 30, p. 127-130.

Mueller, P.A., Burger, H.R., Heatherington, A., Wooden, J, Mogk, D.W., and D'Arcy, K. 2004, Age and Evolution of the Precambrian crust, Tobacco Root Mountains, Montana: in Precambrian geology of the Tobacco Root Mountains, Montana. Edited by J.B. Brady, H.R. Burger, J.T. Cheney, and T.A. Harms: Geological Society of America Special Paper 377, p. 179-201.

Mueller, P.A., Burger, H.R., Wooden, J.L., Brady, J.B., Cheney, J.T., Harms, T.A., Heatherington, A.L., and Mogk, D.W., 2005, Paleoproterozoic metamorphism in the northern Wyoming province: implications for the assembly of Laurentia: Journal of Geology, v. 113, p. 169-179.

Norford, B.S., 1990, Ordovician and Silurian Stratigraphy, paleogeography and depositional history of the Peace River Arch area, Alberta and British Columbia: : in Geology of the Peace River Arch, O'Connell, S.C., and Bell, J.S., eds., Bulletin of Canadian Petroleum Geology, v. 38A.

Oaks, R.Q., and James W.C., 1980, The Kinnikinic Quartzite (Middle Ordovician) in the Type Area, Central Idaho, and a New Reference Section near Arco, Idaho. BYU Geology Studies, v. 27, p. 1-9.

O'Connell, S.C., Dix, G.R., and Barclay, J.E., 1990, The origin, history, and regional structural development of the Peace River Arch, Western Canada: in Geology of the Peace River Arch, O'Connell, S.C., and Bell, J.S., eds., Bulletin of Canadian Petroleum Geology, v. 38A, p. 4-24.

O'Neill, J., and Lopez, D., 1985, Character and regional significance of Great Falls tectonic zone, east-central Idaho and west-central Montana: American Association of Petroleum Geologists Bulletin, v. 69, p. 437-447.

Premo, W.R., and Van Schmus, W.R., 1989, Zircon geochronology of Precambrian rocks in southeastern Wyoming and northern Colorado: in Grambling, J.A., and Tewksbursy, B.J.,

eds., Proterozoic geology of the southern Rocky Mountains: Geological Society of America Special Paper 235, p. 13-48.

Rainbird, R.H., Heaman, L.M., and Young, G.M., 1992, Sampling Laurentia: Detrital zircon geochronology offers evidence for an extensive Neoproterozoic river system originating from the Grenville orogen: Geology, v. 20, p. 351-354.

Rainbird, R.H., McNicoll, V.J., Theriault, R.J., Heaman, L.M., Abbot, J.G., Long, D.G.F., and Thorkelson, D.J., 1997, Pan-continental River System Draining Grenville Orogen Recorded by U-Pb and Sm-Nd Geochronology of Neoproterozoic Quartzarenites and Mudrocks, Northwestern Canada: Geology, v. 105, p. 1-17.

Reading, H.G., ed., 1996, Sedimentary Environments: Processes, Facies and Stratigraphy, 3 ed, Blackwell Science Ltd.

Redden J.A., Peterman, Z.E., Zartman, R.E., and DeWitt, E., 1990, U-Th-Pb geochronology and preliminary interpretations of Precambrian tectonic events in the Black Hills, South Dakota: in Lewry, J.F., and Stauffer, M.R., eds,. The Trans-Hudson orogen: Geological Association of Canada Special Paper 37, p. 229-251.

Ross, C.P., 1937, Geology and ore deposits of the Bayhorse Region, Custer County, Idaho: U.S. Geological Survey Bulletin 877.

Ross, C.P., 1947, Geology of the Borah Peak quadrangle, Idaho: Geological Survey of America Bulletin v. 58, no. 12, p. 1085-1160.

Ross, C.P., 1961, Geology of the southern part of the Lemhi Range, Idaho: U.S. Geological Survey Bulletin 1081-F, p. 189-260.

Ross, G.M., and Bowring, S.A., 1990, Detrital zircon geochronology of the Windermere Supergroup and the tectonic assembly of the southern Canadian Cordillera: Journal of Geology, v. 18, p. 879-893.

Ross, G.M., 1991, Precambrian basement in the Canadian Cordillera: An introduction: Canadian Journal of Earth Sciences, v. 28, p. 1133-1139.

Ross, G.M., Parrish, R.R., and Winston, D., 1992, Provenance and U-Pb geochronology of the Mesoproterozoic Belt Super Group (northwestern United States), implications for the age of deposition and pre-Panthalassa plate reconstructions: Earth and Planetary Science Letters, v. 113, p. 57-76.

Ross, G.M. and Villeneuve, M., 2003, Provenance of the Mesoproterozoic (1.4 Ma) Belt basin (western North America): Another piece in the pre-Rodinia Paleogeographic puzzle: Geological Society of America Bulletin, v. 115, p. 1191-1217.

Ross, R.J., 1959, Brachiopod fauna of the Saturday Mountain Formation, southern Lemhi Range, Idaho: United States Geological Survey Professional Paper 295-L, p. 441-461.

Ross, R.J., 1961, Distribution of Ordovician graptolites in Eugeosynclinal facies in western North America and its paleogeographic implications: American Association of Petroleum Geologists Bulletin, v. 45, p. 330-341.

Runkel, A.C., Miller, J.F., McKay, R.M., Palmer, A.R., and Taylor, J.F. 2007, High-resolution sequence stratigraphy of Lower Paleozoic sheet sandstones in central North America: The role of special conditions of cratonic interiors in development of stratal architecture: Geological Society of America Bulletin, v. 119, p.860-881.

Runkel, A.C., McKay, R.M., and Palmer, A.R., 1998, Origin of a classic cratonic sheet sandstone: Stratigraphy across the Sauk II-Sauk III boundary in the Upper Mississippi Valley: Geological Society of America Bulletin, v. 110, p. 188-210.

Ruppel, E.T., 1986, The Lemhi Arch: A Late Proterozoic and Early Paleozoic Landmass in Central Idaho: In Peterson, J.A., ed., Paleotectonics and sedimentation in the Rocky Mountain region, United States, AAPG Memoir 41, p. 119-130.

Saltzman, M.R., and Young, S.A., 2005, A long-lived glaciation in the Late Ordovician? Isotopic and sequence-stratigraphic evidence from western Laurentia: Geology, v. 113, p. 109-112.

Scholten, R., and Ramspott, L.D., 1968, Tectonic mechanisms indicated by structural framework of central Beaverhead Range, Idaho-Montana: Geological Society of America Special Paper 104, 71 p.

Sears, J., and Price, R.A., 1999, A new look at the Siberian connection; no SWEAT: Geology, v. 28, p. 423-426.

Sims, P.K., Peterman, Z.E. Hildebrand, T.G., and Mahan, S., 1990, Precambrian basement map of the Trans-Hudson orogen and adjacent terranes, northern Great Plains, U.S.A.: U.S. Geological Survey, Stanford, CA.

Sloss, L.L., 1954, Lemhi arch, a mid-Paleozoic positive element in south-central Idaho: Geological Society of America Bulletin, v. 65, p. 365-368.

Sloss, L.L., 1988, Tectonic evolution of the Craton in Phanerozoic time: In Sloss, L.L., ed., Sedimentary Cover, North American Craton; U.S., Geological Society of America, Geology of North America, v. D-2, p. 25-51.

Snyder, G.L., Siems, D.F., Grossman, J.N., Ludwig, K.R., and Nealy, L.D., 1995, Geology, petrochemistry, and geochronology of the Precambrian rock of the Fletcher Park-Johnson Mountain area, Albany and Platt counties, Wyoming with a section on the Fletcher Park

shear zone by B.R. Frost, K.R. Chamberlain, and G.L. Snyder: U.S. Geological Survey, Miscellaneous Investigations Series Map I-2233, 3 sheets, scale 1:24 000.

Sweet, W.C., 2000, Conodonts and biostratigraphy of Upper Ordovician strata along a shelf to basin transect in Central Nevada: Journal of Paleontology, v. 74, p. 1148-1160.

Thomas, R.C., 2007, A field guide to the Cambrian section at Camp Creek, Southwest Montana, in Thomas, R.C., and Gibson, R.I., eds., Introduction to the geology of the Dillon area, Proceedings Volume from the 32nd Annual Field Conference of the Tobacco Root Geological Society: Northwest Geology, v. 36, p. 231-243.

Vermeesch, P., 2004, How Many Grains Are Needed for a Provenance Study?: Earth and Planetary Science Letters, v. 224, p. 441-451.

Webb, G.W., 1958, Middle Ordovician stratigraphy in eastern Nevada and western Utah: American Association of Petroleum Geologists Bulletin, v. 42, no. 40, p. 2335-2377.

Witzke, B.J., 1980, Middle and Upper Ordovician paleogeography of the region bordering the Trans-Continental Arch: in Fouch. T.D., and Magathan, E.R., eds., Paleozoic paleogeography of the west-central United States; Rocky Mountain paleogeography Symposium 1, SEPM, p. 1-18.

Zimmerman, M.K., and Cooper, J.D., 1999, Sequence stratigraphy of the Eureka Quartzite, Southern California and Southern Nevada: Acta Universitatis Carolinae, Geologica, v. 43, p. 147-150.

APPENDIX A
SITE COORDINATES

Location	Latitude (N)	Longitude (W)	UTM Zone	Easting	Northing
Arco Hills (AH)	43° 38' 05"	113° 14' 44"	12 T	318849.7	4833742.9
Clayton Mine (CM)	44° 16' 14"	114° 26' 04"	11 T	704751.3	4905106.8
Elkhorn Creek (EC)	44° 04' 45"	113° 48' 59"	12 T	274504.7	4484510.5
Italian Canyon (IC)	44° 20' 35"	112° 56' 34"	12 T	345140.1	4911778.4
Italian Gulch (IG)	44° 42' 31"	113° 17' 53"	12 T	317963.9	4953162.9
Leadore Hill (LH)	44° 37' 11"	113° 22' 46"	12 T	311236.9	4943467.7
Mahogany Hills (MH)	44° 27' 02"	113° 51' 39"	12 T	272376.0	4925914.7
Twin Peaks Ranch (TPR)	44° 57' 05"	114° 00' 02"	11 T	736598.8	4981925.7

Reference datum is North American Datum of 1927 (NAD 27).

APPENDIX B
DETRITAL ZICON DATA

Sample	$^{238}U/^{206}Pb$	1 σ (%) +/-	$^{207}Pb/^{206}Pb$	1 σ (%)	$^{238}U/^{206}Pb$ Age (Ma)	1 σ (abs) +/-	$^{207}Pb/^{206}Pb$ Age (Ma)	1 σ (abs) +/-
Italian Canyon 3 (Upper) <10% Discordant								
IC3_1	2.32	0.0287	0.1488	0.0067	2313	56	2332	11
IC3_3	2.73	0.0308	0.1295	0.0098	2010	53	2092	17
IC3_4	2.93	0.0275	0.1199	0.0067	1893	45	1954	12
IC3_5	2.91	0.0290	0.1192	0.0071	1904	48	1945	13
IC3_6	2.63	0.0281	0.1310	0.0072	2078	50	2112	13
IC3_7	2.89	0.0269	0.1160	0.0064	1917	44	1896	12
IC3_8	3.00	0.0274	0.1181	0.0064	1855	44	1928	11
IC3_9	2.82	0.0342	0.1278	0.0099	1955	57	2068	17
IC3_10	5.75	0.0307	0.0763	0.0084	1034	29	1102	17
IC3_11	2.39	0.0220	0.1555	0.0081	2250	42	2408	14
IC3_12	3.16	0.0214	0.1122	0.0089	1774	33	1835	16
IC3_13	2.01	0.0220	0.1837	0.0084	2605	47	2686	14
IC3_14	1.96	0.0217	0.1845	0.0081	2660	47	2694	13
IC3_15	3.12	0.0215	0.1141	0.0085	1793	34	1865	15
IC3_16	3.12	0.0234	0.1125	0.0084	1795	37	1840	15
IC3_17	2.18	0.0224	0.1679	0.0085	2431	45	2537	14
IC3_18	3.17	0.0225	0.1113	0.0091	1768	35	1820	16
IC3_19	3.06	0.0277	0.1184	0.0121	1820	44	1932	22
IC3_20	3.04	0.0233	0.1199	0.0096	1832	37	1955	17
IC3_21	2.03	0.0177	0.1831	0.0097	2583	38	2681	16
IC3_22	6.08	0.0181	0.0732	0.0107	982	17	1020	22
IC3_23	3.02	0.0175	0.1132	0.0092	1842	28	1852	17
IC3_24	6.17	0.0169	0.0732	0.0107	969	15	1021	22
IC3_25	2.40	0.0170	0.1519	0.0092	2244	32	2367	16
IC3_26	3.11	0.0161	0.1158	0.0095	1798	25	1892	17
IC3_27	3.20	0.0206	0.1123	0.0112	1755	32	1838	20
IC3_28	3.00	0.0159	0.1134	0.0091	1854	26	1854	16
IC3_29	4.46	0.0177	0.0858	0.0112	1304	21	1333	21
IC3_30	6.12	0.0186	0.0750	0.0103	976	17	1069	20
IC3_31	2.69	0.0349	0.1322	0.0062	2038	61	2127	11
IC3_32	3.24	0.0361	0.1124	0.0087	1736	55	1838	16
IC3_33	3.56	0.0361	0.1001	0.0086	1597	51	1625	16
IC3_34	3.10	0.0357	0.1120	0.0080	1801	56	1832	14
IC3_35	3.16	0.0350	0.1116	0.0065	1774	54	1826	12
IC3_36	3.10	0.0373	0.1120	0.0105	1801	58	1832	19
IC3_37	3.22	0.0386	0.1171	0.0107	1745	59	1913	19
IC3_38	1.95	0.0346	0.1835	0.0056	2667	75	2684	9
IC3_39	5.91	0.0361	0.0735	0.0109	1008	34	1029	22
IC3_40	3.04	0.0358	0.1149	0.0080	1833	57	1878	14
IC3_41	2.05	0.0255	0.1795	0.0094	2560	54	2648	15
IC3_43	3.08	0.0256	0.1118	0.0104	1814	40	1829	19
IC3_45	3.05	0.0260	0.1145	0.0106	1826	41	1872	19
IC3_46	2.99	0.0265	0.1144	0.0103	1861	43	1870	19

IC3_47	2.96	0.0259	0.1164	0.0102	1879	42	1902	18
IC3_48	3.06	0.0257	0.1124	0.0093	1825	41	1839	17
IC3_49	2.98	0.0272	0.1172	0.0106	1867	44	1913	19
IC3_50	3.07	0.0257	0.1123	0.0107	1818	41	1836	19
IC3_51	3.29	0.0219	0.1161	0.0107	1710	33	1897	19
IC3_52	3.19	0.0223	0.1128	0.0097	1760	34	1845	17
IC3_53	3.06	0.0307	0.1167	0.0141	1821	49	1906	25
IC3_54	3.04	0.0219	0.1185	0.0097	1835	35	1934	17
IC3_55	3.10	0.0209	0.1129	0.0095	1803	33	1847	17
IC3_56	2.95	0.0208	0.1163	0.0092	1881	34	1900	16
IC3_57	2.94	0.0203	0.1176	0.0091	1890	33	1920	16
IC3_58	3.00	0.0251	0.1185	0.0103	1854	40	1934	18
IC3_59	3.15	0.0219	0.1129	0.0101	1777	34	1847	18
IC3_60	5.11	0.0209	0.0783	0.0103	1153	22	1154	20
IC3_61	3.16	0.0283	0.1119	0.0073	1773	44	1831	13
IC3_62	3.05	0.0270	0.1121	0.0071	1826	43	1834	13
IC3_63	4.90	0.0269	0.0816	0.0073	1198	29	1237	14
IC3_64	2.39	0.0275	0.1442	0.0068	2252	52	2279	12
IC3_65	2.91	0.0274	0.1215	0.0068	1902	45	1978	12
IC3_67	3.22	0.0271	0.1140	0.0076	1741	41	1864	14
IC3_68	3.12	0.0272	0.1128	0.0073	1792	42	1845	13
IC3_71	2.75	0.0322	0.1269	0.0079	2001	55	2056	14
IC3_72	3.21	0.0316	0.1088	0.0073	1746	48	1779	13
IC3_73	3.15	0.0317	0.1114	0.0079	1776	49	1822	14
IC3_74	3.13	0.0334	0.1100	0.0092	1789	52	1800	17
IC3_75	3.07	0.0318	0.1116	0.0075	1817	50	1825	14
IC3_76	2.29	0.0324	0.1518	0.0079	2334	63	2366	13
IC3_77	3.14	0.0320	0.1139	0.0081	1783	50	1862	15
IC3_78	3.04	0.0325	0.1122	0.0080	1831	52	1836	14
IC3_79	2.91	0.0316	0.1218	0.0077	1902	52	1982	14
IC3_80	2.93	0.0325	0.1169	0.0079	1895	53	1910	14
IC3_81	3.23	0.0147	0.1118	0.0094	1738	22	1829	17
IC3_82	3.02	0.0135	0.1112	0.0097	1842	22	1820	17
IC3_83	2.86	0.0127	0.1269	0.0094	1935	21	2055	16
IC3_84	2.02	0.0152	0.1816	0.0091	2593	32	2668	15
IC3_85	3.04	0.0132	0.1133	0.0090	1836	21	1853	16
IC3_86	2.95	0.0185	0.1182	0.0112	1883	30	1929	20
IC3_87	2.77	0.0192	0.1203	0.0109	1985	33	1960	19
IC3_88	3.02	0.0141	0.1146	0.0101	1842	23	1873	18
IC3_89	3.05	0.0123	0.1119	0.0086	1830	20	1830	16
IC3_90	3.05	0.0131	0.1131	0.0093	1826	21	1851	17
IC3_91	2.72	0.0154	0.1185	0.0052	2019	27	1934	9
IC3_92	2.74	0.0132	0.1295	0.0034	2005	23	2091	6
IC3_93	3.16	0.0127	0.1138	0.0046	1770	20	1861	8
IC3_94	3.06	0.0132	0.1166	0.0048	1821	21	1905	9
IC3_96	3.16	0.0121	0.1129	0.0037	1773	19	1847	7
IC3_97	2.47	0.0126	0.1494	0.0039	2193	23	2339	7

IC3_98	1.95	0.0123	0.1875	0.0038	2668	27	2720	6
IC3_99	3.17	0.0130	0.1168	0.0047	1767	20	1908	8
IC3_100	3.00	0.0132	0.1180	0.0042	1854	21	1926	8
IC3_101	3.16	0.0195	0.1123	0.0049	1771	30	1838	9
IC3_102	2.99	0.0202	0.1182	0.0055	1860	32	1929	10
IC3_103	3.02	0.0199	0.1169	0.0050	1842	32	1909	9
IC3_104	2.70	0.0193	0.1314	0.0040	2033	34	2116	7
IC3_105	3.22	0.0194	0.1122	0.0049	1744	30	1836	9
IC3_106	2.76	0.0201	0.1289	0.0048	1991	34	2083	8
IC3_107	2.71	0.0199	0.1277	0.0045	2023	35	2066	8
IC3_108	2.97	0.0198	0.1183	0.0040	1873	32	1931	7
IC3_109	2.91	0.0195	0.1234	0.0053	1907	32	2006	9
IC3_110	3.20	0.0204	0.1134	0.0059	1754	31	1855	11
IC3_111	2.99	0.0127	0.1175	0.0053	1859	20	1918	9
IC3_112	3.07	0.0118	0.1163	0.0055	1818	19	1900	10
IC3_113	2.93	0.0121	0.1295	0.0056	1892	20	2092	10
IC3_114	3.07	0.0127	0.1134	0.0045	1815	20	1855	8
IC3_115	2.30	0.0115	0.1532	0.0045	2324	22	2382	8
IC3_117	1.93	0.0122	0.2024	0.0046	2697	27	2845	7
IC3_118	2.10	0.0140	0.1777	0.0048	2509	29	2631	8
IC3_119	2.75	0.0136	0.1287	0.0048	2000	23	2080	8
IC3_120	2.79	0.0134	0.1278	0.0057	1977	23	2068	10
IC3_121	3.25	0.0425	0.1121	0.0053	1731	64	1833	10
IC3_122	3.20	0.0422	0.1129	0.0055	1754	65	1847	10
IC3_123	3.25	0.0424	0.1143	0.0071	1729	64	1869	13
IC3_124	3.06	0.0422	0.1170	0.0060	1825	67	1910	11
IC3_125	3.26	0.0424	0.1136	0.0062	1723	64	1857	11
IC3_127	2.44	0.0421	0.1469	0.0048	2215	78	2310	8
IC3_128	2.69	0.0421	0.1292	0.0049	2037	73	2087	9
IC3_129	2.07	0.0422	0.1850	0.0049	2543	88	2699	8
IC3_130	3.03	0.0425	0.1170	0.0049	1836	68	1910	9
IC3_131	3.22	0.0220	0.1162	0.0045	1742	33	1898	8
IC3_132	3.26	0.0231	0.1150	0.0058	1724	35	1879	10
IC3_133	3.50	0.0238	0.1070	0.0051	1620	34	1749	9
IC3_134	2.86	0.0216	0.1285	0.0047	1933	36	2078	8
IC3_135	3.32	0.0220	0.1151	0.0061	1696	33	1882	11
IC3_136	2.09	0.0214	0.1836	0.0041	2516	44	2685	7
IC3_137	3.33	0.0221	0.1132	0.0051	1694	33	1852	9
IC3_138	3.22	0.0215	0.1174	0.0056	1744	33	1917	10
IC3_139	3.39	0.0221	0.1127	0.0045	1665	32	1844	8
IC3_140	2.36	0.0219	0.1607	0.0041	2280	42	2463	7
				>10% Discordant				
IC3_44	3.50	0.0284	0.1270	0.0100	1617	40	2056	17
IC3_66	4.34	0.0318	0.1274	0.0096	1336	38	2063	17
IC3_69	3.17	0.0279	0.1212	0.0067	1767	43	1974	12
IC3_70	4.26	0.0276	0.1485	0.0070	1357	34	2329	12

IC3_95	3.18	0.0128	0.1285	0.0037	1758	20	2078	7
IC3_116	2.89	0.0114	0.1608	0.0085	1912	19	2464	14
IC3_126	3.38	0.0424	0.1200	0.0050	1669	62	1956	9

Sample	$^{238}U/^{206}Pb$	1 σ (%) +/-	$^{207}Pb/^{206}Pb$	1 σ (%)	$^{238}U/^{206}Pb$ Age (Ma)	1 σ (abs) +/-	$^{207}Pb/^{206}Pb$ Age (Ma)	1 σ (abs) +/-
Italian Canyon 2 (Middle) <10% Discordant								
IC2_1	2.89	0.0338	0.1285	0.0064	1918	56	2077	11
IC2_2	3.27	0.0333	0.1146	0.0065	1719	50	1874	12
IC2_3	3.22	0.0343	0.1172	0.0075	1745	52	1914	13
IC2_4	3.25	0.0334	0.1132	0.0061	1728	50	1852	11
IC2_5	3.09	0.0346	0.1169	0.0062	1805	54	1909	11
IC2_7	3.14	0.0352	0.1201	0.0087	1784	55	1957	15
IC2_8	2.88	0.0350	0.1286	0.0078	1920	58	2079	14
IC2_10	2.84	0.0332	0.1288	0.0073	1945	55	2082	13
IC2_11	3.19	0.0180	0.1133	0.0048	1758	28	1853	9
IC2_12	3.12	0.0187	0.1146	0.0049	1792	29	1873	9
IC2_13	3.14	0.0216	0.1128	0.0054	1782	34	1845	10
IC2_14	2.93	0.0198	0.1299	0.0052	1891	32	2096	9
IC2_15	3.09	0.0216	0.1190	0.0065	1806	34	1941	12
IC2_16	3.10	0.0209	0.1119	0.0059	1800	33	1831	11
IC2_17	2.79	0.0212	0.1278	0.0067	1973	36	2068	12
IC2_18	3.12	0.0201	0.1133	0.0055	1794	31	1854	10
IC2_19	2.42	0.0185	0.1495	0.0047	2226	35	2341	8
IC2_21	2.23	0.0089	0.1509	0.0044	2385	18	2356	7
IC2_22	3.21	0.0103	0.1123	0.0064	1747	16	1838	12
IC2_23	3.15	0.0094	0.1112	0.0059	1778	15	1819	11
IC2_24	3.03	0.0088	0.1233	0.0050	1838	14	2005	9
IC2_25	3.07	0.0099	0.1138	0.0056	1818	16	1861	10
IC2_26	1.87	0.0106	0.2066	0.0054	2767	24	2879	9
IC2_28	2.05	0.0102	0.1820	0.0050	2565	22	2671	8
IC2_29	3.13	0.0080	0.1137	0.0046	1787	12	1859	8
IC2_30	3.07	0.0098	0.1119	0.0048	1816	15	1830	9
IC2_31	2.71	0.0115	0.1291	0.0042	2028	20	2085	7
IC2_32	3.03	0.0113	0.1188	0.0033	1839	18	1939	6
IC2_33	3.19	0.0132	0.1134	0.0057	1756	20	1854	10
IC2_35	3.13	0.0144	0.1139	0.0057	1789	22	1863	10
IC2_36	3.30	0.0184	0.1152	0.0096	1705	28	1883	17
IC2_37	5.35	0.0144	0.0798	0.0083	1105	15	1193	16
IC2_38	3.12	0.0264	0.1185	0.0177	1793	41	1934	31
IC2_39	2.71	0.0152	0.1271	0.0036	2026	26	2059	6
IC2_40	3.21	0.0150	0.1133	0.0050	1746	23	1853	9
IC2_42	3.03	0.0235	0.1183	0.0065	1839	38	1931	12
IC2_43	2.03	0.0215	0.1836	0.0062	2579	46	2686	10
IC2_44	3.00	0.0214	0.1195	0.0069	1857	34	1949	12
IC2_45	2.99	0.0209	0.1183	0.0070	1862	34	1931	13

IC2_46	2.72	0.0210	0.1276	0.0069	2017	36	2065	12
IC2_47	3.07	0.0245	0.1165	0.0106	1817	39	1903	19
IC2_48	3.10	0.0218	0.1116	0.0067	1802	34	1826	12
IC2_49	2.74	0.0211	0.1302	0.0063	2008	36	2101	11
IC2_50	1.96	0.0207	0.1992	0.0065	2655	45	2820	11
IC2_51	3.09	0.0135	0.1127	0.0063	1808	21	1843	11
IC2_52	3.00	0.0150	0.1157	0.0077	1855	24	1891	14
IC2_53	3.10	0.0140	0.1123	0.0073	1802	22	1836	13
IC2_54	3.15	0.0139	0.1134	0.0071	1777	22	1855	13
IC2_55	2.85	0.0137	0.1201	0.0064	1938	23	1958	11
IC2_56	2.91	0.0134	0.1181	0.0066	1903	22	1928	12
IC2_57	2.90	0.0139	0.1180	0.0066	1908	23	1927	12
IC2_58	3.13	0.0163	0.1144	0.0089	1785	25	1870	16
IC2_59	1.95	0.0160	0.1861	0.0070	2666	35	2708	12
IC2_60	2.94	0.0173	0.1182	0.0085	1888	28	1929	15
IC2_61	2.69	0.0180	0.1261	0.0054	2036	31	2044	10
IC2_62	3.12	0.0181	0.1115	0.0063	1790	28	1823	11
IC2_63	3.03	0.0204	0.1174	0.0072	1837	32	1917	13
IC2_64	2.56	0.0220	0.1448	0.0073	2123	40	2286	13
IC2_65	3.19	0.0194	0.1100	0.0062	1759	30	1800	11
IC2_66	1.64	0.0180	0.2586	0.0050	3073	44	3238	8
IC2_68	2.46	0.0192	0.1407	0.0060	2197	36	2236	10
IC2_69	1.80	0.0185	0.2212	0.0059	2843	42	2989	10
IC2_72	2.59	0.0281	0.1294	0.0069	2107	50	2090	12
IC2_73	2.77	0.0272	0.1195	0.0053	1984	46	1948	9
IC2_74	2.96	0.0275	0.1117	0.0056	1875	45	1828	10
IC2_75	2.96	0.0285	0.1156	0.0078	1874	46	1889	14
IC2_76	2.10	0.0274	0.1628	0.0055	2510	57	2485	9
IC2_77	3.20	0.0274	0.1081	0.0063	1753	42	1768	11
IC2_78	3.08	0.0279	0.1142	0.0078	1813	44	1868	14
IC2_79	2.65	0.0272	0.1290	0.0054	2063	48	2084	9
IC2_80	3.02	0.0272	0.1111	0.0055	1845	44	1818	10
IC2_81	2.98	0.0172	0.1194	0.0070	1864	28	1948	12
IC2_82	2.80	0.0156	0.1180	0.0045	1970	26	1926	8
IC2_83	2.98	0.0154	0.1177	0.0050	1864	25	1922	9
IC2_84	3.02	0.0158	0.1127	0.0047	1845	25	1843	9
IC2_85	1.92	0.0161	0.1851	0.0047	2702	35	2699	8
IC2_86	2.19	0.0155	0.1585	0.0042	2426	31	2440	7
IC2_87	2.88	0.0156	0.1178	0.0046	1920	26	1923	8
IC2_88	3.04	0.0161	0.1118	0.0053	1832	26	1829	9
IC2_89	2.98	0.0155	0.1119	0.0045	1866	25	1830	8
IC2_90	2.70	0.0175	0.1301	0.0076	2032	30	2099	13
IC2_91	2.05	0.0160	0.1800	0.0060	2563	34	2653	10
IC2_92	2.93	0.0136	0.1170	0.0057	1891	22	1911	10
IC2_93	2.92	0.0145	0.1256	0.0067	1900	24	2038	12
IC2_95	2.92	0.0142	0.1180	0.0060	1901	23	1926	11
IC2_96	2.81	0.0154	0.1191	0.0074	1962	26	1943	13

IC2_97	3.06	0.0131	0.1131	0.0049	1824	21	1850	9
IC2_98	2.89	0.0149	0.1199	0.0059	1913	25	1955	11
IC2_99	3.09	0.0145	0.1130	0.0056	1809	23	1848	10
IC2_100	2.64	0.0135	0.1293	0.0048	2070	24	2088	8
IC2_101	3.06	0.0161	0.1122	0.0073	1822	26	1835	13
IC2_102	3.01	0.0144	0.1127	0.0037	1849	23	1844	7
IC2_103	3.05	0.0159	0.1133	0.0068	1829	25	1853	12
IC2_104	3.07	0.0158	0.1126	0.0060	1819	25	1842	11
IC2_105	2.08	0.0148	0.1719	0.0043	2527	31	2576	7
IC2_106	2.05	0.0143	0.1727	0.0035	2565	30	2584	6
IC2_107	2.41	0.0150	0.1471	0.0050	2234	28	2312	9
IC2_108	3.13	0.0153	0.1112	0.0047	1785	24	1819	8
IC2_109	3.20	0.0175	0.1133	0.0055	1752	27	1853	10
IC2_110	3.05	0.0150	0.1130	0.0048	1828	24	1848	9
IC2_111	2.62	0.0174	0.1282	0.0058	2083	31	2073	10
IC2_112	3.00	0.0197	0.1226	0.0083	1853	32	1995	15
IC2_113	2.05	0.0166	0.1910	0.0036	2565	35	2751	6
IC2_114	2.65	0.0180	0.1401	0.0053	2064	32	2229	9
IC2_116	2.64	0.0225	0.1292	0.0040	2073	40	2087	7
IC2_117	3.12	0.0245	0.1134	0.0056	1794	38	1854	10
IC2_118	2.99	0.0232	0.1137	0.0048	1858	37	1860	9
IC2_119	1.99	0.0240	0.1861	0.0039	2619	51	2708	6
IC2_120	3.10	0.0228	0.1125	0.0049	1803	36	1841	9
IC2_121	2.62	0.0230	0.1392	0.0059	2082	41	2218	10
IC2_122	2.69	0.0239	0.1283	0.0066	2040	42	2075	12
IC2_123	3.07	0.0237	0.1124	0.0085	1818	37	1839	15
IC2_124	3.04	0.0220	0.1142	0.0046	1831	35	1867	8
IC2_125	3.09	0.0233	0.1128	0.0055	1807	37	1845	10
IC2_127	2.64	0.0237	0.1273	0.0037	2072	42	2062	7
IC2_128	2.85	0.0220	0.1190	0.0038	1940	37	1942	7
IC2_129	3.13	0.0238	0.1124	0.0060	1785	37	1838	11
IC2_130	5.70	0.0223	0.0738	0.0059	1041	21	1036	12
IC2_131	5.73	0.0151	0.0744	0.0077	1037	14	1053	15
IC2_132	2.66	0.0156	0.1293	0.0070	2057	27	2089	12
IC2_133	3.22	0.0137	0.1088	0.0059	1744	21	1779	11
IC2_134	2.74	0.0165	0.1288	0.0066	2006	28	2081	12
IC2_135	1.99	0.0128	0.1741	0.0053	2626	28	2597	9
IC2_136	1.95	0.0152	0.1831	0.0062	2673	33	2681	10
IC2_138	2.65	0.0129	0.1296	0.0057	2066	23	2093	10
IC2_139	3.07	0.0140	0.1116	0.0081	1819	22	1826	15
IC2_140	2.97	0.0125	0.1141	0.0059	1870	20	1866	11
IC2_141	2.57	0.0123	0.1280	0.0057	2118	22	2071	10
IC2_142	2.88	0.0127	0.1217	0.0064	1922	21	1981	11
IC2_143	2.98	0.0131	0.1236	0.0063	1867	21	2009	11
IC2_144	5.62	0.0118	0.0747	0.0062	1055	11	1060	12
IC2_145	2.88	0.0130	0.1183	0.0061	1921	21	1931	11
IC2_146	3.11	0.0102	0.1130	0.0054	1797	16	1849	10

IC2_147	3.10	0.0139	0.1113	0.0051	1802	22	1820	9
IC2_148	1.98	0.0120	0.1812	0.0039	2636	26	2664	7
IC2_149	1.96	0.0073	0.1814	0.0030	2654	16	2665	5
IC2_150	1.97	0.0088	0.1832	0.0042	2646	19	2682	7
IC2_151	2.64	0.0102	0.1291	0.0055	2072	18	2085	10
IC2_152	2.51	0.0099	0.1420	0.0060	2164	18	2252	10
IC2_153	3.02	0.0101	0.1128	0.0040	1842	16	1846	7
IC2_154	3.19	0.0135	0.1151	0.0074	1760	21	1881	13
IC2_155	2.67	0.0137	0.1294	0.00495	2048	24	2090	9
			>10% Discordant					
IC2_6	3.512	0.0360	0.1261	0.0080	1615	51	2044	14
IC2_9	3.370	0.0324	0.1151	0.0063	1675	48	1882	11
IC2_20	3.219	0.0186	0.1191	0.0071	1744	28	1943	13
IC2_34	2.110	0.0137	0.2187	0.0095	2500	28	2971	15
IC2_67	3.958	0.0195	0.1160	0.0084	1452	25	1895	15
IC2_70	2.812	0.0201	0.1694	0.0054	1961	34	2551	9
IC2_71	3.299	0.0316	0.1207	0.0060	1707	47	1967	11
IC2_94	3.139	0.0139	0.1840	0.0065	1783	22	2689	11
IC2_115	3.237	0.0261	0.1215	0.0070	1735	40	1979	12
IC2_126	3.248	0.0233	0.1210	0.0044	1730	35	1971	8

Sample	$^{238}U/^{206}Pb$	1 σ (%) +/-	$^{207}Pb/^{206}Pb$	1 σ (%)	$^{238}U/^{206}Pb$ Age (Ma)	1 σ (abs) +/-	$^{207}Pb/^{206}Pb$ Age (Ma)	1 σ (abs) +/-
Italian Canyon 5 (Basal) <10% Discordant								
IC5_1	2.99	0.0245	0.1191	0.0040	1857	39	1943	7
IC5_2	2.43	0.0242	0.1556	0.0039	2221	45	2409	7
IC5_3	3.16	0.0240	0.1117	0.0041	1773	37	1828	7
IC5_4	2.04	0.0243	0.1809	0.0035	2570	51	2661	6
IC5_5	3.10	0.0238	0.1110	0.0036	1804	37	1816	7
IC5_6	3.00	0.0234	0.1165	0.0037	1854	38	1903	7
IC5_7	3.11	0.0238	0.1137	0.0053	1795	37	1860	9
IC5_8	2.10	0.0248	0.1788	0.0041	2511	51	2642	7
IC5_9	2.06	0.0248	0.1808	0.0034	2546	52	2661	6
IC5_10	3.18	0.0247	0.1125	0.0037	1765	38	1840	7
IC5_11	3.07	0.0235	0.1119	0.0044	1818	37	1831	8
IC5_12	3.12	0.0229	0.1114	0.0046	1792	36	1822	8
IC5_13	2.73	0.0237	0.1279	0.0059	2011	41	2069	10
IC5_14	3.16	0.0242	0.1128	0.0050	1774	37	1845	9
IC5_15	1.70	0.0238	0.2230	0.0047	2975	56	3003	7
IC5_16	2.70	0.0234	0.1300	0.0050	2029	41	2097	9
IC5_17	3.12	0.0230	0.1126	0.0053	1793	36	1841	10
IC5_19	3.14	0.0218	0.1115	0.0044	1784	34	1823	8
IC5_20	1.98	0.0224	0.1878	0.0044	2633	48	2723	7
IC5_21	2.03	0.0079	0.1812	0.0044	2578	17	2664	7
IC5_22	2.13	0.0139	0.1873	0.0036	2479	28	2719	6

IC5_23	2.99	0.0098	0.1188	0.0054	1860	16	1939	10
IC5_24	4.46	0.0117	0.0870	0.0065	1303	14	1360	13
IC5_25	3.08	0.0092	0.1138	0.0042	1815	15	1861	8
IC5_26	3.00	0.0093	0.1149	0.0044	1854	15	1878	8
IC5_27	2.73	0.0110	0.1284	0.0043	2011	19	2076	8
IC5_28	3.01	0.0102	0.1183	0.0050	1852	16	1930	9
IC5_29	3.07	0.0082	0.1095	0.0041	1820	13	1791	7
IC5_30	3.06	0.0090	0.1141	0.0043	1824	14	1866	8
IC5_31	5.96	0.0095	0.0735	0.0056	999	9	1029	11
IC5_32	2.03	0.0095	0.1892	0.0032	2578	20	2735	5
IC5_33	3.15	0.0094	0.1139	0.0041	1777	15	1863	7
IC5_34	2.01	0.0098	0.1837	0.0032	2603	21	2686	5
IC5_35	3.32	0.0131	0.1120	0.0060	1698	19	1832	11
IC5_36	3.05	0.0130	0.1182	0.0057	1828	21	1929	10
IC5_37	2.12	0.0126	0.1818	0.0047	2489	26	2670	8
IC5_38	3.08	0.0120	0.1125	0.0039	1812	19	1840	7
IC5_39	2.90	0.0105	0.1177	0.0039	1908	17	1922	7
IC5_40	3.23	0.0143	0.1142	0.0057	1741	22	1867	10
IC5_41	3.05	0.0240	0.1131	0.0071	1829	38	1849	13
IC5_42	3.14	0.0237	0.1118	0.0080	1784	37	1828	14
IC5_43	3.34	0.0234	0.1046	0.0065	1687	35	1708	12
IC5_44	3.05	0.0230	0.1139	0.0076	1827	36	1862	14
IC5_45	2.12	0.0236	0.1905	0.0064	2487	48	2747	10
IC5_46	3.08	0.0225	0.1124	0.0065	1814	36	1838	12
IC5_47	3.10	0.0234	0.1131	0.0067	1805	37	1849	12
IC5_48	2.21	0.0229	0.1614	0.0066	2404	46	2471	11
IC5_49	2.74	0.0237	0.1279	0.0069	2007	41	2070	12
IC5_50	1.89	0.0234	0.1897	0.0064	2740	52	2739	10
IC5_51	2.97	0.0123	0.1143	0.0075	1871	20	1868	14
IC5_52	5.71	0.0114	0.0746	0.0074	1040	11	1056	15
IC5_53	3.08	0.0107	0.1122	0.0059	1811	17	1835	11
IC5_54	3.10	0.0110	0.1129	0.0067	1804	17	1847	12
IC5_55	2.96	0.0129	0.1183	0.0061	1874	21	1931	11
IC5_56	3.07	0.0127	0.1114	0.0059	1818	20	1822	11
IC5_58	3.04	0.0134	0.1146	0.0067	1835	21	1874	12
IC5_59	1.93	0.0147	0.1918	0.0070	2693	32	2758	11
IC5_60	3.11	0.0147	0.1200	0.0077	1797	23	1956	14
IC5_61	1.92	0.0150	0.1941	0.0050	2700	33	2778	8
IC5_62	2.00	0.0126	0.1811	0.0036	2616	27	2663	6
IC5_63	2.98	0.0142	0.1171	0.0051	1864	23	1913	9
IC5_64	1.97	0.0132	0.1876	0.0041	2652	29	2721	7
IC5_65	2.96	0.0143	0.1176	0.0057	1875	23	1920	10
IC5_66	1.99	0.0130	0.1857	0.0039	2623	28	2704	6
IC5_67	3.11	0.0130	0.1129	0.0039	1796	20	1846	7
IC5_68	3.10	0.0144	0.1122	0.0065	1803	23	1835	12
IC5_69	2.14	0.0130	0.1698	0.0045	2469	27	2556	7
IC5_70	3.11	0.0118	0.1128	0.0038	1798	19	1845	7

IC5_71	2.66	0.0173	0.1298	0.0062	2056	30	2095	11
IC5_72	2.99	0.0170	0.1133	0.0057	1859	27	1852	10
IC5_73	2.09	0.0163	0.1698	0.0051	2524	34	2556	8
IC5_74	3.03	0.0178	0.1117	0.0064	1836	28	1827	12
IC5_75	3.09	0.0175	0.1115	0.0064	1805	28	1824	12
IC5_76	3.05	0.0161	0.1112	0.0058	1826	26	1819	10
IC5_77	1.89	0.0169	0.1854	0.0053	2741	38	2702	9
IC5_78	1.95	0.0170	0.1985	0.0065	2664	37	2814	11
IC5_79	3.10	0.0162	0.1124	0.0061	1805	25	1838	11
IC5_80	1.91	0.0176	0.1976	0.0052	2715	39	2807	8
IC5_81	3.07	0.0185	0.1128	0.0079	1818	29	1845	14
IC5_82	3.20	0.0161	0.1094	0.0053	1754	25	1790	10
IC5_83	3.02	0.0160	0.1132	0.0052	1846	26	1851	9
IC5_84	1.97	0.0168	0.1868	0.0054	2648	36	2714	9
IC5_86	3.04	0.0152	0.1154	0.0061	1832	24	1885	11
IC5_87	3.14	0.0139	0.1148	0.0064	1783	22	1876	12
IC5_88	3.13	0.0130	0.1144	0.0050	1788	20	1871	9
IC5_89	2.03	0.0150	0.1879	0.0050	2577	32	2724	8
IC5_90	2.14	0.0127	0.1710	0.0046	2468	26	2568	8
IC5_91	2.77	0.0144	0.1277	0.0056	1987	25	2066	10
IC5_92	2.95	0.0132	0.1181	0.0049	1879	22	1927	9
IC5_93	3.17	0.0143	0.1118	0.0057	1766	22	1829	10
IC5_94	2.70	0.0148	0.1301	0.0059	2033	26	2099	10
IC5_95	3.04	0.0142	0.1135	0.0047	1836	23	1856	9
IC5_96	3.26	0.0147	0.1114	0.0053	1723	22	1823	10
IC5_97	3.09	0.0143	0.1121	0.0051	1809	23	1834	9
IC5_98	2.67	0.0146	0.1283	0.0055	2049	26	2075	10
IC5_99	2.00	0.0143	0.1820	0.0057	2617	31	2672	9
IC5_100	3.02	0.0155	0.1140	0.0071	1842	25	1864	13
IC5_101	2.82	0.0152	0.1276	0.0047	1956	26	2066	8
IC5_102	1.83	0.0172	0.2096	0.0059	2807	39	2902	10
IC5_103	3.23	0.0171	0.1137	0.0048	1737	26	1860	9
IC5_104	3.24	0.0162	0.1141	0.0069	1732	25	1866	12
IC5_105	3.16	0.0149	0.1117	0.0045	1774	23	1827	8
IC5_106	3.02	0.0159	0.1164	0.0056	1843	25	1902	10
IC5_107	3.22	0.0154	0.1124	0.0046	1745	23	1839	8
IC5_108	2.69	0.0151	0.1276	0.0051	2040	26	2065	9
IC5_109	3.09	0.0148	0.1154	0.0055	1809	23	1886	10
IC5_110	3.10	0.0141	0.1138	0.0048	1801	22	1861	9
IC5_111	1.77	0.0144	0.2168	0.0048	2881	33	2957	8
IC5_112	2.96	0.0160	0.1177	0.0077	1877	26	1921	14
IC5_114	3.09	0.0147	0.1128	0.0053	1808	23	1846	10
IC5_115	3.05	0.0156	0.1190	0.0073	1827	25	1941	13
IC5_116	2.06	0.0219	0.1806	0.0049	2549	46	2658	8
IC5_117	3.34	0.0221	0.1102	0.0058	1690	33	1803	10
IC5_118	2.70	0.0220	0.1269	0.0054	2030	38	2055	9
IC5_119	2.00	0.0217	0.1848	0.0047	2618	46	2696	8

IC5_120	2.79	0.0214	0.1278	0.0051	1974	36	2067	9
IC5_121	2.83	0.0208	0.1283	0.0048	1952	35	2075	8
IC5_122	2.93	0.0218	0.1197	0.0063	1892	36	1952	11
IC5_123	2.72	0.0216	0.1290	0.0051	2019	37	2084	9
IC5_124	3.12	0.0214	0.1119	0.0058	1795	33	1830	10
IC5_125	3.14	0.0214	0.1129	0.0055	1784	33	1847	10
IC5_126	3.22	0.0206	0.1140	0.0052	1741	31	1864	9
IC5_127	2.94	0.0235	0.1163	0.0085	1885	38	1900	15
IC5_128	2.93	0.0216	0.1171	0.0049	1893	35	1913	9
IC5_129	3.21	0.0207	0.1122	0.0056	1751	32	1835	10
IC5_130	2.97	0.0233	0.1200	0.0083	1871	38	1956	15
IC5_131	2.82	0.0105	0.1285	0.0051	1957	18	2077	9
IC5_132	3.06	0.0098	0.1136	0.0042	1823	16	1858	7
IC5_133	2.03	0.0100	0.1834	0.0043	2584	21	2684	7
IC5_134	3.23	0.0095	0.1122	0.0041	1740	15	1835	7
IC5_135	1.94	0.0097	0.1886	0.0040	2680	21	2730	7
IC5_136	1.77	0.0099	0.2167	0.0041	2881	23	2957	7
IC5_137	2.75	0.0112	0.1287	0.0060	1998	19	2080	10
IC5_138	3.01	0.0093	0.1264	0.0041	1849	15	2048	7
IC5_139	3.18	0.0115	0.1122	0.0066	1761	18	1835	12
IC5_140	2.02	0.0107	0.1790	0.0046	2590	23	2644	8
			>10% Discordant					
IC5_18	4.42	0.0225	0.1074	0.0045	1315	27	1755	8
IC5_85	2.82	0.0211	0.1470	0.0061	1955	35	2312	10
IC5_113	2.68	0.0156	0.1716	0.0047	2046	27	2573	8

Sample	$^{238}U/^{206}Pb$	1 σ (%) +/-	$^{207}Pb/^{206}Pb$	1 σ (%)	$^{238}U/^{206}Pb$ Age (Ma)	1 σ (abs) +/-	$^{207}Pb/^{206}Pb$ Age (Ma)	1 σ (abs) +/-
Twin Peaks Ranch 2 (Upper) <10% Discordant								
TPR2_1	3.03	0.0291	0.1140	0.0044	1838	46	1864	8
TPR2_2	3.06	0.0290	0.1141	0.0056	1821	46	1866	10
TPR2_3	2.00	0.0290	0.1787	0.0041	2610	62	2641	7
TPR2_4	1.95	0.0284	0.1884	0.0042	2670	62	2728	7
TPR2_5	3.15	0.0279	0.1108	0.0043	1779	43	1813	8
TPR2_6	2.75	0.0292	0.1222	0.0045	1999	50	1988	8
TPR2_7	3.01	0.0287	0.1169	0.0052	1848	46	1909	9
TPR2_8	2.10	0.0288	0.1781	0.0047	2515	60	2635	8
TPR2_9	3.07	0.0299	0.1166	0.0071	1819	47	1905	13
TPR2_10	3.04	0.0280	0.1138	0.0043	1835	45	1862	8
TPR2_11	1.99	0.0315	0.1880	0.0049	2625	68	2725	8
TPR2_12	1.85	0.0315	0.2200	0.0049	2791	71	2981	8
TPR2_13	3.13	0.0315	0.1120	0.0058	1786	49	1832	10
TPR2_14	2.00	0.0324	0.1842	0.0054	2614	69	2691	9
TPR2_15	3.17	0.0315	0.1138	0.0060	1766	48	1861	11
TPR2_16	3.22	0.0314	0.1131	0.0053	1742	48	1850	10

TPR2_17	1.91	0.0309	0.1946	0.0045	2719	68	2782	7
TPR2_18	3.20	0.0311	0.1147	0.0052	1751	47	1874	9
TPR2_19	3.20	0.0311	0.1121	0.0050	1754	48	1834	9
TPR2_20	3.16	0.0313	0.1113	0.0050	1771	48	1821	9
TPR2_21	2.94	0.0276	0.1177	0.0043	1888	45	1922	8
TPR2_22	3.16	0.0280	0.1117	0.0049	1771	43	1828	9
TPR2_23	2.03	0.0275	0.1807	0.0038	2583	58	2659	6
TPR2_25	3.19	0.0281	0.1130	0.0054	1758	43	1849	10
TPR2_26	1.96	0.0277	0.1788	0.0041	2652	60	2642	7
TPR2_27	1.95	0.0274	0.1880	0.0040	2673	60	2724	7
TPR2_28	3.12	0.0276	0.1138	0.0051	1794	43	1861	9
TPR2_29	3.19	0.0283	0.1126	0.0059	1760	43	1841	11
TPR2_30	3.13	0.0277	0.1119	0.0051	1789	43	1831	9
TPR2_31	2.18	0.0148	0.1702	0.0031	2433	30	2559	5
TPR2_32	2.95	0.0143	0.1200	0.0033	1880	23	1956	6
TPR2_33	3.22	0.0153	0.1117	0.0050	1745	23	1828	9
TPR2_34	2.76	0.0152	0.1214	0.0036	1996	26	1977	6
TPR2_36	1.99	0.0153	0.1893	0.0036	2630	33	2736	6
TPR2_37	2.01	0.0148	0.1819	0.0033	2604	32	2671	5
TPR2_38	2.84	0.0154	0.1236	0.0042	1947	26	2010	8
TPR2_39	6.31	0.0145	0.0713	0.0039	949	13	965	8
TPR2_40	1.90	0.0165	0.1996	0.0041	2725	37	2823	7
TPR2_41	1.96	0.0121	0.1858	0.0024	2662	26	2705	4
TPR2_42	3.35	0.0187	0.1119	0.0091	1684	28	1830	16
TPR2_43	1.93	0.0148	0.1958	0.0045	2696	33	2792	7
TPR2_44	3.20	0.0132	0.1117	0.0045	1753	20	1827	8
TPR2_45	3.08	0.0132	0.1141	0.0044	1811	21	1865	8
TPR2_46	3.09	0.0114	0.1117	0.0028	1809	18	1827	5
TPR2_47	3.16	0.0126	0.1116	0.0042	1773	19	1825	8
TPR2_48	2.71	0.0127	0.1281	0.0045	2026	22	2072	8
TPR2_49	1.76	0.0117	0.2210	0.0027	2904	27	2988	4
TPR2_50	3.16	0.0118	0.1135	0.0035	1771	18	1857	6
TPR2_51	3.14	0.0292	0.1143	0.0062	1782	45	1869	11
TPR2_52	1.99	0.0290	0.1870	0.0034	2620	62	2716	6
TPR2_53	3.12	0.0291	0.1117	0.0043	1794	45	1827	8
TPR2_54	3.13	0.0289	0.1133	0.0043	1785	45	1853	8
TPR2_55	3.20	0.0287	0.1110	0.0041	1754	44	1816	7
TPR2_56	2.02	0.0290	0.1879	0.0035	2588	62	2724	6
TPR2_57	3.12	0.0290	0.1150	0.0042	1791	45	1880	7
TPR2_58	1.95	0.0286	0.1853	0.0029	2674	62	2701	5
TPR2_59	3.03	0.0287	0.1134	0.0034	1837	46	1854	6
TPR2_60	3.17	0.0286	0.1118	0.0032	1765	44	1829	6
TPR2_61	2.02	0.0274	0.1794	0.0066	2590	58	2647	11
TPR2_62	3.16	0.0266	0.1124	0.0060	1774	41	1839	11
TPR2_63	2.73	0.0265	0.1278	0.0062	2012	46	2067	11
TPR2_64	2.00	0.0276	0.1878	0.0067	2616	59	2723	11
TPR2_65	3.11	0.0268	0.1167	0.0063	1797	42	1907	11

TPR2_66	3.11	0.0271	0.1132	0.0069	1798	42	1852	12
TPR2_67	2.79	0.0266	0.1292	0.0064	1976	45	2087	11
TPR2_68	2.30	0.0271	0.1610	0.0067	2324	53	2466	11
TPR2_69	1.89	0.0266	0.1980	0.0060	2742	59	2809	10
TPR2_70	3.27	0.0267	0.1075	0.0076	1721	40	1758	14
TPR2_71	3.03	0.0103	0.1165	0.0068	1837	16	1903	12
TPR2_72	3.18	0.0110	0.1112	0.0070	1764	17	1819	13
TPR2_73	1.98	0.0097	0.1871	0.0060	2637	21	2717	10
TPR2_74	3.25	0.0098	0.1115	0.0072	1728	15	1824	13
TPR2_75	2.01	0.0135	0.1899	0.0074	2605	29	2741	12
TPR2_76	3.19	0.0096	0.1119	0.0063	1759	15	1830	11
TPR2_77	3.02	0.0101	0.1175	0.0065	1846	16	1918	12
TPR2_78	2.36	0.0088	0.1598	0.0062	2280	17	2453	10
TPR2_79	3.05	0.0130	0.1159	0.0081	1825	21	1894	15
TPR2_80	3.24	0.0108	0.1115	0.0073	1734	16	1824	13
TPR2_81	3.13	0.0128	0.1146	0.0054	1788	20	1874	10
TPR2_82	3.21	0.0137	0.1121	0.0061	1747	21	1833	11
TPR2_83	3.27	0.0125	0.1091	0.0058	1719	19	1784	11
TPR2_84	3.11	0.0133	0.1127	0.0053	1797	21	1844	10
TPR2_85	1.97	0.0135	0.1986	0.0057	2652	29	2815	9
TPR2_86	2.82	0.0138	0.1296	0.0055	1957	23	2092	10
TPR2_87	3.23	0.0123	0.1119	0.0052	1738	19	1831	9
TPR2_88	2.07	0.0127	0.1788	0.0051	2539	27	2642	9
TPR2_89	3.00	0.0125	0.1195	0.0059	1855	20	1949	11
TPR2_90	2.11	0.0134	0.1840	0.0054	2504	28	2689	9
TPR2_92	2.00	0.0251	0.1859	0.0056	2619	54	2706	9
TPR2_93	1.98	0.0248	0.1864	0.0055	2637	53	2711	9
TPR2_94	3.09	0.0247	0.1139	0.0055	1807	39	1863	10
TPR2_95	3.10	0.0248	0.1121	0.0056	1802	39	1834	10
TPR2_96	3.11	0.0249	0.1142	0.0063	1797	39	1868	11
TPR2_97	2.23	0.0250	0.1765	0.0059	2384	50	2620	10
TPR2_98	6.10	0.0245	0.0749	0.0061	979	22	1066	12
TPR2_99	3.12	0.0248	0.1120	0.0057	1794	39	1833	10
TPR2_100	2.30	0.0252	0.1668	0.0062	2324	49	2526	10
TPR2_101	3.17	0.0263	0.1116	0.0059	1769	41	1826	11
TPR2_102	3.19	0.0267	0.1119	0.0061	1760	41	1830	11
TPR2_103	6.14	0.0259	0.0736	0.0053	973	23	1031	11
TPR2_104	3.20	0.0261	0.1117	0.0046	1755	40	1828	8
TPR2_105	1.88	0.0264	0.2024	0.0042	2749	59	2846	7
TPR2_106	3.24	0.0257	0.1097	0.0041	1736	39	1794	7
TPR2_107	2.80	0.0256	0.1250	0.0039	1971	43	2029	7
TPR2_108	1.98	0.0259	0.1844	0.0039	2635	56	2693	6
TPR2_109	3.20	0.0258	0.1112	0.0047	1754	40	1819	9
TPR2_110	3.20	0.0261	0.1119	0.0048	1751	40	1830	9
TPR2_111	3.17	0.0237	0.1139	0.0039	1766	36	1862	7
TPR2_112	2.23	0.0243	0.1568	0.0031	2389	48	2422	5
TPR2_113	2.65	0.0242	0.1386	0.0047	2063	43	2210	8

TPR2_114	3.04	0.0253	0.1173	0.0054	1831	40	1916	10
TPR2_115	3.18	0.0257	0.1120	0.0062	1761	40	1832	11
TPR2_116	2.01	0.0248	0.1887	0.0033	2607	53	2731	5
TPR2_117	3.04	0.0244	0.1166	0.0058	1834	39	1904	10
TPR2_118	2.02	0.0238	0.1850	0.0028	2595	51	2698	5
TPR2_119	3.09	0.0236	0.1161	0.0039	1807	37	1898	7
TPR2_120	2.05	0.0235	0.1871	0.0031	2559	49	2716	5
TPR2_121	1.98	0.0206	0.1873	0.0033	2632	44	2719	5
TPR2_122	2.02	0.0208	0.1850	0.0038	2591	44	2698	6
TPR2_123	1.84	0.0204	0.2114	0.0032	2804	46	2916	5
TPR2_124	3.22	0.0204	0.1099	0.0032	1742	31	1798	6
TPR2_125	2.01	0.0203	0.1852	0.0031	2606	43	2700	5
			>10% Discordant					
TPR2_24	3.21	0.0293	0.1276	0.0050	1749	45	2066	9
TPR2_35	3.99	0.0187	0.1107	0.0056	1442	24	1811	10

Sample	$^{238}U/^{206}Pb$	1 σ (%) +/-	$^{207}Pb/^{206}Pb$	1 σ (%)	$^{238}U/^{206}Pb$ Age (Ma)	1 σ (abs) +/-	$^{207}Pb/^{206}Pb$ Age (Ma)	1 σ (abs) +/-
Twin Peaks Ranch 4 (Upper Middle) <10% Discordant								
TPR4_1	2.66	0.0114	0.1280	0.0047	2056	20	2071	8
TPR4_2	1.97	0.0120	0.1877	0.0049	2644	26	2722	8
TPR4_3	3.16	0.0186	0.1110	0.0118	1772	29	1816	21
TPR4_4	2.13	0.0117	0.1675	0.0047	2479	24	2533	8
TPR4_5	2.96	0.0121	0.1155	0.0059	1878	20	1888	11
TPR4_6	3.05	0.0113	0.1120	0.0049	1827	18	1833	9
TPR4_7	3.08	0.0114	0.1128	0.0055	1810	18	1845	10
TPR4_8	2.84	0.0119	0.1290	0.0058	1946	20	2084	10
TPR4_9	2.09	0.0118	0.1663	0.0052	2519	25	2520	9
TPR4_10	1.99	0.0114	0.1822	0.0047	2622	25	2673	8
TPR4_11	3.13	0.0115	0.1125	0.0053	1789	18	1840	10
TPR4_12	2.88	0.0123	0.1193	0.0056	1920	20	1946	10
TPR4_13	2.66	0.0113	0.1283	0.0049	2060	20	2074	9
TPR4_14	2.98	0.0118	0.1163	0.0051	1864	19	1901	9
TPR4_15	2.81	0.0110	0.1218	0.0049	1962	19	1982	9
TPR4_16	3.14	0.0221	0.1128	0.0087	1785	34	1846	16
TPR4_17	2.71	0.0219	0.1283	0.0079	2023	38	2074	14
TPR4_18	2.85	0.0221	0.1178	0.0081	1938	37	1923	14
TPR4_19	2.99	0.0222	0.1158	0.0086	1860	36	1893	15
TPR4_20	3.07	0.0220	0.1137	0.0078	1817	35	1859	14
TPR4_21	2.96	0.0223	0.1143	0.0090	1876	36	1869	16
TPR4_22	2.99	0.0225	0.1161	0.0086	1863	36	1898	15
TPR4_23	3.08	0.0219	0.1182	0.0080	1815	34	1930	14
TPR4_24	2.73	0.0217	0.1230	0.0075	2011	37	2000	13
TPR4_25	2.99	0.0244	0.1209	0.0110	1860	39	1969	19
TPR4_26	2.95	0.0220	0.1173	0.0081	1884	36	1915	15

TPR4_27	2.63	0.0217	0.1281	0.0082	2074	38	2072	14
TPR4_28	2.67	0.0234	0.1294	0.0088	2050	41	2091	15
TPR4_29	3.00	0.0221	0.1127	0.0081	1854	35	1844	15
TPR4_30	3.01	0.0228	0.1129	0.0088	1847	37	1847	16
TPR4_31	3.01	0.0312	0.1135	0.0059	1850	50	1857	11
TPR4_32	2.67	0.0307	0.1287	0.0054	2050	54	2081	10
TPR4_33	3.03	0.0311	0.1131	0.0056	1837	50	1850	10
TPR4_34	2.59	0.0305	0.1284	0.0054	2102	55	2076	10
TPR4_35	2.91	0.0310	0.1177	0.0056	1905	51	1922	10
TPR4_36	3.08	0.0308	0.1103	0.0065	1814	49	1804	12
TPR4_37	2.99	0.0305	0.1122	0.0047	1860	49	1835	9
TPR4_38	2.89	0.0308	0.1176	0.0057	1916	51	1921	10
TPR4_39	3.11	0.0306	0.1114	0.0056	1795	48	1822	10
TPR4_40	3.07	0.0304	0.1115	0.0056	1817	48	1824	10
TPR4_41	2.93	0.0236	0.1179	0.0061	1893	39	1925	11
TPR4_42	2.96	0.0236	0.1192	0.0064	1877	38	1944	11
TPR4_43	2.90	0.0238	0.1179	0.0064	1912	39	1925	11
TPR4_44	2.88	0.0233	0.1138	0.0052	1924	39	1860	9
TPR4_45	2.90	0.0236	0.1167	0.0057	1908	39	1906	10
TPR4_46	3.01	0.0244	0.1134	0.0074	1848	39	1855	13
TPR4_47	2.79	0.0239	0.1231	0.0060	1976	41	2002	11
TPR4_48	1.85	0.0241	0.2001	0.0058	2791	54	2827	9
TPR4_49	2.79	0.0235	0.1208	0.0056	1973	40	1969	10
TPR4_50	2.41	0.0236	0.1459	0.0056	2238	45	2298	10
TPR4_51	3.02	0.0405	0.1144	0.0060	1844	65	1870	11
TPR4_52	2.60	0.0404	0.1293	0.0057	2095	72	2089	10
TPR4_53	2.92	0.0404	0.1123	0.0057	1898	66	1837	10
TPR4_54	3.07	0.0404	0.1124	0.0056	1817	64	1838	10
TPR4_55	2.90	0.0404	0.1194	0.0059	1908	66	1947	10
TPR4_56	2.97	0.0405	0.1375	0.0064	1870	65	2196	11
TPR4_57	2.89	0.0406	0.1176	0.0060	1915	67	1920	11
TPR4_58	2.88	0.0403	0.1176	0.0066	1922	67	1920	12
TPR4_59	2.19	0.0408	0.1560	0.0063	2428	82	2413	11
TPR4_60	3.00	0.0409	0.1123	0.0054	1853	66	1837	10
TPR4_61	2.93	0.0152	0.1174	0.0070	1892	25	1916	12
TPR4_62	2.95	0.0129	0.1164	0.0060	1880	21	1902	11
TPR4_63	2.99	0.0141	0.1134	0.0068	1861	23	1854	12
TPR4_64	2.91	0.0146	0.1167	0.0075	1903	24	1907	13
TPR4_65	3.13	0.0152	0.1115	0.0085	1786	24	1824	15
TPR4_66	2.68	0.0132	0.1281	0.0060	2046	23	2071	10
TPR4_67	1.98	0.0146	0.1847	0.0058	2637	31	2696	10
TPR4_68	2.67	0.0131	0.1272	0.0060	2052	23	2059	11
TPR4_69	3.11	0.0137	0.1126	0.0061	1799	22	1842	11
TPR4_70	3.09	0.0145	0.1121	0.0067	1808	23	1833	12
TPR4_71	3.08	0.0087	0.1125	0.0075	1810	14	1839	13
TPR4_72	2.94	0.0080	0.1168	0.0074	1889	13	1908	13
TPR4_73	2.91	0.0083	0.1189	0.0078	1905	14	1940	14

TPR4_74	3.01	0.0106	0.1109	0.0080	1850	17	1814	14
TPR4_75	2.69	0.0111	0.1277	0.0084	2038	19	2066	15
TPR4_76	3.28	0.0141	0.1060	0.0100	1715	21	1731	18
TPR4_77	2.69	0.0079	0.1283	0.0076	2037	14	2075	13
TPR4_78	3.16	0.0095	0.1111	0.0083	1771	15	1818	15
TPR4_79	2.94	0.0116	0.1171	0.0087	1885	19	1912	15
TPR4_80	2.69	0.0087	0.1263	0.0081	2035	15	2048	14
TPR4_81	3.02	0.0115	0.1146	0.0076	1842	18	1874	14
TPR4_82	2.00	0.0128	0.1791	0.0074	2617	28	2645	12
TPR4_83	2.91	0.0096	0.1188	0.0069	1905	16	1938	12
TPR4_84	2.92	0.0124	0.1182	0.0073	1897	20	1930	13
TPR4_85	2.68	0.0137	0.1292	0.0081	2043	24	2087	14
TPR4_87	2.94	0.0115	0.1181	0.0077	1889	19	1928	14
TPR4_88	2.90	0.0122	0.1167	0.0078	1912	20	1906	14
TPR4_90	3.02	0.0107	0.1205	0.0081	1846	17	1964	14
TPR4_91	2.69	0.0090	0.1293	0.0070	2037	16	2089	12
TPR4_92	2.46	0.0066	0.1449	0.0055	2196	12	2287	10
TPR4_93	2.80	0.0096	0.1346	0.0061	1966	16	2159	11
TPR4_94	3.10	0.0066	0.1133	0.0060	1802	10	1853	11
TPR4_95	2.92	0.0073	0.1189	0.0059	1899	12	1939	10
TPR4_96	2.61	0.0090	0.1314	0.0056	2092	16	2116	10
TPR4_97	2.96	0.0076	0.1174	0.0066	1878	12	1916	12
TPR4_98	3.12	0.0114	0.1129	0.0072	1792	18	1846	13
TPR4_99	2.59	0.0102	0.1309	0.0064	2107	18	2111	11
TPR4_100	2.64	0.0102	0.1291	0.0060	2069	18	2086	11
TPR4_101	3.01	0.0103	0.1135	0.0046	1852	17	1856	8
TPR4_102	1.85	0.0121	0.2026	0.0053	2783	27	2847	9
TPR4_103	3.07	0.0107	0.1133	0.0049	1820	17	1852	9
TPR4_104	1.90	0.0098	0.2026	0.0045	2721	22	2847	7
TPR4_105	3.01	0.0131	0.1130	0.0067	1850	21	1847	12
TPR4_106	3.05	0.0144	0.1176	0.0091	1829	23	1920	16
TPR4_107	2.94	0.0119	0.1176	0.0052	1888	19	1920	9
TPR4_108	1.74	0.0121	0.2082	0.0046	2932	28	2891	8
TPR4_109	3.00	0.0115	0.1130	0.0045	1856	18	1848	8
TPR4_110	3.03	0.0119	0.1128	0.0045	1836	19	1844	8
TPR4_111	3.01	0.0115	0.1127	0.0069	1849	18	1844	12
TPR4_112	2.65	0.0113	0.1294	0.0069	2067	20	2090	12
TPR4_113	2.70	0.0126	0.1282	0.0069	2033	22	2074	12
TPR4_114	2.67	0.0132	0.1276	0.0076	2052	23	2065	13
TPR4_115	3.13	0.0114	0.1127	0.0063	1785	18	1844	11
TPR4_116	3.12	0.0120	0.1124	0.0066	1792	19	1838	12
TPR4_117	1.75	0.0160	0.2163	0.0074	2920	38	2953	12
TPR4_118	3.00	0.0122	0.1121	0.0061	1854	20	1834	11
TPR4_119	2.69	0.0127	0.1280	0.0068	2035	22	2071	12
TPR4_120	2.09	0.0119	0.1700	0.0060	2519	25	2558	10
TPR4_121	2.99	0.0133	0.1178	0.0071	1862	22	1923	13
TPR4_122	2.93	0.0133	0.1178	0.0076	1895	22	1923	14

TPR4_123	3.08	0.0105	0.1126	0.0067	1810	17	1842	12
TPR4_124	2.88	0.0119	0.1177	0.0064	1921	20	1921	11
TPR4_126	2.76	0.0189	0.1204	0.0052	1995	32	1962	9
TPR4_127	2.90	0.0176	0.1177	0.0048	1912	29	1921	9
TPR4_128	2.96	0.0174	0.1208	0.0065	1874	28	1968	12
TPR4_129	3.12	0.0179	0.1132	0.0061	1793	28	1851	11
TPR4_130	2.76	0.0176	0.1289	0.0060	1996	30	2083	10
TPR4_131	2.72	0.0187	0.1275	0.0057	2018	32	2063	10
TPR4_132	1.97	0.0200	0.1838	0.0053	2641	43	2687	9
TPR4_133	2.98	0.0189	0.1138	0.0057	1868	31	1861	10
TPR4_134	3.05	0.0207	0.1148	0.0068	1826	33	1876	12
TPR4_135	3.18	0.0177	0.1129	0.0051	1761	27	1847	9
TPR4_136	2.66	0.0210	0.1266	0.0066	2058	37	2051	12
TPR4_137	2.95	0.0186	0.1183	0.0054	1883	30	1931	10
			>10% Discordant					
TPR4_89	3.15	0.0123	0.1324	0.0099	1776	19	2130	17
TPR4_125	2.73	0.0107	0.1806	0.0061	2011	18	2658	10

Sample	$^{238}U/^{206}Pb$	1 σ (%) +/-	$^{207}Pb/^{206}Pb$	1 σ (%)	$^{238}U/^{206}Pb$ Age (Ma)	1 σ (abs) +/-	$^{207}Pb/^{206}Pb$ Age (Ma)	1 σ (abs) +/-
Twin Peaks Ranch 3 (Lower Middle) <10% Discordant								
TPR3_1	2.73	0.0177	0.1179	0.0052	2009	30	1924	9
TPR3_2	2.76	0.0171	0.1191	0.0050	1992	29	1943	9
TPR3_3	2.92	0.0165	0.1119	0.0041	1899	27	1831	7
TPR3_4	2.78	0.0160	0.1177	0.0038	1982	27	1922	7
TPR3_5	2.82	0.0161	0.1192	0.0039	1959	27	1944	7
TPR3_6	1.93	0.0162	0.1857	0.0036	2695	36	2705	6
TPR3_7	3.15	0.0181	0.1148	0.0049	1779	28	1877	9
TPR3_8	2.95	0.0165	0.1126	0.0049	1881	27	1843	9
TPR3_9	3.05	0.0162	0.1100	0.0042	1828	26	1799	8
TPR3_10	2.97	0.0173	0.1140	0.0044	1868	28	1864	8
TPR3_11	2.78	0.0145	0.1188	0.0040	1980	25	1938	7
TPR3_12	3.02	0.0144	0.1119	0.0043	1843	23	1830	8
TPR3_13	3.10	0.0141	0.1112	0.0044	1802	22	1820	8
TPR3_14	2.90	0.0145	0.1115	0.0043	1913	24	1824	8
TPR3_15	2.90	0.0145	0.1199	0.0054	1909	24	1955	10
TPR3_16	2.27	0.0143	0.1521	0.0041	2352	28	2370	7
TPR3_17	2.89	0.0161	0.1211	0.0075	1916	27	1973	13
TPR3_19	3.03	0.0158	0.1126	0.0076	1839	25	1842	14
TPR3_20	2.82	0.0142	0.1169	0.0047	1957	24	1909	8
TPR3_21	3.03	0.0135	0.1132	0.0042	1838	22	1851	8
TPR3_22	2.05	0.0129	0.1699	0.0039	2564	27	2556	7
TPR3_23	2.97	0.0132	0.1169	0.0039	1872	21	1909	7
TPR3_24	2.38	0.0126	0.1464	0.0038	2261	24	2304	7
TPR3_25	3.04	0.0139	0.1132	0.0061	1832	22	1851	11

TPR3_26	3.12	0.0140	0.1137	0.0044	1790	22	1860	8
TPR3_27	3.08	0.0136	0.1131	0.0047	1813	21	1849	9
TPR3_28	2.07	0.0126	0.1692	0.0036	2537	26	2549	6
TPR3_29	2.93	0.0153	0.1254	0.0067	1895	25	2034	12
TPR3_30	3.08	0.0138	0.1112	0.0056	1814	22	1819	10
TPR3_31	2.03	0.0098	0.1733	0.0054	2582	21	2590	9
TPR3_32	2.59	0.0107	0.1272	0.0055	2104	19	2060	10
TPR3_33	1.84	0.0111	0.1907	0.0061	2795	25	2748	10
TPR3_34	3.03	0.0124	0.1198	0.0064	1838	20	1953	11
TPR3_35	2.88	0.0099	0.1177	0.0059	1919	16	1922	11
TPR3_36	2.93	0.0106	0.1165	0.0072	1892	17	1903	13
TPR3_37	2.46	0.0094	0.1463	0.0056	2196	18	2303	10
TPR3_38	2.92	0.0112	0.1161	0.0065	1901	18	1897	12
TPR3_39	1.92	0.0116	0.1897	0.0058	2707	26	2740	10
TPR3_40	3.34	0.0122	0.1145	0.0063	1687	18	1873	11
TPR3_41	3.01	0.0110	0.1128	0.0051	1848	18	1844	9
TPR3_42	1.99	0.0127	0.1746	0.0051	2629	27	2602	8
TPR3_43	3.41	0.0117	0.1053	0.0055	1658	17	1719	10
TPR3_44	2.23	0.0110	0.1527	0.0047	2390	22	2376	8
TPR3_45	3.04	0.0117	0.1111	0.0058	1836	19	1818	10
TPR3_46	3.10	0.0120	0.1117	0.0065	1803	19	1827	12
TPR3_47	3.12	0.0118	0.1120	0.0060	1790	18	1832	11
TPR3_48	2.25	0.0109	0.1616	0.0049	2373	22	2472	8
TPR3_49	2.19	0.0113	0.1683	0.0049	2428	23	2540	8
TPR3_50	2.41	0.0117	0.1571	0.0054	2240	22	2425	9
TPR3_51	3.12	0.0090	0.1116	0.0047	1791	14	1826	8
TPR3_52	3.16	0.0097	0.1101	0.0051	1772	15	1801	9
TPR3_53	1.99	0.0086	0.1859	0.0038	2624	18	2706	6
TPR3_54	2.01	0.0090	0.1849	0.0042	2605	19	2697	7
TPR3_56	2.95	0.0087	0.1178	0.0044	1880	14	1923	8
TPR3_57	3.13	0.0091	0.1118	0.0043	1789	14	1829	8
TPR3_59	3.07	0.0089	0.1165	0.0044	1819	14	1903	8
TPR3_60	2.85	0.0088	0.1234	0.0041	1941	15	2006	7
TPR3_61	3.07	0.0096	0.1142	0.0047	1817	15	1867	8
TPR3_62	5.95	0.0093	0.0735	0.0068	1001	9	1027	14
TPR3_63	3.25	0.0100	0.1117	0.0054	1732	15	1828	10
TPR3_64	3.25	0.0090	0.1123	0.0044	1730	14	1838	8
TPR3_65	3.18	0.0100	0.1109	0.0050	1761	15	1814	9
TPR3_66	3.58	0.0098	0.1076	0.0045	1588	14	1760	8
TPR3_67	3.01	0.0095	0.1174	0.0047	1848	15	1917	8
TPR3_68	3.10	0.0240	0.1140	0.0050	1804	38	1864	9
TPR3_69	1.97	0.0095	0.1865	0.0042	2646	21	2711	7
TPR3_70	2.38	0.0092	0.1454	0.0044	2265	18	2293	8
TPR3_71	3.11	0.0074	0.1064	0.0036	1796	12	1739	7
TPR3_72	2.96	0.0099	0.1182	0.0046	1874	16	1929	8
TPR3_73	3.16	0.0193	0.1135	0.0136	1772	30	1857	24
TPR3_74	2.92	0.0098	0.1180	0.0042	1899	16	1927	7

TPR3_75	2.32	0.0102	0.1463	0.0043	2310	20	2303	7
TPR3_76	2.94	0.0122	0.1157	0.0060	1886	20	1891	11
TPR3_77	1.94	0.0121	0.1816	0.0040	2676	26	2667	7
TPR3_78	3.12	0.0114	0.1124	0.0052	1795	18	1839	9
TPR3_79	3.02	0.0125	0.1152	0.0054	1841	20	1882	10
TPR3_80	2.64	0.0124	0.1285	0.0055	2072	22	2078	10
TPR3_81	2.68	0.0116	0.1291	0.0056	2043	20	2086	10
TPR3_82	3.04	0.0133	0.1167	0.0062	1836	21	1906	11
TPR3_83	3.17	0.0115	0.1134	0.0061	1770	18	1854	11
TPR3_84	3.02	0.0131	0.1204	0.0056	1846	21	1962	10
TPR3_85	1.97	0.0102	0.1833	0.0038	2645	22	2683	6
TPR3_87	3.19	0.0108	0.1096	0.0043	1759	17	1793	8
TPR3_88	2.03	0.0114	0.1742	0.0042	2578	24	2598	7
TPR3_89	2.97	0.0122	0.1163	0.0049	1872	20	1901	9
TPR3_90	3.17	0.0111	0.1125	0.0051	1767	17	1840	9
TPR3_91	3.00	0.0179	0.1182	0.0056	1854	29	1930	10
TPR3_92	2.42	0.0176	0.1513	0.0052	2233	33	2361	9
TPR3_93	2.90	0.0172	0.1181	0.0048	1907	28	1928	8
TPR3_94	2.45	0.0176	0.1508	0.0054	2206	33	2355	9
TPR3_95	2.66	0.0172	0.1304	0.0048	2055	30	2104	8
TPR3_96	3.01	0.0174	0.1174	0.0055	1852	28	1916	10
TPR3_97	1.99	0.0179	0.2042	0.0049	2626	38	2860	8
TPR3_98	3.15	0.0171	0.1165	0.0049	1776	26	1904	9
TPR3_99	3.13	0.0171	0.1130	0.0046	1788	27	1848	8
TPR3_100	1.85	0.0172	0.2038	0.0044	2783	39	2857	7
TPR3_101	3.13	0.0166	0.1126	0.0045	1787	26	1841	8
TPR3_102	2.60	0.0167	0.1344	0.0048	2098	30	2156	8
TPR3_103	2.66	0.0172	0.1311	0.0049	2054	30	2113	9
TPR3_104	3.04	0.0168	0.1127	0.0057	1831	27	1844	10
TPR3_105	2.99	0.0166	0.1178	0.0051	1858	27	1923	9
TPR3_106	3.21	0.0234	0.1103	0.0042	1750	36	1805	8
TPR3_107	3.11	0.0234	0.1117	0.0044	1795	37	1828	8
TPR3_108	3.03	0.0235	0.1140	0.0045	1837	38	1864	8
TPR3_109	3.11	0.0240	0.1140	0.0065	1798	38	1864	12
TPR3_110	2.96	0.0237	0.1177	0.0042	1879	38	1921	8
TPR3_111	2.87	0.0236	0.1303	0.0046	1924	39	2103	8
TPR3_112	2.84	0.0236	0.1222	0.0044	1947	39	1989	8
TPR3_113	3.11	0.0244	0.1120	0.0055	1797	38	1833	10
TPR3_114	3.10	0.0240	0.1175	0.0069	1801	38	1919	12
TPR3_115	3.25	0.0258	0.1136	0.0109	1729	39	1857	20
TPR3_116	3.14	0.0270	0.1151	0.0043	1782	42	1881	8
TPR3_117	2.08	0.0269	0.1715	0.0035	2528	56	2572	6
TPR3_118	2.85	0.0270	0.1274	0.0040	1936	45	2062	7
TPR3_119	5.80	0.0269	0.0732	0.0052	1026	25	1020	11
TPR3_120	2.97	0.0270	0.1188	0.0048	1870	44	1938	9
TPR3_121	3.06	0.0270	0.1144	0.0042	1822	43	1870	8
TPR3_124	2.00	0.0278	0.1877	0.0052	2613	59	2722	9

TPR3_125	2.05	0.0269	0.1746	0.0032	2559	57	2602	5
TPR3_126	3.00	0.0252	0.1176	0.0068	1856	40	1920	12
TPR3_127	3.19	0.0247	0.1119	0.0047	1757	38	1831	9
TPR3_128	3.20	0.0246	0.1122	0.0050	1755	38	1836	9
TPR3_129	3.22	0.0245	0.1112	0.0047	1744	37	1819	8
TPR3_130	3.22	0.0253	0.1112	0.0073	1745	39	1818	13
TPR3_131	3.18	0.0245	0.1111	0.0048	1763	38	1818	9
TPR3_132	3.27	0.0246	0.1126	0.0046	1721	37	1841	8
TPR3_133	3.24	0.0245	0.1119	0.0049	1736	37	1830	9
TPR3_134	2.94	0.0250	0.1156	0.0051	1888	41	1889	9
TPR3_135	2.89	0.0247	0.1199	0.0044	1913	41	1955	8
TPR3_136	2.81	0.0060	0.1141	0.0037	1961	10	1866	7
TPR3_137	5.45	0.0055	0.0734	0.0061	1086	6	1026	12
TPR3_138	2.97	0.0065	0.1117	0.0045	1870	11	1827	8
TPR3_139	2.97	0.0052	0.1123	0.0033	1868	8	1837	6
TPR3_140	2.91	0.0066	0.1108	0.0041	1902	11	1813	7
TPR3_141	3.28	0.0062	0.1076	0.0035	1717	9	1759	6
TPR3_142	2.76	0.0059	0.1174	0.0037	1994	10	1917	7
TPR3_143	2.83	0.0210	0.1139	0.0041	1948	35	1863	7
TPR3_144	1.80	0.0058	0.1864	0.0031	2843	13	2711	5
TPR3_145	2.18	0.0054	0.1454	0.0033	2438	11	2292	6
TPR3_146	3.11	0.0074	0.1064	0.0036	1796	12	1739	7
			>10% Discordant					
TPR3_58	2.44	0.0095	0.1692	0.0041	2217	18	2550	7
TPR3_55	2.32	0.0102	0.2010	0.0068	2314	20	2834	11
TPR3_86	3.30	0.0225	0.1716	0.0044	1706	34	2574	7
TPR3_123	3.17	0.0269	0.1344	0.0045	1769	42	2156	8
TPR3_122	3.33	0.0273	0.1156	0.0060	1691	40	1889	11

Sample	$^{238}U/^{206}Pb$	1 σ (%) +/-	$^{207}Pb/^{206}Pb$	1 σ (%)	$^{238}U/^{206}Pb$ Age (Ma)	1 σ (abs) +/-	$^{207}Pb/^{206}Pb$ Age (Ma)	1 σ (abs) +/-
Twin Peaks Ranch 5 (Basal) <10% Discordant								
TPR5_1	3.01	0.0245	0.1165	0.0051	1849	39	1903	9
TPR5_2	2.09	0.0243	0.1649	0.0041	2516	50	2507	7
TPR5_3	1.94	0.0247	0.1847	0.0046	2674	54	2695	8
TPR5_4	3.04	0.0241	0.1142	0.0048	1831	38	1867	9
TPR5_5	3.08	0.0241	0.1198	0.0097	1811	38	1953	17
TPR5_6	3.13	0.0265	0.1161	0.0073	1790	41	1897	13
TPR5_7	3.06	0.0240	0.1122	0.0052	1823	38	1835	9
TPR5_8	1.96	0.0247	0.1818	0.0050	2662	54	2669	8
TPR5_9	2.99	0.0240	0.1137	0.0046	1857	39	1859	8
TPR5_10	3.07	0.0248	0.1119	0.0062	1818	39	1830	11
TPR5_12	2.66	0.0182	0.1286	0.0045	2056	32	2078	8
TPR5_13	3.02	0.0183	0.1162	0.0058	1842	29	1899	10
TPR5_14	2.64	0.0174	0.1286	0.0035	2072	31	2079	6

TPR5_16	3.09	0.0177	0.1116	0.0040	1810	28	1826	7
TPR5_17	3.12	0.0169	0.1115	0.0033	1790	26	1823	6
TPR5_19	2.10	0.0180	0.1714	0.0044	2515	37	2572	7
TPR5_20	1.80	0.0177	0.2046	0.0034	2849	41	2863	6
TPR5_21	2.11	0.0179	0.1707	0.0023	2502	37	2564	4
TPR5_22	3.06	0.0177	0.1127	0.0022	1821	28	1843	4
TPR5_23	3.05	0.0176	0.1125	0.0022	1828	28	1840	4
TPR5_24	2.65	0.0181	0.1285	0.0034	2061	32	2077	6
TPR5_25	2.69	0.0174	0.1289	0.0023	2038	30	2084	4
TPR5_26	1.96	0.0183	0.1854	0.0021	2653	40	2702	3
TPR5_27	2.70	0.0177	0.1280	0.0025	2033	31	2071	4
TPR5_28	1.98	0.0178	0.1836	0.0028	2640	39	2686	5
TPR5_29	3.06	0.0177	0.1134	0.0023	1824	28	1855	4
TPR5_30	3.11	0.0181	0.1118	0.0037	1798	28	1830	7
TPR5_31	1.93	0.0146	0.1875	0.0030	2694	32	2721	5
TPR5_33	1.88	0.0143	0.1897	0.0026	2755	32	2739	4
TPR5_34	2.91	0.0174	0.1189	0.0061	1903	29	1939	11
TPR5_35	3.10	0.0150	0.1119	0.0041	1805	24	1831	7
TPR5_36	3.05	0.0145	0.1121	0.0035	1829	23	1833	6
TPR5_37	2.94	0.0149	0.1177	0.0040	1889	24	1922	7
TPR5_38	2.63	0.0145	0.1276	0.0032	2077	26	2065	6
TPR5_39	3.06	0.0143	0.1138	0.0028	1821	23	1861	5
TPR5_41	3.08	0.0162	0.1124	0.0026	1815	26	1839	5
TPR5_42	3.13	0.0176	0.1126	0.0043	1785	27	1842	8
TPR5_43	3.10	0.0177	0.1105	0.0045	1803	28	1807	8
TPR5_44	3.00	0.0198	0.1204	0.0073	1856	32	1963	13
TPR5_45	2.65	0.0166	0.1272	0.0029	2065	29	2059	5
TPR5_47	3.08	0.0167	0.1128	0.0037	1812	26	1845	7
TPR5_48	3.09	0.0181	0.1141	0.0032	1808	28	1865	6
TPR5_49	1.88	0.0166	0.1867	0.0026	2752	37	2713	4
TPR5_50	2.99	0.0164	0.1125	0.0026	1858	26	1840	5
TPR5_51	2.76	0.0151	0.1276	0.0064	1991	26	2066	11
TPR5_52	3.05	0.0129	0.1121	0.0057	1830	21	1834	10
TPR5_53	3.04	0.0121	0.1150	0.0052	1833	19	1880	9
TPR5_54	1.91	0.0128	0.1853	0.0056	2718	28	2701	9
TPR5_55	3.05	0.0123	0.1142	0.0056	1826	20	1867	10
TPR5_56	1.89	0.0119	0.2189	0.0049	2733	27	2973	8
TPR5_57	3.16	0.0117	0.1110	0.0052	1775	18	1815	9
TPR5_58	1.92	0.0121	0.1879	0.0050	2698	27	2724	8
TPR5_59	2.68	0.0128	0.1271	0.0060	2042	22	2058	11
TPR5_60	3.11	0.0128	0.1130	0.0058	1799	20	1848	11
TPR5_61	1.93	0.0121	0.1861	0.0054	2695	27	2708	9
TPR5_62	2.94	0.0116	0.1177	0.0055	1885	19	1921	10
TPR5_63	2.77	0.0133	0.1285	0.0061	1986	23	2077	11
TPR5_64	1.89	0.0146	0.1981	0.0065	2737	32	2811	11
TPR5_65	1.98	0.0128	0.1844	0.0055	2635	28	2693	9
TPR5_66	3.12	0.0117	0.1124	0.0055	1794	18	1838	10

TPR5_67	3.14	0.0156	0.1133	0.0082	1784	24	1853	15
TPR5_68	3.18	0.0166	0.1146	0.0085	1760	26	1874	15
TPR5_70	2.02	0.0137	0.1818	0.0061	2593	29	2669	10
TPR5_71	2.90	0.0143	0.1167	0.0064	1908	24	1906	11
TPR5_72	2.51	0.0132	0.1322	0.0056	2163	24	2128	10
TPR5_73	3.15	0.0144	0.1127	0.0072	1777	22	1844	13
TPR5_74	1.94	0.0143	0.1850	0.0058	2680	31	2698	10
TPR5_75	2.92	0.0135	0.1188	0.0058	1899	22	1939	10
TPR5_76	1.98	0.0189	0.1833	0.0043	2634	41	2683	7
TPR5_77	2.01	0.0183	0.1846	0.0030	2603	39	2694	5
TPR5_78	3.17	0.0180	0.1123	0.0038	1767	28	1837	7
TPR5_79	3.10	0.0197	0.1180	0.0064	1801	31	1926	11
TPR5_80	2.67	0.0183	0.1290	0.0039	2054	32	2084	7
TPR5_81	2.98	0.0184	0.1172	0.0046	1868	30	1914	8
TPR5_82	3.20	0.0185	0.1107	0.0045	1751	28	1811	8
TPR5_83	2.07	0.0200	0.1793	0.0046	2539	42	2646	8
TPR5_84	3.15	0.0178	0.1114	0.0036	1777	28	1822	7
TPR5_85	1.93	0.0188	0.1903	0.0041	2686	41	2745	7
TPR5_86	2.70	0.0182	0.1281	0.0035	2034	32	2072	6
TPR5_87	3.05	0.0188	0.1137	0.0041	1828	30	1859	7
TPR5_88	3.07	0.0183	0.1125	0.0039	1815	29	1840	7
TPR5_89	2.91	0.0179	0.1175	0.0034	1902	29	1919	6
TPR5_90	1.95	0.0178	0.1859	0.0030	2664	39	2706	5
TPR5_91	3.19	0.0136	0.1156	0.0066	1760	21	1889	12
TPR5_92	3.28	0.0136	0.1137	0.0071	1713	20	1859	13
TPR5_93	3.17	0.0126	0.1107	0.0051	1767	19	1812	9
TPR5_94	2.91	0.0128	0.1157	0.0047	1901	21	1890	8
TPR5_95	2.97	0.0125	0.1152	0.0049	1873	20	1883	9
TPR5_96	3.11	0.0123	0.1120	0.0046	1797	19	1832	8
TPR5_97	2.73	0.0133	0.1272	0.0052	2014	23	2060	9
TPR5_98	2.72	0.0126	0.1283	0.0047	2017	22	2075	8
TPR5_99	3.06	0.0126	0.1120	0.0050	1824	20	1832	9
TPR5_100	3.06	0.0139	0.1156	0.0056	1821	22	1890	10
TPR5_101	2.68	0.0125	0.1278	0.0047	2043	22	2068	8
TPR5_102	3.18	0.0132	0.1120	0.0056	1760	20	1832	10
TPR5_103	1.99	0.0125	0.1863	0.0047	2622	27	2710	8
TPR5_104	3.10	0.0121	0.1120	0.0048	1800	19	1832	9
TPR5_105	3.18	0.0125	0.1122	0.0052	1763	19	1835	9
TPR5_106	2.06	0.0114	0.1672	0.0053	2550	24	2530	9
TPR5_107	3.15	0.0153	0.1114	0.0085	1776	24	1822	15
TPR5_108	3.19	0.0120	0.1125	0.0061	1758	18	1841	11
TPR5_109	2.09	0.0134	0.1808	0.0066	2516	28	2660	11
TPR5_111	2.01	0.0121	0.1790	0.0053	2600	26	2644	9
TPR5_112	3.19	0.0124	0.1109	0.0065	1757	19	1814	12
TPR5_113	1.95	0.0128	0.1808	0.0058	2668	28	2660	10
TPR5_114	3.05	0.0117	0.1152	0.0058	1826	19	1882	10
TPR5_115	2.89	0.0118	0.1212	0.0054	1913	20	1973	10

TPR5_116	3.04	0.0123	0.1141	0.0055	1835	20	1865	10
TPR5_117	2.01	0.0116	0.1814	0.0053	2598	25	2666	9
TPR5_118	1.95	0.0120	0.1877	0.0053	2668	26	2722	9
TPR5_119	3.14	0.0115	0.1119	0.0056	1781	18	1831	10
TPR5_120	3.14	0.0123	0.1123	0.0058	1783	19	1836	11
TPR5_121	2.09	0.0185	0.1706	0.0045	2516	38	2564	8
TPR5_122	1.97	0.0181	0.1818	0.0041	2650	39	2669	7
TPR5_123	2.93	0.0184	0.1214	0.0052	1894	30	1977	9
TPR5_124	3.05	0.0181	0.1127	0.0045	1826	29	1844	8
TPR5_125	3.07	0.0180	0.1132	0.0043	1820	29	1852	8
TPR5_126	1.99	0.0179	0.1854	0.0040	2624	38	2702	7
TPR5_127	2.76	0.0182	0.1284	0.0044	1991	31	2076	8
TPR5_128	3.15	0.0179	0.1123	0.0042	1776	28	1838	8
TPR5_129	3.00	0.0182	0.1197	0.0044	1853	29	1952	8
TPR5_130	3.16	0.0194	0.1105	0.0057	1772	30	1807	10
TPR5_131	3.17	0.0181	0.1121	0.0045	1766	28	1833	8
TPR5_132	3.06	0.0178	0.1138	0.0045	1825	28	1861	8
TPR5_133	3.12	0.0182	0.1150	0.0050	1790	28	1880	9
TPR5_134	3.16	0.0186	0.1123	0.0048	1772	29	1837	9
TPR5_135	2.95	0.0182	0.1178	0.0050	1883	30	1923	9
			>10% Discordant					
TPR5_18	3.25	0.0194	0.1191	0.0048	1731	29	1942	9
TPR5_40	3.36	0.0154	0.1149	0.0035	1681	23	1878	6
TPR5_110	3.74	0.0141	0.1123	0.0064	1528	19	1837	12

Sample	$^{238}U/^{206}Pb$	1 σ (%) +/-	$^{207}Pb/^{206}Pb$	1 σ (%)	$^{238}U/^{206}Pb$ Age (Ma)	1 σ (abs) +/-	$^{207}Pb/^{206}Pb$ Age (Ma)	1 σ (abs) +/-
Clayton Mine 3 (Upper) <10% Discordant								
CM3_1	3.09	0.0207	0.1128	0.0043	1806	32	1845	8
CM3_2	3.15	0.0209	0.1152	0.0051	1777	32	1883	9
CM3_3	2.02	0.0205	0.1838	0.0036	2587	43	2687	6
CM3_4	3.14	0.0209	0.1131	0.0054	1784	32	1849	10
CM3_6	2.92	0.0207	0.1175	0.0042	1901	34	1919	8
CM3_7	3.21	0.0207	0.1125	0.0044	1747	32	1840	8
CM3_8	2.32	0.0207	0.1546	0.0037	2308	40	2398	6
CM3_9	3.19	0.0207	0.1137	0.0046	1757	32	1860	8
CM3_10	3.13	0.0204	0.1139	0.0038	1788	32	1863	7
CM3_11	3.01	0.0148	0.1154	0.0040	1847	24	1886	7
CM3_12	2.06	0.0158	0.1798	0.0048	2553	33	2651	8
CM3_13	2.93	0.0148	0.1183	0.0042	1892	24	1930	7
CM3_14	1.96	0.0149	0.1875	0.0038	2655	32	2721	6
CM3_15	3.13	0.0148	0.1115	0.0042	1789	23	1824	8
CM3_16	1.98	0.0152	0.1852	0.0043	2640	33	2700	7
CM3_17	3.19	0.0154	0.1137	0.0053	1756	24	1860	10
CM3_18	2.85	0.0146	0.1296	0.0037	1936	24	2092	7

CM3_19	2.95	0.0157	0.1140	0.0059	1882	26	1865	11
CM3_20	3.15	0.0157	0.1120	0.0063	1778	24	1832	11
CM3_21	3.10	0.0151	0.1135	0.0049	1804	24	1856	9
CM3_22	2.98	0.0157	0.1167	0.0056	1866	25	1906	10
CM3_23	3.16	0.0154	0.1123	0.0052	1770	24	1837	9
CM3_24	3.28	0.0156	0.1166	0.0063	1717	23	1905	11
CM3_25	3.06	0.0149	0.1165	0.0043	1825	24	1904	8
CM3_26	3.05	0.0077	0.1112	0.0035	1826	12	1819	6
CM3_27	3.05	0.0086	0.1126	0.0052	1829	14	1842	9
CM3_28	3.17	0.0091	0.1161	0.0067	1769	14	1896	12
CM3_29	2.96	0.0071	0.1178	0.0035	1876	11	1922	6
CM3_30	2.73	0.0079	0.1288	0.0047	2011	14	2082	8
CM3_31	2.99	0.0074	0.1141	0.0040	1860	12	1865	7
CM3_32	3.07	0.0081	0.1113	0.0047	1819	13	1821	9
CM3_33	3.07	0.0083	0.1132	0.0051	1819	13	1851	9
CM3_34	3.09	0.0088	0.1125	0.0061	1807	14	1841	11
CM3_35	2.31	0.0081	0.1584	0.0039	2322	16	2439	7
CM3_36	2.66	0.0107	0.1283	0.0051	2059	19	2074	9
CM3_37	2.66	0.0076	0.1290	0.0037	2054	13	2084	6
CM3_38	2.64	0.0069	0.1304	0.0033	2071	12	2104	6
CM3_39	3.06	0.0084	0.1142	0.0050	1822	13	1868	9
CM3_40	2.70	0.0081	0.1282	0.0042	2029	14	2074	7
CM3_41	2.97	0.0082	0.1185	0.0044	1870	13	1934	8
CM3_42	3.00	0.0085	0.1178	0.0045	1856	14	1923	8
CM3_43	3.07	0.0116	0.1109	0.0076	1819	18	1814	14
CM3_44	2.97	0.0096	0.1163	0.0062	1870	16	1900	11
CM3_45	2.68	0.0080	0.1291	0.0044	2046	14	2086	8
CM3_46	2.96	0.0088	0.1181	0.0048	1875	14	1927	9
CM3_47	3.12	0.0077	0.1126	0.0043	1795	12	1842	8
CM3_48	3.29	0.0082	0.1075	0.0050	1710	12	1758	9
CM3_49	3.11	0.0129	0.1109	0.0093	1797	20	1815	17
CM3_50	3.06	0.0090	0.1153	0.0056	1822	14	1885	10
CM3_51	3.05	0.0076	0.1131	0.0037	1827	12	1850	7
CM3_52	2.96	0.0080	0.1174	0.0040	1874	13	1917	7
CM3_53	2.97	0.0083	0.1181	0.0043	1870	13	1928	8
CM3_55	3.10	0.0099	0.1109	0.0066	1804	16	1814	12
CM3_56	2.87	0.0137	0.1182	0.0040	1929	23	1929	7
CM3_57	3.01	0.0133	0.1159	0.0035	1851	21	1894	6
CM3_58	3.16	0.0139	0.1118	0.0046	1771	22	1829	8
CM3_59	2.00	0.0135	0.1854	0.0037	2616	29	2701	6
CM3_60	3.17	0.0137	0.1131	0.0045	1767	21	1850	8
CM3_61	2.97	0.0139	0.1199	0.0058	1871	22	1955	10
CM3_62	2.96	0.0135	0.1176	0.0042	1874	22	1921	8
CM3_63	2.67	0.0133	0.1277	0.0038	2052	23	2067	7
CM3_64	2.84	0.0146	0.1286	0.0049	1943	24	2079	9
CM3_65	3.20	0.0135	0.1123	0.0041	1754	21	1838	7
CM3_66	2.67	0.0138	0.1282	0.0042	2051	24	2073	7

CM3_67	3.07	0.0141	0.1114	0.0055	1818	22	1822	10
CM3_68	2.95	0.0134	0.1164	0.0040	1884	22	1902	7
CM3_69	2.93	0.0144	0.1189	0.0054	1894	24	1940	10
CM3_70	2.94	0.0142	0.1123	0.0054	1887	23	1837	10
CM3_71	3.06	0.0063	0.1112	0.0046	1823	10	1820	8
CM3_72	2.57	0.0076	0.1289	0.0046	2120	14	2083	8
CM3_74	3.05	0.0060	0.1126	0.0042	1829	9	1843	8
CM3_75	3.14	0.0065	0.1119	0.0046	1780	10	1831	8
CM3_76	3.14	0.0057	0.1116	0.0039	1783	9	1826	7
CM3_77	3.16	0.0069	0.1122	0.0048	1772	11	1835	9
CM3_78	2.02	0.0061	0.1833	0.0040	2593	13	2683	7
CM3_79	3.16	0.0069	0.1118	0.0051	1774	11	1828	9
CM3_80	3.18	0.0068	0.1114	0.0046	1762	10	1823	8
CM3_81	2.70	0.0061	0.1281	0.0045	2033	11	2072	8
CM3_82	1.73	0.0085	0.2173	0.0052	2946	20	2961	8
CM3_83	2.90	0.0068	0.1170	0.0049	1907	11	1910	9
CM3_84	3.00	0.0085	0.1123	0.0061	1853	14	1837	11
CM3_85	2.92	0.0067	0.1184	0.0053	1898	11	1933	9
CM3_86	2.95	0.0066	0.1171	0.0068	1884	11	1912	12
CM3_87	5.77	0.0058	0.0737	0.0072	1030	6	1033	14
CM3_88	2.66	0.0061	0.1316	0.0066	2058	11	2120	12
CM3_89	2.99	0.0059	0.1163	0.0065	1857	9	1900	12
CM3_90	3.12	0.0053	0.1133	0.0068	1794	8	1853	12
CM3_91	2.89	0.0047	0.1216	0.0062	1913	8	1980	11
CM3_92	2.92	0.0050	0.1184	0.0061	1901	8	1932	11
CM3_93	2.97	0.0049	0.1173	0.0062	1873	8	1915	11
CM3_94	2.95	0.0044	0.1175	0.0059	1879	7	1919	11
CM3_95	3.06	0.0064	0.1133	0.0071	1821	10	1853	13
CM3_96	3.18	0.0045	0.1087	0.0059	1761	7	1778	11
CM3_97	1.92	0.0049	0.1863	0.0059	2697	11	2710	10
CM3_98	2.71	0.0064	0.1282	0.0070	2025	11	2074	12
CM3_99	2.00	0.0064	0.1823	0.0065	2609	14	2674	11
CM3_100	3.00	0.0052	0.1140	0.0060	1854	8	1864	11
CM3_101	3.02	0.0072	0.1121	0.0073	1842	12	1834	13
CM3_102	2.94	0.0082	0.1180	0.0075	1890	13	1926	13
CM3_103	3.00	0.0077	0.1157	0.0076	1855	12	1891	14
CM3_104	1.93	0.0068	0.1843	0.0066	2690	15	2692	11
CM3_105	3.16	0.0070	0.1127	0.0076	1773	11	1844	14
CM3_106	2.02	0.0058	0.1802	0.0063	2595	12	2655	10
CM3_107	3.01	0.0070	0.1133	0.0074	1847	11	1852	13
CM3_108	3.11	0.0098	0.1134	0.0078	1797	15	1855	14
CM3_109	2.74	0.0073	0.1286	0.0081	2008	13	2079	14
CM3_110	3.12	0.0068	0.1121	0.0075	1791	11	1833	14
CM3_111	1.91	0.0071	0.1871	0.0066	2712	16	2717	11
CM3_112	2.98	0.0067	0.1183	0.0071	1864	11	1930	13
CM3_113	3.19	0.0073	0.1103	0.0075	1758	11	1805	14
CM3_114	2.01	0.0058	0.1786	0.0063	2605	12	2640	10

CM3_115	3.15	0.0060	0.1121	0.0066	1778	9	1833	12
CM3_116	3.08	0.0066	0.1130	0.0048	1811	10	1848	9
CM3_117	2.05	0.0062	0.1822	0.0032	2563	13	2673	5
CM3_118	2.22	0.0052	0.1636	0.0025	2395	10	2493	4
CM3_119	3.16	0.0072	0.1138	0.0051	1773	11	1861	9
CM3_120	3.18	0.0061	0.1131	0.0039	1764	9	1849	7
CM3_121	2.22	0.0058	0.1652	0.0031	2396	12	2510	5
CM3_122	3.23	0.0075	0.1138	0.0053	1740	11	1862	10
CM3_123	1.99	0.0073	0.1886	0.0042	2623	16	2730	7
CM3_124	3.25	0.0071	0.1126	0.0050	1729	11	1842	9
CM3_126	3.05	0.0053	0.1146	0.0029	1826	8	1874	5
CM3_127	2.71	0.0078	0.1291	0.0045	2022	13	2086	8
CM3_128	3.01	0.0083	0.1201	0.0070	1850	13	1958	12
CM3_129	3.09	0.0063	0.1130	0.0044	1805	10	1848	8
CM3_130	3.06	0.0074	0.1121	0.0048	1825	12	1834	9
CM3_131	2.95	0.0063	0.1179	0.0045	1883	10	1924	8
CM3_132	3.17	0.0070	0.1131	0.0059	1766	11	1849	11
CM3_133	3.11	0.0059	0.1126	0.0052	1799	9	1842	9
CM3_134	2.83	0.0049	0.1175	0.0036	1949	8	1918	7
CM3_135	2.91	0.0067	0.1180	0.0047	1905	11	1925	8
CM3_136	3.15	0.0051	0.1138	0.0040	1775	8	1861	7
CM3_137	2.70	0.0047	0.1292	0.0037	2031	8	2088	6
CM3_139	2.65	0.0114	0.1282	0.0083	2066	20	2073	15
CM3_140	2.87	0.0081	0.1170	0.0062	1927	14	1911	11
CM3_141	2.93	0.0048	0.1170	0.0040	1890	8	1912	7
			>10% Discordant					
CM3_5	3.45	0.0208	0.1181	0.0039	1640	30	1928	7
CM3_54	2.18	0.0104	0.1927	0.0046	2430	21	2765	7
CM3_73	3.44	0.0065	0.1161	0.0045	1644	9	1896	8
CM3_125	3.28	0.0057	0.1176	0.0034	1715	9	1921	6

Sample	$^{238}U/^{206}Pb$	1 σ (%) +/-	$^{207}Pb/^{206}Pb$	1 σ (%)	$^{238}U/^{206}Pb$ Age (Ma)	1 σ (abs) +/-	$^{207}Pb/^{206}Pb$ Age (Ma)	1 σ (abs) +/-
Clayton Mine 2 (Middle) <10% Discordant								
CM2_1	3.27	0.0194	0.1119	0.0074	1721	29	1831	13
CM2_3	2.93	0.0190	0.1184	0.0066	1893	31	1932	12
CM2_4	3.18	0.0192	0.1129	0.0076	1761	30	1847	14
CM2_5	3.03	0.0194	0.1136	0.0066	1839	31	1857	12
CM2_6	3.19	0.0191	0.1119	0.0064	1759	29	1831	12
CM2_7	2.79	0.0198	0.1300	0.0067	1977	34	2097	12
CM2_8	2.66	0.0194	0.1294	0.0073	2055	34	2090	13
CM2_9	3.22	0.0210	0.1165	0.0082	1741	32	1903	15
CM2_10	2.71	0.0195	0.1277	0.0070	2027	34	2066	12
CM2_11	2.78	0.0205	0.1231	0.0084	1980	35	2002	15
CM2_12	2.80	0.0212	0.1289	0.0102	1971	36	2083	18

CM2_13	2.98	0.0191	0.1167	0.0067	1867	31	1907	12
CM2_14	3.15	0.0376	0.1153	0.0106	1776	58	1884	19
CM2_15	2.64	0.0558	0.1270	0.0228	2069	98	2057	40
CM2_16	3.27	0.0175	0.1126	0.0081	1719	26	1842	15
CM2_17	3.24	0.0176	0.1174	0.0083	1734	27	1918	15
CM2_18	3.19	0.0195	0.1146	0.0096	1760	30	1873	17
CM2_19	3.12	0.0178	0.1126	0.0089	1793	28	1842	16
CM2_20	2.36	0.0163	0.1458	0.0076	2277	31	2297	13
CM2_21	3.04	0.0174	0.1203	0.0111	1836	28	1960	20
CM2_22	3.11	0.0164	0.1167	0.0089	1799	26	1906	16
CM2_23	2.17	0.0160	0.1781	0.0072	2439	32	2635	12
CM2_24	3.02	0.0197	0.1168	0.0092	1845	31	1907	16
CM2_25	3.15	0.0161	0.1140	0.0087	1779	25	1865	16
CM2_26	1.81	0.0173	0.2024	0.0086	2838	40	2846	14
CM2_27	3.15	0.0184	0.1122	0.0100	1778	29	1835	18
CM2_28	1.92	0.0173	0.1889	0.0078	2702	38	2732	13
CM2_29	3.00	0.0162	0.1116	0.0081	1852	26	1826	15
CM2_30	2.92	0.0151	0.1183	0.0072	1898	25	1931	13
CM2_31	3.15	0.0195	0.1100	0.0096	1778	30	1799	17
CM2_32	3.22	0.0188	0.1120	0.0107	1744	29	1832	19
CM2_33	2.05	0.0218	0.1847	0.0103	2561	46	2696	17
CM2_34	3.10	0.0140	0.1176	0.0067	1804	22	1920	12
CM2_35	3.13	0.0153	0.1125	0.0081	1787	24	1840	15
CM2_36	1.97	0.0142	0.1853	0.0061	2641	31	2701	10
CM2_37	2.02	0.0188	0.1893	0.0073	2591	40	2736	12
CM2_38	2.96	0.0138	0.1180	0.0073	1875	22	1926	13
CM2_39	2.81	0.0148	0.1177	0.0077	1965	25	1921	14
CM2_40	3.09	0.0135	0.1192	0.0063	1806	21	1945	11
CM2_41	3.17	0.0166	0.1113	0.0094	1767	26	1820	17
CM2_42	2.88	0.0153	0.1110	0.0076	1919	25	1816	14
CM2_43	2.17	0.0134	0.1652	0.0060	2445	27	2509	10
CM2_44	3.32	0.0146	0.1100	0.0081	1698	22	1799	15
CM2_45	3.00	0.0316	0.1134	0.0241	1856	51	1855	43
CM2_46	1.98	0.0181	0.1854	0.0071	2638	39	2702	12
CM2_48	3.37	0.0523	0.1109	0.0668	1674	77	1815	117
CM2_49	2.96	0.0146	0.1159	0.0077	1874	24	1893	14
CM2_50	3.00	0.0144	0.1179	0.0067	1855	23	1924	12
CM2_51	6.04	0.0178	0.0721	0.0126	988	16	988	25
CM2_52	3.51	0.0219	0.1076	0.0107	1617	31	1760	19
CM2_53	2.93	0.0150	0.1135	0.0065	1890	25	1857	12
CM2_54	3.21	0.0154	0.1109	0.0076	1751	24	1814	14
CM2_55	3.11	0.0195	0.1120	0.0102	1797	30	1832	18
CM2_56	3.26	0.0164	0.1098	0.0095	1727	25	1795	17
CM2_57	3.30	0.0149	0.1154	0.0071	1708	22	1887	13
CM2_59	1.97	0.0164	0.1847	0.0076	2647	35	2696	12
CM2_60	2.64	0.0146	0.1272	0.0069	2070	26	2060	12
CM2_61	3.03	0.0229	0.1123	0.0041	1836	36	1837	7

CM2_62	2.82	0.0245	0.1227	0.0049	1957	41	1995	9
CM2_63	3.06	0.0272	0.1123	0.0071	1821	43	1836	13
CM2_64	2.27	0.0240	0.1691	0.0043	2354	47	2549	7
CM2_65	3.12	0.0237	0.1176	0.0060	1794	37	1920	11
CM2_67	2.49	0.0230	0.1463	0.0046	2174	42	2303	8
CM2_68	2.03	0.0235	0.1958	0.0046	2583	50	2792	7
CM2_69	3.17	0.0230	0.1123	0.0049	1766	35	1837	9
CM2_70	3.04	0.0237	0.1168	0.0059	1831	38	1908	11
CM2_71	2.82	0.0060	0.1181	0.0048	1955	10	1928	9
CM2_72	2.93	0.0101	0.1201	0.0064	1893	16	1958	11
CM2_73	3.12	0.0102	0.1143	0.0077	1794	16	1869	14
CM2_74	3.04	0.0071	0.1122	0.0048	1835	11	1835	9
CM2_75	3.15	0.0055	0.1119	0.0045	1777	9	1830	8
CM2_76	3.19	0.0057	0.1142	0.0050	1758	9	1867	9
CM2_77	3.05	0.0095	0.1158	0.0063	1826	15	1892	11
CM2_78	2.77	0.0084	0.1265	0.0055	1984	14	2051	10
CM2_79	3.10	0.0070	0.1125	0.0053	1802	11	1841	10
CM2_80	3.12	0.0110	0.1208	0.0049	1793	17	1969	9
CM2_81	3.34	0.0152	0.1129	0.0050	1690	23	1846	9
CM2_82	3.15	0.0139	0.1128	0.0039	1776	21	1846	7
CM2_83	3.16	0.0203	0.1153	0.0101	1773	31	1884	18
CM2_84	2.56	0.0137	0.1279	0.0038	2129	25	2069	7
CM2_85	2.98	0.0147	0.1181	0.0051	1867	24	1927	9
CM2_86	3.04	0.0144	0.1112	0.0050	1834	23	1819	9
CM2_87	2.98	0.0138	0.1185	0.0044	1863	22	1934	8
CM2_88	3.23	0.0174	0.1170	0.0048	1741	26	1910	9
CM2_89	1.99	0.0137	0.1873	0.0037	2630	29	2719	6
CM2_90	3.18	0.0176	0.1165	0.0071	1763	27	1903	13
CM2_91	3.13	0.0118	0.1139	0.0045	1790	18	1862	8
CM2_92	3.12	0.0150	0.1172	0.0062	1794	23	1915	11
CM2_93	2.30	0.0135	0.1681	0.0045	2328	26	2539	8
CM2_94	3.11	0.0127	0.1142	0.0049	1798	20	1867	9
CM2_95	2.21	0.0133	0.1736	0.0058	2410	27	2593	10
CM2_96	2.02	0.0140	0.1656	0.0060	2590	30	2513	10
CM2_97	3.10	0.0130	0.1177	0.0052	1802	20	1922	9
CM2_98	3.16	0.0133	0.1188	0.0049	1773	21	1938	9
CM2_99	3.24	0.0147	0.1114	0.0071	1734	22	1823	13
CM2_100	2.05	0.0162	0.1822	0.0073	2562	34	2673	12
CM2_101	2.02	0.0130	0.1916	0.0051	2595	28	2756	8
CM2_102	3.18	0.0160	0.1132	0.0087	1762	25	1851	16
CM2_103	3.03	0.0145	0.1136	0.0065	1837	23	1858	12
CM2_104	3.31	0.0141	0.1150	0.0050	1702	21	1880	9
CM2_105	2.74	0.0149	0.1287	0.0062	2007	26	2080	11
CM2_106	2.71	0.0109	0.1290	0.0079	2022	19	2084	14
CM2_107	1.96	0.0125	0.1886	0.0079	2660	27	2730	13
CM2_108	3.19	0.0153	0.1129	0.0108	1759	23	1846	19
CM2_109	3.10	0.0109	0.1074	0.0080	1802	17	1756	15

CM2_110	2.95	0.0098	0.1173	0.0074	1883	16	1916	13
CM2_111	3.01	0.0106	0.1179	0.0081	1849	17	1925	14
CM2_112	1.94	0.0151	0.1879	0.0087	2685	33	2724	14
CM2_113	3.26	0.0117	0.1150	0.0090	1723	18	1879	16
CM2_114	2.99	0.0107	0.1189	0.0082	1859	17	1940	15
CM2_115	2.93	0.0101	0.1183	0.0075	1894	17	1931	13
CM2_116	3.10	0.0120	0.1135	0.0093	1800	19	1855	17
CM2_117	3.29	0.0146	0.1122	0.0094	1713	22	1835	17
CM2_118	2.93	0.0108	0.1187	0.0082	1891	18	1936	15
CM2_119	2.03	0.0123	0.1884	0.0085	2583	26	2728	14
CM2_120	1.94	0.0124	0.1834	0.0076	2679	27	2683	12
CM2_121	3.39	0.0202	0.1120	0.0134	1667	30	1832	24
CM2_123	2.81	0.0099	0.1316	0.0096	1965	17	2119	17
CM2_124	2.88	0.0096	0.1256	0.0091	1923	16	2037	16
CM2_125	3.11	0.0092	0.1167	0.0091	1797	14	1907	16
CM2_126	3.36	0.0098	0.1124	0.0090	1680	14	1839	16
CM2_127	2.91	0.0101	0.1179	0.0094	1903	17	1925	17
CM2_128	5.82	0.0113	0.0762	0.0132	1022	11	1099	26
CM2_130	1.96	0.0107	0.1956	0.0089	2655	23	2789	15
CM2_131	3.08	0.0104	0.1147	0.0089	1812	16	1876	16
CM2_132	1.73	0.0111	0.2277	0.0090	2942	26	3036	14
CM2_133	3.11	0.0091	0.1141	0.0090	1796	14	1866	16
CM2_134	3.21	0.0093	0.1126	0.0090	1746	14	1841	16
CM2_135	3.20	0.0102	0.1169	0.0087	1752	16	1910	16
			>10% Discordant					
CM2_58	3.977	0.0238	0.1098	0.0091	1446	31	1796	16
CM2_66	2.581	0.0240	0.1690	0.0046	2111	43	2548	8

Sample	$^{238}U/^{206}Pb$	1 σ (%) +/-	$^{207}Pb/^{206}Pb$	1 σ (%)	$^{238}U/^{206}Pb$ Age (Ma)	1 σ (abs) +/-	$^{207}Pb/^{206}Pb$ Age (Ma)	1 σ (abs) +/-
Clayton Mine 1 (Basal) <10% Discordant								
CM1_1	5.80	0.0171	0.0766	0.0070	1026	16	1112	14
CM1_3	2.92	0.0208	0.1130	0.0083	1898	34	1849	15
CM1_4	3.20	0.0156	0.1133	0.0053	1752	24	1853	9
CM1_6	2.95	0.0184	0.1183	0.0081	1881	30	1930	14
CM1_7	2.75	0.0220	0.1304	0.0145	2002	38	2103	25
CM1_8	2.16	0.0150	0.1632	0.0054	2451	31	2489	9
CM1_9	2.95	0.0187	0.1136	0.0071	1881	30	1857	13
CM1_10	1.94	0.0168	0.1708	0.0056	2676	37	2565	9
CM1_12	2.00	0.0182	0.1739	0.0060	2612	39	2596	10
CM1_13	2.88	0.0137	0.1193	0.0081	1923	23	1946	14
CM1_14	1.94	0.0179	0.1795	0.0074	2685	39	2648	12
CM1_15	3.18	0.0162	0.1131	0.0096	1761	25	1850	17

CM1_16	3.06	0.0173	0.1132	0.0069	1822	27	1851	12
CM1_17	3.12	0.0153	0.1151	0.0058	1790	24	1882	10
CM1_18	2.81	0.0190	0.1170	0.0083	1961	32	1910	15
CM1_20	3.04	0.0280	0.1147	0.0143	1835	45	1875	26
CM1_21	2.06	0.0252	0.1777	0.0097	2554	53	2632	16
CM1_22	1.89	0.0184	0.1862	0.0068	2735	41	2709	11
CM1_23	1.93	0.0216	0.1819	0.0088	2686	47	2671	14
CM1_24	5.91	0.0158	0.0753	0.0086	1008	15	1077	17
CM1_25	1.93	0.0180	0.1775	0.0076	2689	40	2629	13
CM1_27	3.14	0.0173	0.1162	0.0060	1781	27	1898	11
CM1_29	2.21	0.0144	0.1650	0.0055	2410	29	2508	9
CM1_30	2.44	0.0175	0.1356	0.0069	2213	33	2172	12
CM1_31	3.15	0.0245	0.1128	0.0075	1776	38	1844	13
CM1_32	3.30	0.0267	0.1136	0.0070	1708	40	1858	13
CM1_33	2.76	0.0274	0.1291	0.0047	1991	47	2086	8
CM1_34	2.03	0.0247	0.1870	0.0051	2578	52	2716	8
CM1_35	3.03	0.0258	0.1148	0.0090	1839	41	1877	16
CM1_36	2.71	0.0240	0.1302	0.0044	2027	42	2100	8
CM1_37	2.44	0.0266	0.1553	0.0057	2213	50	2405	10
CM1_39	2.87	0.0256	0.1203	0.0090	1930	43	1961	16
CM1_40	3.07	0.0300	0.1229	0.0130	1818	47	1999	23
CM1_41	2.63	0.0212	0.1314	0.0075	2076	38	2116	13
CM1_43	2.73	0.0203	0.1223	0.0108	2010	35	1990	19
CM1_44	2.05	0.0151	0.1814	0.0064	2560	32	2666	11
CM1_45	5.82	0.0140	0.0771	0.0067	1023	13	1123	13
CM1_46	3.23	0.0162	0.1139	0.0087	1738	25	1862	16
CM1_47	2.10	0.0153	0.1724	0.0067	2507	32	2581	11
CM1_48	2.21	0.0259	0.1676	0.0061	2405	52	2534	10
CM1_51	3.26	0.0189	0.1121	0.0078	1726	29	1834	14
CM1_52	3.15	0.0278	0.1207	0.0192	1776	43	1967	34
CM1_53	2.94	0.0340	0.1145	0.0443	1889	55	1873	78
CM1_54	2.63	0.0245	0.1375	0.0159	2078	43	2195	27
CM1_55	2.61	0.0208	0.1318	0.0101	2094	37	2122	18
CM1_56	2.30	0.0402	0.1068	0.0225	2326	78	1745	41
CM1_57	1.94	0.0177	0.1929	0.0076	2676	39	2767	12
CM1_58	3.12	0.0145	0.1141	0.0064	1791	23	1866	11
CM1_59	3.18	0.0171	0.1164	0.0095	1762	26	1901	17
CM1_60	2.90	0.0172	0.1242	0.0077	1913	28	2018	14
CM1_61	1.85	0.0171	0.2149	0.0160	2784	39	2943	26
CM1_62	3.03	0.0158	0.1152	0.0091	1840	25	1883	16
CM1_63	2.97	0.0169	0.1187	0.0108	1873	27	1937	19
CM1_64	3.03	0.0164	0.1214	0.0073	1840	26	1976	13
CM1_65	2.98	0.0235	0.1229	0.0156	1864	38	1999	27
CM1_66	2.04	0.0140	0.1835	0.0077	2573	30	2685	13
CM1_67	3.09	0.0131	0.1128	0.0085	1806	21	1844	15
CM1_68	1.96	0.0151	0.1962	0.0071	2656	33	2795	12

CM1_69	1.97	0.0213	0.1892	0.0096	2643	46	2736	16
CM1_70	2.72	0.0278	0.1318	0.0186	2015	48	2122	32
CM1_72	3.17	0.0146	0.1158	0.0084	1769	23	1892	15
CM1_73	2.95	0.0116	0.1201	0.0086	1879	19	1958	15
CM1_74	3.04	0.0219	0.1112	0.0105	1833	35	1818	19
CM1_75	2.35	0.0152	0.1504	0.0077	2289	29	2350	13
CM1_77	2.49	0.0113	0.1315	0.0073	2174	21	2118	13
CM1_78	3.07	0.0179	0.1198	0.0147	1818	28	1953	26
CM1_79	2.14	0.0189	0.1864	0.0093	2469	39	2710	15
CM1_80	2.95	0.0152	0.1178	0.0069	1880	25	1923	12
CM1_83	3.59	0.0150	0.1009	0.0099	1585	21	1641	18
CM1_85	2.87	0.0162	0.1239	0.0103	1925	27	2013	18
CM1_86	2.34	0.0156	0.1517	0.0083	2297	30	2366	14
CM1_87	3.17	0.0198	0.1170	0.0162	1767	31	1912	29
CM1_89	2.20	0.0137	0.1681	0.0069	2414	27	2539	12
CM1_90	2.26	0.0180	0.1664	0.0118	2366	36	2521	20
CM1_88	2.14	0.0141	0.1626	0.0064	2467	29	2483	11
CM1_91	3.05	0.0138	0.1160	0.0064	1829	22	1895	12
CM1_92	3.01	0.0143	0.1167	0.0065	1851	23	1906	12
CM1_93	2.95	0.0143	0.1208	0.0076	1884	23	1968	13
CM1_94	2.01	0.0191	0.1806	0.0080	2599	41	2658	13
CM1_95	3.24	0.0172	0.1111	0.0098	1736	26	1817	18
CM1_96	1.74	0.0108	0.2346	0.0067	2929	25	3084	11
CM1_97	3.10	0.0173	0.1135	0.0115	1800	27	1857	21
CM1_98	3.29	0.0189	0.1118	0.0091	1711	28	1829	16
CM1_99	3.19	0.0140	0.1162	0.0099	1756	21	1898	18
CM1_100	2.36	0.0150	0.1365	0.0086	2274	29	2183	15
CM1_101	3.07	0.0140	0.1172	0.0101	1819	22	1913	18
CM1_102	3.05	0.0131	0.1141	0.0090	1827	21	1866	16
CM1_103	2.97	0.0149	0.1196	0.0142	1872	24	1950	25
CM1_104	2.57	0.0142	0.1297	0.0105	2119	26	2095	18
CM1_105	2.87	0.0105	0.1148	0.0082	1930	18	1877	15
CM1_106	2.15	0.0121	0.1773	0.0086	2460	25	2627	14
CM1_107	3.05	0.0105	0.1140	0.0082	1828	17	1864	15
CM1_108	2.08	0.0177	0.1703	0.0099	2531	37	2561	17
CM1_109	3.26	0.0171	0.1133	0.0120	1725	26	1853	22
CM1_110	2.68	0.0118	0.1290	0.0075	2041	21	2085	13
CM1_112	2.70	0.0108	0.1299	0.0082	2034	19	2096	14
CM1_114	3.30	0.0135	0.1136	0.0084	1709	20	1857	15
CM1_115	2.93	0.0123	0.1172	0.0090	1891	20	1914	16
CM1_116	3.09	0.0115	0.1122	0.0076	1808	18	1835	14
CM1_117	3.21	0.0236	0.1144	0.0105	1751	36	1870	19
CM1_118	2.73	0.0239	0.1205	0.0119	2012	41	1963	21
CM1_119	2.34	0.0160	0.1539	0.0068	2293	31	2389	12
CM1_120	3.26	0.0163	0.1124	0.0094	1724	25	1838	17
CM1_121	3.04	0.0102	0.1167	0.0069	1832	16	1906	12
CM1_122	2.92	0.0133	0.1249	0.0085	1899	22	2028	15

CM1_123	3.06	0.0128	0.1161	0.0095	1823	20	1897	17
CM1_124	2.73	0.0134	0.1295	0.0068	2012	23	2091	12
CM1_125	1.96	0.0144	0.1872	0.0074	2656	31	2718	12
CM1_126	2.17	0.0238	0.1681	0.0097	2440	48	2539	16
CM1_127	3.02	0.0196	0.1256	0.0091	1842	31	2038	16
CM1_128	2.96	0.0137	0.1200	0.0081	1879	22	1956	14
CM1_129	3.07	0.0111	0.1125	0.0085	1819	18	1840	15
CM1_132	3.28	0.0164	0.1160	0.0111	1716	25	1895	20
				>10% Discordant				
CM1_2	4.05	0.0155	0.1030	0.0130	1421	20	1679	24
CM1_5	2.60	0.0273	0.1935	0.0100	2101	49	2772	16
CM1_11	6.66	0.0242	0.0758	0.0109	902	20	1089	22
CM1_19	3.17	0.0332	0.1355	0.0197	1767	51	2171	34
CM1_26	3.24	0.0206	0.1381	0.0133	1733	31	2204	23
CM1_28	3.84	0.0162	0.1490	0.0124	1491	22	2334	21
CM1_38	5.01	0.0594	0.1396	0.0332	1174	63	2222	56
CM1_42	4.11	0.0220	0.1337	0.0116	1405	28	2147	20
CM1_49	3.25	0.0230	0.1499	0.0115	1731	35	2345	20
CM1_50	3.25	0.0300	0.1281	0.0237	1727	45	2072	41
CM1_71	4.13	0.0229	0.1144	0.0128	1398	29	1871	23
CM1_76	4.01	0.0296	0.2016	0.0259	1435	38	2839	42
CM1_81	3.53	0.0212	0.1461	0.0123	1607	30	2301	21
CM1_82	5.61	0.0387	0.2279	0.0671	1057	38	3037	104
CM1_84	6.10	0.0195	0.0761	0.0154	979	18	1098	30
CM1_111	3.63	0.0166	0.1307	0.0109	1567	23	2108	19
CM1_113	5.81	0.0115	0.0783	0.0107	1024	11	1153	21
CM1_130	2.22	0.0121	0.1824	0.0081	2401	24	2675	13
CM1_131	3.30	0.0119	0.1178	0.0086	1707	18	1924	15
CM1_133	3.21	0.0135	0.1196	0.0090	1747	21	1951	16
CM1_135	2.76	0.0204	0.1949	0.0100	1995	35	2784	16

Sample	$^{238}U/^{206}Pb$	1 σ (%) +/-	$^{207}Pb/^{206}Pb$	1 σ (%)	$^{238}U/^{206}Pb$ Age (Ma)	1 σ (abs) +/-	$^{207}Pb/^{206}Pb$ Age (Ma)	1 σ (abs) +/-
				Italian Gulch <10% Discordant				
IG_1	3.02	0.0212	0.1182	0.0072	1844	34	1929	13
IG_2	3.20	0.0215	0.1119	0.0080	1755	33	1831	14
IG_3	1.99	0.0212	0.1844	0.0070	2628	46	2693	12
IG_4	2.84	0.0212	0.1222	0.0071	1946	36	1989	13
IG_5	3.26	0.0214	0.1085	0.0076	1724	32	1775	14
IG_6	3.16	0.0214	0.1126	0.0076	1772	33	1842	14
IG_7	3.20	0.0216	0.1134	0.0080	1754	33	1854	14
IG_8	2.73	0.0213	0.1289	0.0075	2014	37	2083	13
IG_9	3.03	0.0213	0.1164	0.0077	1840	34	1901	14
IG_10	2.01	0.0215	0.1846	0.0072	2605	46	2695	12

IG_11	3.14	0.0212	0.1126	0.0073	1784	33	1841	13
IG_12	2.05	0.0215	0.1791	0.0074	2562	45	2645	12
IG_13	3.13	0.0224	0.1190	0.0093	1788	35	1942	16
IG_15	1.53	0.0211	0.2829	0.0068	3244	53	3379	11
IG_16	2.99	0.0065	0.1220	0.0050	1858	11	1986	9
IG_17	2.15	0.0089	0.1741	0.0043	2459	18	2598	7
IG_18	2.94	0.0071	0.1170	0.0050	1887	12	1911	9
IG_19	2.55	0.0060	0.1343	0.0041	2135	11	2155	7
IG_20	3.15	0.0072	0.1125	0.0055	1777	11	1840	10
IG_21	1.96	0.0063	0.1981	0.0039	2652	14	2811	6
IG_22	2.06	0.0072	0.1739	0.0045	2549	15	2596	8
IG_23	2.71	0.0073	0.1289	0.0047	2026	13	2082	8
IG_24	2.96	0.0076	0.1177	0.0056	1877	12	1922	10
IG_25	3.13	0.0072	0.1125	0.0055	1788	11	1841	10
IG_26	3.09	0.0064	0.1129	0.0042	1806	10	1846	8
IG_27	3.16	0.0067	0.1121	0.0050	1774	10	1833	9
IG_28	1.91	0.0066	0.2010	0.0042	2710	15	2835	7
IG_29	2.08	0.0064	0.1718	0.0045	2527	13	2576	7
IG_30	2.07	0.0137	0.1883	0.0052	2538	29	2727	9
IG_31	2.82	0.0119	0.1304	0.0050	1958	20	2103	9
IG_32	3.28	0.0139	0.1131	0.0056	1717	21	1851	10
IG_33	2.68	0.0122	0.1283	0.0056	2045	21	2074	10
IG_34	2.99	0.0114	0.1161	0.0049	1862	18	1897	9
IG_35	2.92	0.0116	0.1179	0.0053	1897	19	1925	9
IG_36	2.96	0.0114	0.1171	0.0045	1876	19	1912	8
IG_37	3.16	0.0118	0.1126	0.0058	1770	18	1841	11
IG_39	2.99	0.0117	0.1189	0.0051	1863	19	1940	9
IG_40	3.06	0.0121	0.1128	0.0058	1821	19	1845	11
IG_41	3.04	0.0126	0.1172	0.0061	1835	20	1914	11
IG_42	4.81	0.0118	0.0833	0.0052	1218	13	1276	10
IG_43	3.10	0.0114	0.1143	0.0045	1804	18	1869	8
IG_44	3.00	0.0122	0.1178	0.0057	1856	20	1923	10
IG_45	2.02	0.0118	0.1738	0.0045	2595	25	2594	7
IG_46	5.57	0.0075	0.0769	0.0067	1064	7	1118	13
IG_47	2.92	0.0066	0.1162	0.0054	1900	11	1899	10
IG_48	2.66	0.0084	0.1302	0.0076	2058	15	2100	13
IG_49	3.08	0.0064	0.1150	0.0058	1812	10	1880	10
IG_50	2.99	0.0074	0.1174	0.0070	1862	12	1917	12
IG_51	2.88	0.0051	0.1173	0.0047	1919	8	1916	8
IG_52	3.05	0.0063	0.1144	0.0058	1829	10	1870	10
IG_53	3.10	0.0064	0.1128	0.0063	1801	10	1844	11
IG_54	3.10	0.0062	0.1112	0.0056	1804	10	1819	10
IG_55	3.27	0.0061	0.1064	0.0058	1722	9	1739	11
IG_56	3.06	0.0070	0.1140	0.0063	1824	11	1865	11
IG_57	2.64	0.0064	0.1292	0.0053	2071	11	2087	9
IG_58	1.97	0.0059	0.1842	0.0049	2645	13	2691	8
IG_59	1.96	0.0059	0.1881	0.0055	2661	13	2726	9

IG_60	3.02	0.0067	0.1138	0.0056	1842	11	1861	10
IG_61	3.05	0.0085	0.1120	0.0065	1827	14	1831	12
IG_62	3.00	0.0078	0.1127	0.0056	1854	13	1844	10
IG_63	3.01	0.0079	0.1122	0.0048	1850	13	1835	9
IG_64	3.04	0.0071	0.1137	0.0053	1833	11	1860	10
IG_65	3.04	0.0085	0.1117	0.0063	1833	14	1827	11
IG_66	3.13	0.0066	0.1116	0.0049	1789	10	1826	9
IG_67	3.17	0.0086	0.1168	0.0055	1766	13	1907	10
IG_68	2.08	0.0064	0.1723	0.0047	2531	13	2580	8
IG_69	2.01	0.0068	0.1732	0.0049	2600	15	2588	8
IG_70	2.00	0.0069	0.1860	0.0050	2609	15	2707	8
IG_71	3.13	0.0073	0.1118	0.0053	1788	11	1828	10
IG_72	3.10	0.0070	0.1112	0.0049	1801	11	1819	9
IG_73	2.94	0.0077	0.1171	0.0055	1885	13	1912	10
IG_74	2.93	0.0071	0.1168	0.0059	1892	12	1907	11
IG_75	3.09	0.0080	0.1120	0.0057	1810	13	1832	10
IG_76	3.10	0.0085	0.1143	0.0083	1804	13	1870	15
IG_77	2.79	0.0095	0.1226	0.0070	1972	16	1994	12
IG_78	2.73	0.0078	0.1244	0.0076	2011	13	2020	13
IG_79	3.16	0.0111	0.1167	0.0089	1775	17	1907	16
IG_80	2.94	0.0082	0.1184	0.0067	1889	13	1932	12
IG_81	3.24	0.0073	0.1087	0.0065	1735	11	1778	12
IG_82	2.92	0.0071	0.1173	0.0069	1901	12	1915	12
IG_83	1.96	0.0077	0.1891	0.0067	2657	17	2734	11
IG_84	3.21	0.0079	0.1124	0.0070	1746	12	1839	13
IG_85	3.06	0.0081	0.1123	0.0070	1820	13	1837	13
IG_86	3.10	0.0084	0.1115	0.0078	1805	13	1824	14
IG_87	2.93	0.0076	0.1165	0.0069	1893	12	1903	12
IG_88	1.95	0.0066	0.1861	0.0063	2669	14	2708	10
IG_89	3.16	0.0071	0.1129	0.0069	1772	11	1847	12
IG_90	2.94	0.0073	0.1184	0.0073	1885	12	1932	13
IG_91	2.95	0.0087	0.1174	0.0042	1881	14	1916	8
IG_92	2.25	0.0105	0.1744	0.0055	2368	21	2600	9
IG_93	2.67	0.0085	0.1298	0.0038	2051	15	2096	7
IG_94	3.04	0.0083	0.1119	0.0035	1832	13	1830	6
IG_95	3.15	0.0098	0.1187	0.0048	1775	15	1936	8
IG_96	5.91	0.0104	0.0743	0.0094	1008	10	1051	19
IG_97	2.88	0.0086	0.1179	0.0042	1919	14	1925	8
IG_98	2.92	0.0088	0.1179	0.0040	1897	14	1925	7
IG_99	2.92	0.0091	0.1173	0.0046	1897	15	1915	8
IG_100	2.95	0.0085	0.1183	0.0041	1883	14	1930	7
IG_101	1.72	0.0094	0.2207	0.0043	2949	22	2986	7
IG_102	2.78	0.0091	0.1245	0.0051	1979	16	2021	9
IG_103	2.94	0.0084	0.1171	0.0038	1886	14	1913	7
IG_104	2.40	0.0087	0.1467	0.0036	2248	16	2308	6
IG_105	2.74	0.0092	0.1203	0.0044	2003	16	1961	8
IG_106	3.28	0.0118	0.1098	0.0048	1716	18	1796	9

IG_107	5.27	0.0115	0.0773	0.0038	1120	12	1129	8
IG_108	3.08	0.0116	0.1126	0.0044	1814	18	1842	8
IG_109	2.72	0.0115	0.1284	0.0041	2019	20	2077	7
IG_110	2.85	0.0119	0.1167	0.0038	1938	20	1907	7
IG_111	3.09	0.0122	0.1150	0.0050	1808	19	1880	9
IG_112	2.81	0.0121	0.1165	0.0042	1960	20	1904	8
IG_113	3.02	0.0122	0.1132	0.0043	1844	20	1851	8
IG_114	2.82	0.0123	0.1172	0.0044	1957	21	1913	8
IG_115	2.92	0.0126	0.1162	0.0048	1896	21	1898	9
IG_116	3.08	0.0129	0.1128	0.0045	1812	20	1846	8
IG_117	1.99	0.0126	0.1858	0.0041	2624	27	2705	7
IG_118	1.93	0.0121	0.1856	0.0038	2695	26	2704	6
IG_119	2.00	0.0119	0.1799	0.0039	2615	26	2652	7
IG_120	2.95	0.0116	0.1181	0.0039	1881	19	1927	7
IG_121	2.93	0.0084	0.1170	0.0050	1895	14	1911	9
IG_122	3.11	0.0072	0.1121	0.0030	1796	11	1833	5
IG_123	2.99	0.0071	0.1177	0.0036	1860	11	1922	6
IG_124	2.71	0.0070	0.1275	0.0033	2022	12	2063	6
IG_125	2.89	0.0075	0.1200	0.0031	1913	12	1956	6
IG_126	2.94	0.0088	0.1168	0.0040	1888	14	1908	7
IG_127	3.20	0.0087	0.1134	0.0041	1755	13	1854	7
IG_128	3.02	0.0089	0.1135	0.0046	1844	14	1856	8
IG_129	2.89	0.0083	0.1163	0.0040	1913	14	1900	7
IG_130	2.07	0.0092	0.1754	0.0048	2542	19	2610	8
			>10% Discordant					
IG_14	2.91	0.0217	0.1834	0.0100	1902	36	2684	16
IG_38	3.29	0.0113	0.1186	0.0045	1709	17	1935	8

Sample	$^{238}U/^{206}Pb$	1 σ (%) +/-	$^{207}Pb/^{206}Pb$	1 σ (%)	$^{238}U/^{206}Pb$ Age (Ma)	1 σ (abs) +/-	$^{207}Pb/^{206}Pb$ Age (Ma)	1 σ (abs) +/-
Italian Canyon Wilbert Formation <10% Discordant								
IC4_3	2.19	0.0569	0.1737	0.0087	2423	114	2594	14
IC4_5	3.42	0.0395	0.1044	0.0085	1653	57	1705	16
IC4_6	3.48	0.0399	0.1034	0.0083	1628	57	1686	15
IC4_7	2.33	0.0400	0.1603	0.0083	2305	77	2459	14
IC4_8	3.71	0.0496	0.1031	0.0105	1540	68	1680	19
IC4_9	2.34	0.0447	0.1578	0.0084	2294	86	2432	14
IC4_11	3.42	0.0462	0.1060	0.0084	1653	67	1732	15
IC4_13	3.25	0.0456	0.1047	0.0077	1730	69	1709	14
IC4_16	3.27	0.0429	0.1076	0.0068	1719	64	1759	12
IC4_17	3.48	0.0425	0.1069	0.0065	1630	61	1747	12
IC4_18	3.47	0.0487	0.1040	0.0078	1634	70	1696	14
IC4_19	3.44	0.0450	0.1044	0.0076	1646	65	1703	14
IC4_20	2.07	0.0472	0.1810	0.0078	2537	98	2662	13
IC4_21	3.34	0.0546	0.1028	0.0085	1687	81	1676	16

IC4_22	3.30	0.0392	0.1058	0.0061	1708	59	1729	11
IC4_23	3.22	0.0424	0.1052	0.0066	1741	64	1717	12
IC4_24	3.31	0.0428	0.1073	0.0060	1703	64	1755	11
IC4_26	1.71	0.0385	0.2411	0.0051	2973	91	3127	8
IC4_27	3.49	0.0440	0.1067	0.0069	1623	63	1743	13
IC4_28	3.46	0.0424	0.1041	0.0064	1637	61	1698	12
IC4_29	3.71	0.0526	0.1026	0.0068	1537	72	1671	13
IC4_30	3.58	0.0490	0.1026	0.0066	1588	69	1671	12
IC4_31	2.37	0.0293	0.1600	0.0078	2272	56	2455	13
IC4_32	3.43	0.0523	0.1003	0.0100	1651	76	1630	19
IC4_33	3.67	0.0272	0.1041	0.0084	1555	37	1699	15
IC4_34	2.21	0.0440	0.1588	0.0098	2404	88	2443	17
IC4_35	2.21	0.0252	0.1616	0.0077	2403	50	2472	13
IC4_36	3.36	0.0383	0.1044	0.0100	1680	56	1705	18
IC4_37	3.62	0.0311	0.1033	0.0084	1574	43	1684	15
IC4_38	3.42	0.0257	0.1058	0.0086	1654	37	1728	16
IC4_39	3.18	0.0207	0.1074	0.0077	1760	32	1756	14
IC4_40	3.47	0.0196	0.1055	0.0082	1633	28	1723	15
IC4_41	3.22	0.0467	0.1052	0.0121	1742	71	1717	22
IC4_42	3.27	0.0505	0.1024	0.0124	1721	76	1667	23
IC4_43	3.26	0.0264	0.1050	0.0101	1725	40	1714	19
IC4_44	3.26	0.0283	0.1043	0.0098	1726	43	1702	18
IC4_45	3.42	0.0442	0.1017	0.0109	1654	64	1655	20
IC4_46	3.25	0.0372	0.1022	0.0106	1729	56	1665	19
IC4_47	3.57	0.0451	0.0995	0.0125	1592	63	1615	23
IC4_48	3.17	0.0362	0.1036	0.0107	1766	56	1689	20
IC4_49	3.44	0.0300	0.1054	0.0102	1646	43	1722	19
IC4_50	3.19	0.0367	0.1017	0.0105	1757	56	1655	19
IC4_51	3.13	0.0354	0.1084	0.0094	1786	55	1773	17
IC4_52	3.29	0.0319	0.1063	0.0090	1712	48	1737	16
IC4_53	3.47	0.0321	0.0938	0.0098	1631	46	1504	18
IC4_54	3.60	0.0350	0.1056	0.0092	1581	49	1724	17
IC4_55	3.02	0.0315	0.1135	0.0083	1844	50	1857	15
IC4_56	3.30	0.0325	0.1050	0.0084	1705	48	1715	15
IC4_57	3.33	0.0322	0.1057	0.0088	1694	48	1727	16
IC4_58	3.33	0.0352	0.1051	0.0096	1692	52	1715	17
IC4_59	2.24	0.0350	0.1620	0.0093	2379	69	2476	16
IC4_60	3.11	0.0450	0.1069	0.0104	1796	70	1747	19
IC4_61	3.07	0.0262	0.1080	0.0081	1816	41	1765	15
IC4_62	3.83	0.0338	0.0903	0.0092	1494	45	1431	18
IC4_63	3.32	0.0272	0.1042	0.0083	1697	40	1701	15
IC4_64	3.13	0.0305	0.1043	0.0082	1787	47	1702	15
IC4_65	3.31	0.0311	0.1044	0.0084	1700	46	1703	15
IC4_66	3.31	0.0342	0.1039	0.0093	1702	51	1694	17
IC4_67	3.21	0.0267	0.1059	0.0083	1750	41	1730	15
IC4_68	3.29	0.0456	0.1044	0.0115	1712	68	1704	21
IC4_69	3.33	0.0336	0.1041	0.0088	1694	50	1699	16

IC4_70	3.14	0.0310	0.1046	0.0087	1783	48	1707	16
IC4_71	3.30	0.0309	0.1036	0.0080	1704	46	1690	15
IC4_72	3.32	0.0277	0.1054	0.0077	1697	41	1722	14
IC4_73	3.29	0.0257	0.1047	0.0075	1710	39	1708	14
IC4_74	3.18	0.0251	0.1045	0.0075	1762	39	1706	14
IC4_75	3.27	0.0248	0.1089	0.0081	1720	37	1781	15
IC4_76	3.28	0.0246	0.1038	0.0073	1718	37	1692	13
IC4_77	3.76	0.0281	0.1008	0.0086	1519	38	1638	16
IC4_78	3.54	0.0334	0.1032	0.0087	1605	47	1683	16
IC4_79	3.39	0.0241	0.1052	0.0075	1664	35	1718	14
IC4_80	3.31	0.0275	0.1068	0.0079	1702	41	1746	14
IC4_81	2.18	0.0217	0.1623	0.0059	2430	44	2480	10
IC4_82	3.39	0.0226	0.1052	0.0062	1665	33	1719	11
IC4_83	2.22	0.0217	0.1591	0.0060	2401	43	2447	10
IC4_85	3.76	0.0198	0.1033	0.0058	1521	27	1685	11
IC4_86	3.27	0.0200	0.1043	0.0062	1719	30	1701	11
IC4_87	3.27	0.0206	0.1043	0.0063	1719	31	1702	12
IC4_88	3.19	0.0226	0.1058	0.0067	1760	35	1729	12
IC4_89	2.12	0.0214	0.1613	0.0058	2493	44	2469	10
IC4_91	3.66	0.0333	0.1041	0.0083	1559	46	1698	15
IC4_92	3.25	0.0292	0.1033	0.0080	1730	44	1684	15
IC4_93	3.51	0.0286	0.1050	0.0081	1618	41	1714	15
IC4_94	3.38	0.0297	0.1056	0.0078	1671	44	1725	14
IC4_95	3.32	0.0197	0.1054	0.0068	1696	29	1721	12
IC4_96	3.41	0.0219	0.1034	0.0067	1658	32	1685	12
IC4_97	3.49	0.0208	0.1047	0.0070	1624	30	1708	13
IC4_98	3.46	0.0194	0.1015	0.0069	1638	28	1651	13
IC4_99	3.54	0.0196	0.1025	0.0073	1606	28	1670	13
IC4_100	3.30	0.0209	0.1049	0.0072	1708	31	1713	13
IC4_101	3.46	0.0157	0.1050	0.0052	1635	23	1715	10
IC4_102	3.51	0.0162	0.1059	0.0060	1617	23	1730	11
IC4_103	3.45	0.0132	0.1047	0.0050	1643	19	1710	9
IC4_104	2.22	0.0125	0.1613	0.0043	2400	25	2470	7
IC4_105	3.43	0.0168	0.1050	0.0053	1650	24	1714	10
IC4_106	3.44	0.0127	0.1053	0.0052	1644	18	1720	10
IC4_107	2.24	0.0142	0.1629	0.0046	2378	28	2486	8
IC4_108	3.37	0.0146	0.1054	0.0052	1673	21	1721	10
IC4_109	3.34	0.0171	0.1048	0.0059	1686	25	1711	11
IC4_110	2.16	0.0148	0.1615	0.0046	2451	30	2471	8
IC4_111	3.48	0.0155	0.1046	0.0057	1629	22	1707	10
IC4_112	3.41	0.0268	0.1047	0.0061	1657	39	1709	11
IC4_113	3.40	0.0205	0.1022	0.0054	1661	30	1665	10
IC4_114	3.47	0.0221	0.1065	0.0060	1633	32	1740	11
IC4_115	3.43	0.0239	0.1043	0.0070	1649	35	1703	13
IC4_116	3.60	0.0177	0.1052	0.0059	1582	25	1717	11
IC4_117	3.47	0.0231	0.1059	0.0067	1632	33	1730	12
IC4_118	3.31	0.0185	0.1053	0.0060	1702	28	1720	11

IC4_119	3.29	0.0337	0.1034	0.0078	1713	50	1685	14
IC4_120	3.39	0.0232	0.1049	0.0063	1665	34	1712	12
IC4_121	3.20	0.0160	0.1042	0.0051	1752	25	1700	9
IC4_122	3.50	0.0225	0.1039	0.0063	1621	32	1694	12
IC4_123	3.29	0.0308	0.1040	0.0073	1711	46	1696	13
IC4_124	3.37	0.0206	0.1058	0.0057	1677	30	1729	10
IC4_125	3.42	0.0198	0.1045	0.0054	1653	29	1706	10
IC4_126	3.62	0.0271	0.1053	0.0067	1574	38	1720	12
IC4_127	3.94	0.0233	0.0920	0.0075	1458	30	1467	14
IC4_128	3.30	0.0231	0.1056	0.0062	1707	35	1726	11
IC4_129	3.34	0.0197	0.1054	0.0059	1690	29	1722	11
IC4_130	3.56	0.0201	0.1050	0.0059	1597	28	1715	11
IC4_131	2.23	0.0144	0.1608	0.0098	2387	29	2464	17
IC4_132	3.43	0.0139	0.1072	0.0098	1651	20	1752	18
IC4_133	3.29	0.0163	0.1048	0.0099	1712	24	1711	18
IC4_134	3.45	0.0136	0.1050	0.0096	1640	20	1714	17
IC4_135	3.48	0.0111	0.1055	0.0095	1629	16	1723	17
				>10% Discordant				
IC4_1	3.87	0.0447	0.1042	0.0096	1480	59	1700	18
IC4_2	4.35	0.0560	0.1021	0.0097	1333	67	1662	18
IC4_4	3.85	0.0728	0.1029	0.0099	1489	96	1677	18
IC4_10	4.40	0.0530	0.1026	0.0093	1321	63	1671	17
IC4_15	3.79	0.0522	0.1039	0.0077	1508	70	1695	14
IC4_14	3.86	0.0724	0.1020	0.0104	1484	95	1661	19
IC4_12	4.11	0.0611	0.1024	0.0088	1403	77	1667	16
IC4_84	5.22	0.0328	0.1037	0.0066	1129	34	1691	12

APPENDIX C
FRACTIONATION FACTORS

Fractionation Factor (FF)	Samples Corrected by FF	$^{207}Pb/^{235}U$	%1stdev	$^{206}Pb/^{238}U$	%1stdev	$^{207}Pb/^{206}Pb$	%1stdev
IC3_A	IC3_1_10	0.7125	1.62	0.7107	1.74	1.0025	0.50
IC3_B	IC3_11_20	0.7204	1.05	0.7176	1.30	1.0038	0.72
IC3_C	IC3_21_30	0.7226	0.83	0.7188	0.80	1.0053	0.82
IC3_D	IC3_31_40	0.7328	2.36	0.7320	2.38	1.0010	0.38
IC3_E	IC3_41_50	0.7404	2.04	0.7385	1.67	1.0027	0.86
IC3_F	IC3_51_60	0.7403	1.76	0.7369	1.25	1.0047	0.81
IC3_G	IC3_61_70	0.7394	2.03	0.7380	1.81	1.0019	0.54
IC3_H	IC3_71_80	0.7520	2.51	0.7498	2.24	1.0030	0.62
IC3_I	IC3_81_90	0.7634	1.11	0.7619	0.51	1.0020	0.76
IC3_J	IC3_91_100	0.8068	0.90	0.8087	0.75	0.9977	0.20
IC3_K	IC3_101_110	0.8274	1.71	0.8266	1.45	1.0010	0.27
IC3_L	IC3_111_121	0.8364	0.62	0.8353	0.72	1.0014	0.34
IC3_M	IC3_121_130	0.8314	3.32	0.8301	3.43	1.0015	0.39
IC3_N	IC3_131_140	0.8017	1.43	0.8009	1.55	1.0010	0.30
IC2_A	IC2_1_10	0.7335	2.08	0.7331	2.27	1.0004	0.50
IC2_B	IC2_11_20	0.7547	1.34	0.7561	1.17	0.9982	0.31
IC2_C	IC2_21_30	0.7661	0.65	0.7659	0.45	1.0003	0.37
IC2_D	IC2_31_40	0.7673	0.57	0.7663	0.65	1.0013	0.11
IC2_E	IC2_41_50	0.7778	1.73	0.7763	1.49	1.0019	0.54
IC2_F	IC2_51_60	0.7894	1.20	0.7873	0.95	1.0026	0.56
IC2_G	IC2_61_70	0.7861	1.32	0.7861	1.11	1.0000	0.43
IC2_H	IC2_71_80	0.7942	2.49	0.7938	2.11	1.0005	0.48
IC2_I	IC2_81_90	0.8037	1.21	0.8017	1.16	1.0024	0.35
IC2_J	IC2_91_100	0.7979	1.00	0.7962	0.94	1.0022	0.33
IC2_K	IC2_101_114	0.7988	1.27	0.7965	1.03	1.0030	0.25
IC2_L	IC2_115_130	0.8087	1.84	0.8057	1.64	1.0038	0.25
IC2_M	IC2_131_145	0.8111	1.26	0.8100	0.84	1.0014	0.44
IC2_N	IC2_146_155	0.8021	0.37	0.8024	0.40	0.9997	0.24
IC5_A	IC5_1_10	0.7899	1.75	0.7887	1.78	1.0016	0.25
IC5_B	IC5_11_20	0.8163	1.97	0.8127	1.72	1.0045	0.37
IC5_C	IC5_21_30	0.8286	0.48	0.8244	0.35	1.0051	0.32
IC5_D	IC5_31_40	0.8263	0.40	0.8256	0.61	1.0008	0.25
IC5_E	IC5_41_50	0.8407	1.88	0.8390	1.82	1.0020	0.59
IC5_F	IC5_51_60	0.8513	0.51	0.8491	0.82	1.0025	0.55
IC5_G	IC5_61_70	0.8498	0.53	0.8488	0.74	1.0013	0.25
IC5_H	IC5_71_85	0.8577	1.07	0.8583	1.30	0.9994	0.44
IC5_I	IC5_86_100	0.8596	0.91	0.8598	1.03	0.9997	0.42
IC5_J	IC5_101_114	0.8496	1.49	0.8491	1.12	1.0006	0.39
IC5_K	IC5_116_130	0.8553	1.95	0.8559	1.71	0.9993	0.41
IC5_L	IC5_131_140	0.8630	0.63	0.8620	0.69	1.0011	0.31
TPR2_A	TPR2_1_10	0.6490	1.61	0.6499	1.74	0.9986	0.30
TPR2_B	TPR2_11_20	0.6478	2.30	0.6484	1.93	0.9992	0.39
TPR2_C	TPR2_21_30	0.6634	1.74	0.6634	1.75	1.0000	0.32
TPR2_D	TPR2_31_40	0.6627	0.75	0.6642	0.84	0.9978	0.19
TPR2_E	TPR2_41_50	0.6648	0.49	0.6660	0.60	0.9982	0.13
TPR2_F	TPR2_51_60	0.6722	1.83	0.6722	1.86	1.0000	0.21

TPR2_G	TPR2_61_70	0.6749	1.85	0.6769	1.73	0.9971	0.55
TPR2_H	TPR2_71_80	0.6695	0.38	0.6707	0.40	0.9982	0.57
TPR2_I	TPR2_81_90	0.6714	0.83	0.6698	0.70	1.0024	0.48
TPR2_J	TPR2_91_100	0.6767	1.36	0.6748	1.59	1.0028	0.49
TPR2_K	TPR2_101_110	0.6755	1.59	0.6762	1.68	0.9990	0.34
TPR2_L	TPR2_111_120	0.6763	1.55	0.6779	1.52	0.9977	0.19
TPR2_M	TPR2_121_125	0.6868	1.52	0.6878	1.33	0.9984	0.25
TPR4_A	TPR4_1_15	0.8030	0.69	0.8042	0.77	0.9985	0.37
TPR4_B	TPR4_16_30	0.8177	2.23	0.8163	1.70	1.0018	0.70
TPR4_C	TPR4_31_40	0.7680	2.44	0.7709	2.29	0.9963	0.42
TPR4_D	TPR4_41_50	0.7999	2.05	0.8019	1.82	0.9976	0.45
TPR4_E	TPR4_51_60	0.7924	2.98	0.7920	3.15	1.0005	0.45
TPR4_F	TPR4_61_70	0.7770	0.58	0.7774	0.89	0.9995	0.49
TPR4_G	TPR4_71_80	0.7836	0.53	0.7842	0.35	0.9991	0.66
TPR4_H	TPR4_81_90	0.7907	0.64	0.7876	0.53	1.0040	0.63
TPR4_I	TPR4_91_100	0.7915	0.66	0.7890	0.27	1.0032	0.49
TPR4_J	TPR4_101_110	0.7867	0.53	0.7846	0.57	1.0027	0.38
TPR4_K	TPR4_111_125	0.7845	0.23	0.7843	0.51	1.0003	0.53
TPR4_L	TPR4_126_135	0.7901	1.23	0.7906	1.15	0.9994	0.41
TPR3_A	TPR3_1_10	0.9207	1.42	0.9222	1.32	0.9984	0.24
TPR3_B	TPR3_11_20	0.9067	0.83	0.9105	1.07	0.9958	0.25
TPR3_C	TPR3_21_30	0.9041	0.76	0.9070	0.96	0.9968	0.23
TPR3_D	TPR3_31_40	0.9079	0.59	0.9085	0.63	0.9994	0.46
TPR3_E	TPR3_41_50	0.9123	0.93	0.9111	0.86	1.0013	0.41
TPR3_F	TPR3_51_60	0.9141	0.92	0.9127	0.64	1.0015	0.30
TPR3_G	TPR3_61_75	0.9159	0.44	0.9155	0.64	1.0004	0.29
TPR3_H	TPR3_76_90	0.9168	0.46	0.9183	0.71	0.9984	0.28
TPR3_I	TPR3_91_105	0.9072	1.15	0.9065	1.43	1.0007	0.38
TPR3_J	TPR3_106_115	0.9127	2.00	0.9113	2.09	1.0015	0.31
TPR3_K	TPR3_115_125	0.9100	2.34	0.9090	2.39	1.0011	0.19
TPR3_L	TPR3_126_135	0.9069	1.87	0.9075	2.16	0.9992	0.34
TPR5_A	TPR5_1_10	0.6881	1.44	0.6880	1.59	1.0001	0.36
TPR5_B	TPR5_11_20	0.6496	0.83	0.6495	1.04	1.0001	0.27
TPR5_C	TPR5_21_30	0.6575	1.12	0.6587	1.08	0.9983	0.09
TPR5_D	TPR5_31_40	0.6647	0.88	0.6665	0.87	0.9974	0.19
TPR5_E	TPR5_41_50	0.6687	1.08	0.6716	0.99	0.9958	0.13
TPR5_F	TPR5_51_60	0.6695	0.84	0.6721	0.66	0.9961	0.45
TPR5_G	TPR5_61_75	0.6672	0.66	0.6696	0.69	0.9964	0.50
TPR5_H	TPR5_76_90	0.6746	1.02	0.6762	1.12	0.9977	0.24
TPR5_I	TPR5_91_105	0.6763	0.79	0.6776	0.72	0.9980	0.41
TPR5_J	TPR5_106_120	0.6775	0.88	0.6780	0.64	0.9992	0.48
TPR5_K	TPR5_121_135	0.6841	1.27	0.6854	1.15	0.9981	0.35
CM3_A	CM3_1_10	0.8153	1.57	0.8145	1.63	1.0010	0.29
CM3_B	CM3_11_25	0.8376	1.23	0.8369	1.19	1.0008	0.32
CM3_C	CM3_26_40	0.8475	0.49	0.8479	0.51	0.9995	0.28
CM3_D	CM3_41_55	0.8542	0.70	0.8543	0.58	0.9998	0.32
CM3_E	CM3_56_70	0.8660	0.90	0.8660	1.11	1.0000	0.27
CM3_F	CM3_71_85	0.8778	0.69	0.8769	0.41	1.0010	0.33
CM3_G	CM3_86_100	0.8772	0.79	0.8783	0.27	0.9987	0.56

CM3_H	CM3_101_115	0.8787	0.98	0.8793	0.42	0.9993	0.61
CM3_I	CM3_116_130	0.8877	0.44	0.8837	0.34	1.0046	0.17
CM3_J	CM3_131_140	0.8864	0.52	0.8841	0.23	1.0025	0.29
CM2_A	CM2_1_15	0.8688	1.52	0.8695	1.60	0.9992	0.60
CM2_B	CM2_16_30	0.8590	0.77	0.8591	1.18	0.9998	0.63
CM2_C	CM2_31_45	0.8537	1.05	0.8541	0.94	0.9994	0.47
CM2_D	CM2_46_60	0.8514	1.25	0.8523	1.00	0.9990	0.45
CM2_E	CM2_61_70	0.9021	1.93	0.9073	2.01	0.9943	0.33
CM2_F	CM2_71_80	0.9254	0.18	0.9287	0.27	0.9964	0.35
CM2_G	CM2_81_90	0.9207	0.95	0.9189	1.17	1.0019	0.31
CM2_H	CM2_91_105	0.9134	1.11	0.9121	0.99	1.0015	0.37
CM2_I	CM2_106_120	0.9142	0.87	0.9140	0.68	1.0002	0.66
CM2_J	CM2_126_135	0.9165	0.39	0.9182	0.47	0.9981	0.79
CM1_A	CM1_1_15	0.9151	0.60	0.9222	0.77	0.9923	0.22
CM1_B	CM1_16_30	0.9125	0.78	0.9211	0.80	0.9906	0.25
CM1_C	CM1_31_40	0.8940	1.92	0.8927	1.93	1.0014	0.29
CM1_D	CM1_41_50	0.9136	0.47	0.9142	0.78	0.9993	0.35
CM1_E	CM1_51_65	0.9269	1.43	0.9262	0.98	1.0007	0.46
CM1_F	CM1_66_80	0.9305	1.09	0.9297	0.61	1.0010	0.53
CM1_G	CM1_81_95	0.9281	0.76	0.9328	0.89	0.9950	0.44
CM1_H	CM1_96_110	0.9340	0.41	0.9376	0.36	0.9961	0.59
CM1_I	CM1_111_125	0.9303	0.70	0.9310	0.58	0.9993	0.51
CM1_J	CM1_126_135	0.9297	0.81	0.9276	0.64	1.0023	0.52
IG_A	IG_1_15	0.9274	2.43	0.9328	1.94	0.9942	0.66
IG_B	IG_16_30	0.9479	0.12	0.9496	0.45	0.9982	0.33
IG_C	IG_31_45	0.9581	1.28	0.9590	1.02	0.9990	0.37
IG_D	IG_45_60	0.9686	0.50	0.9696	0.37	0.9990	0.44
IG_E	IG_61_75	0.9697	0.31	0.9752	0.50	0.9944	0.42
IG_F	IG_76_90	0.9713	0.35	0.9750	0.49	0.9962	0.60
IG_G	IG_91_105	0.9755	0.54	0.9753	0.73	1.0002	0.27
IG_H	IG_106_120	0.9707	1.19	0.9732	1.05	0.9974	0.28
IG_I	IG_121_130	0.9624	0.69	0.9665	0.57	0.9957	0.16
ICWF_A	ICWF_1_10	0.7337	2.50	0.7314	2.33	1.0032	0.64
ICWF_B	ICWF_11_20	0.7633	2.94	0.7575	3.11	1.0076	0.52
ICWF_C	ICWF_21_30	0.7745	2.57	0.7679	2.69	1.0086	0.31
ICWF_D	ICWF_31_40	0.7807	0.44	0.7774	0.87	1.0042	0.62
ICWF_E	ICWF_41_50	0.7926	1.56	0.7903	1.63	1.0029	0.87
ICWF_F	ICWF_51_60	0.8114	2.14	0.8075	2.26	1.0048	0.75
ICWF_G	ICWF_61_70	0.8154	1.89	0.8138	1.82	1.0020	0.67
ICWF_H	ICWF_71_80	0.8070	1.37	0.8062	1.64	1.0009	0.62
ICWF_I	ICWF_81_90	0.8085	1.20	0.8058	1.26	1.0034	0.42
ICWF_J	ICWF_91_100	0.8051	0.98	0.8021	1.11	1.0037	0.52
ICWF_K	ICWF_101_115	0.7997	0.39	0.7943	0.32	1.0067	0.29
ICWF_L	ICWF_116_130	0.8093	1.00	0.8006	0.72	1.0108	0.33
ICWF_M	ICWF_131_135	0.8089	1.07	0.8042	0.24	1.0059	0.88

APPENDIX D
DETRITAL ZIRCON WETHERILL PLOTS

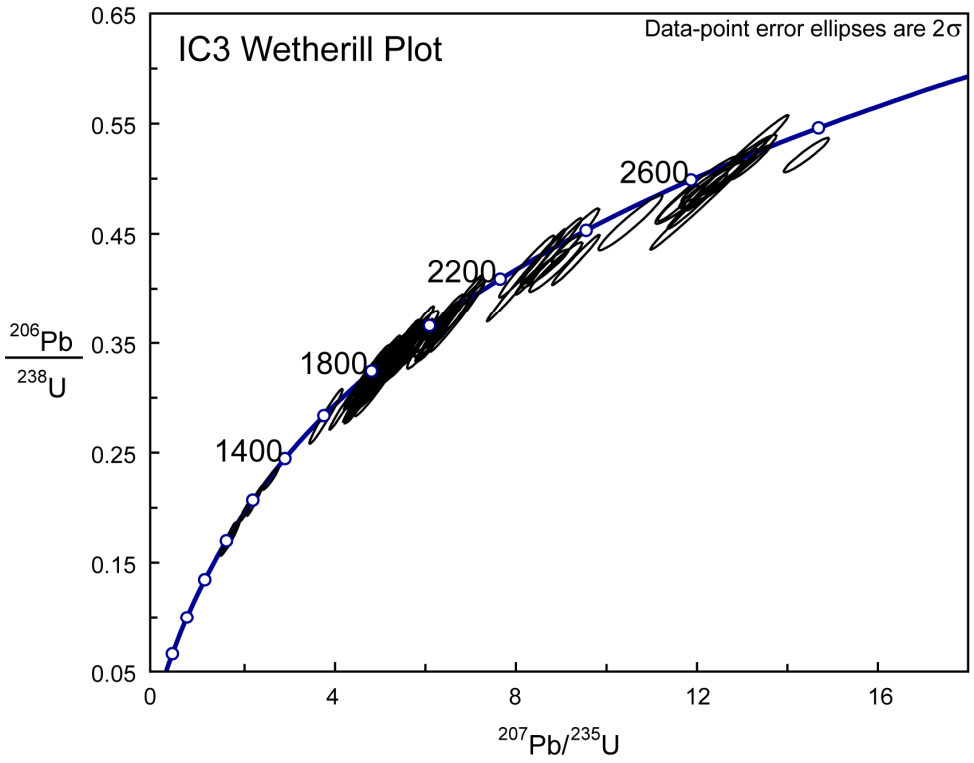
IC3 Wetherill Plot
Data-point error ellipses are 2σ
0.65
0.55
0.45
0.35
0.25
0.15
0.05
206Pb/238U
2600
2200
1800
1400
0
4
8
12
16
207Pb/235U

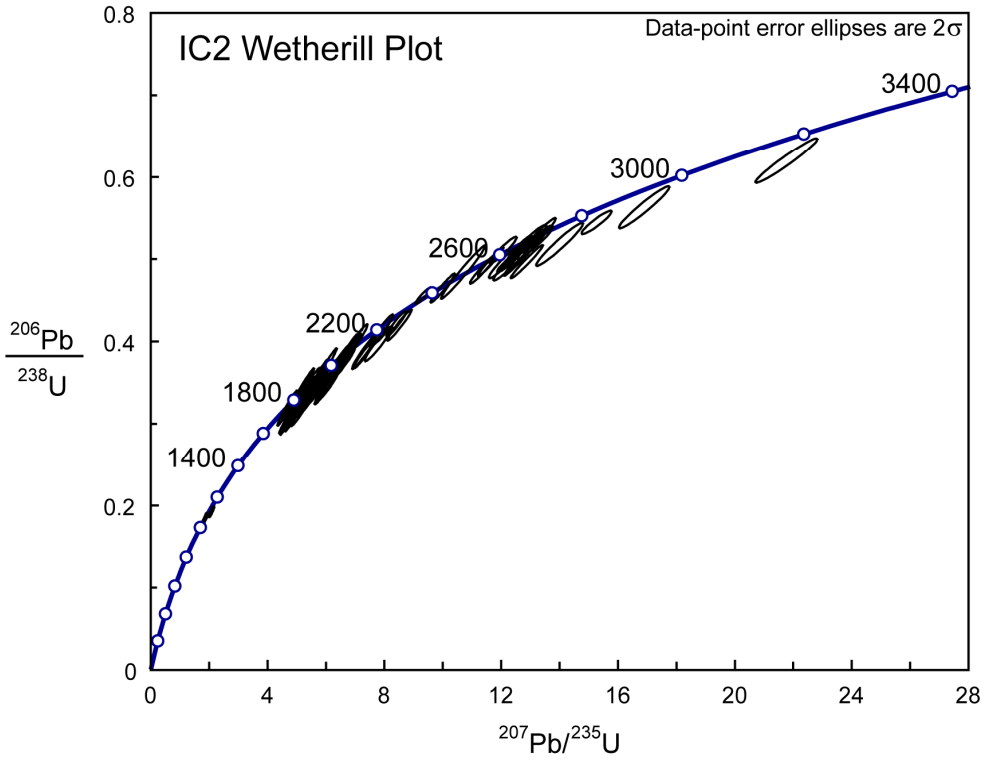
IC2 Wetherill Plot
Data-point error ellipses are 2σ
0.8
0.6
0.4
0.2
0
206Pb/238U
3400
3000
2600
2200
1800
1400
0
4
8
12
16
20
24
28
207Pb/235U

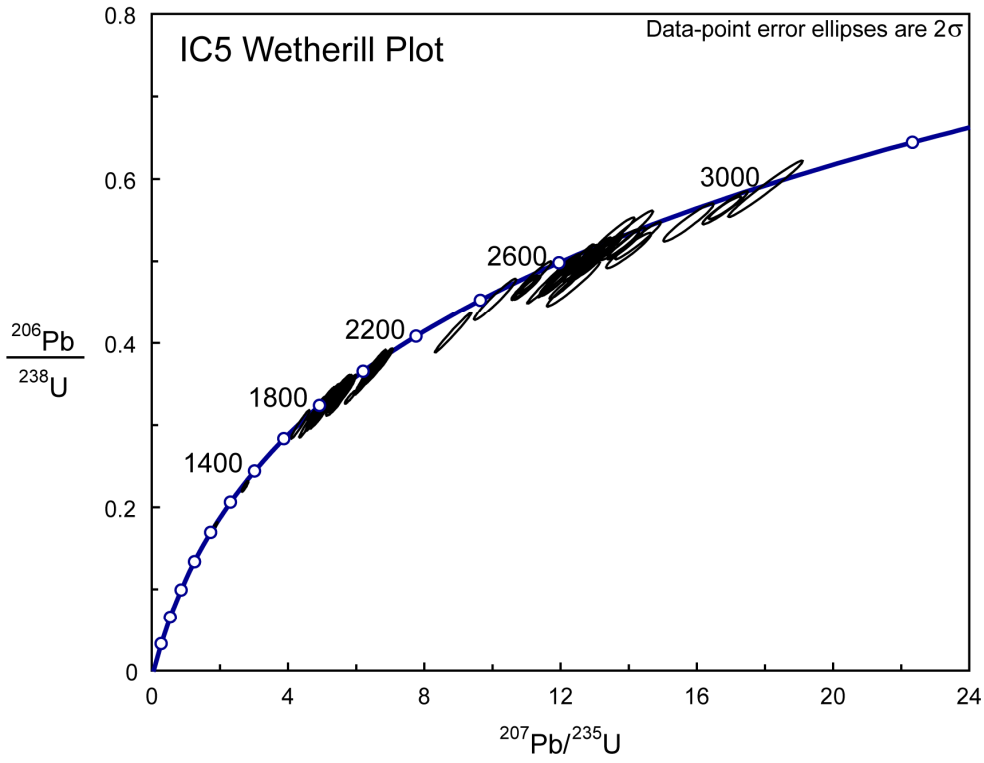
IC5 Wetherill Plot
Data-point error ellipses are 2σ
$^{206}Pb/^{238}U$
$^{207}Pb/^{235}U$
0.8
0.6
0.4
0.2
0
0
4
8
12
16
20
24
1400
1800
2200
2600
3000

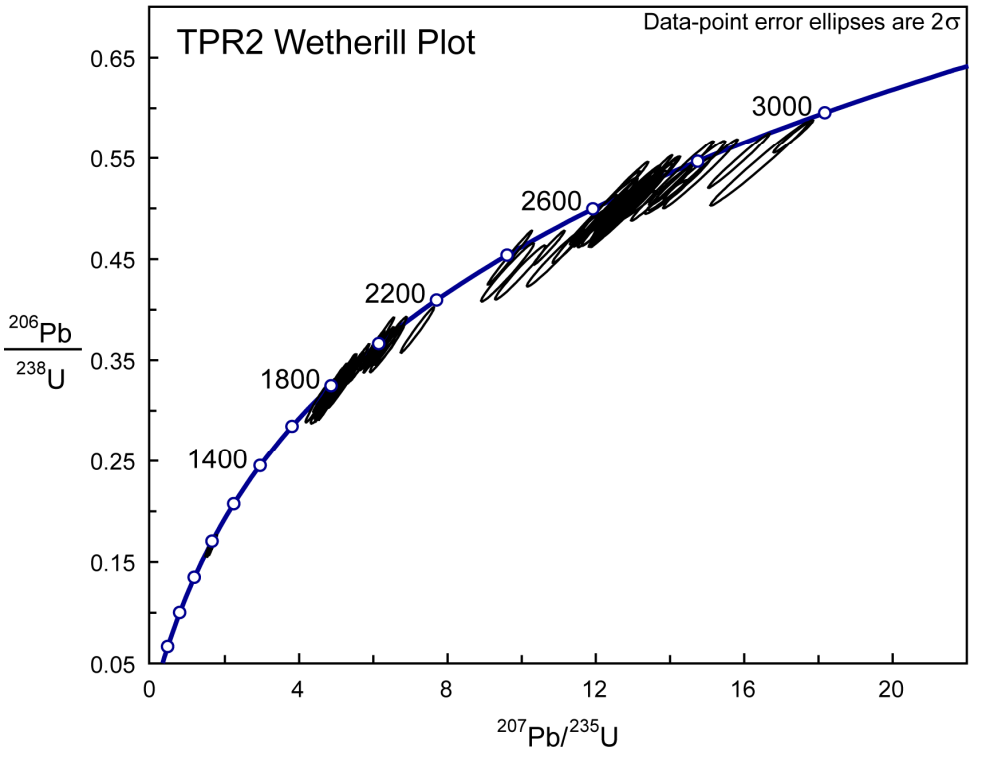
TPR2 Wetherill Plot
Data-point error ellipses are 2σ
$^{206}Pb/^{238}U$
$^{207}Pb/^{235}U$
0.65
0.55
0.45
0.35
0.25
0.15
0.05
0
4
8
12
16
20
1400
1800
2200
2600
3000

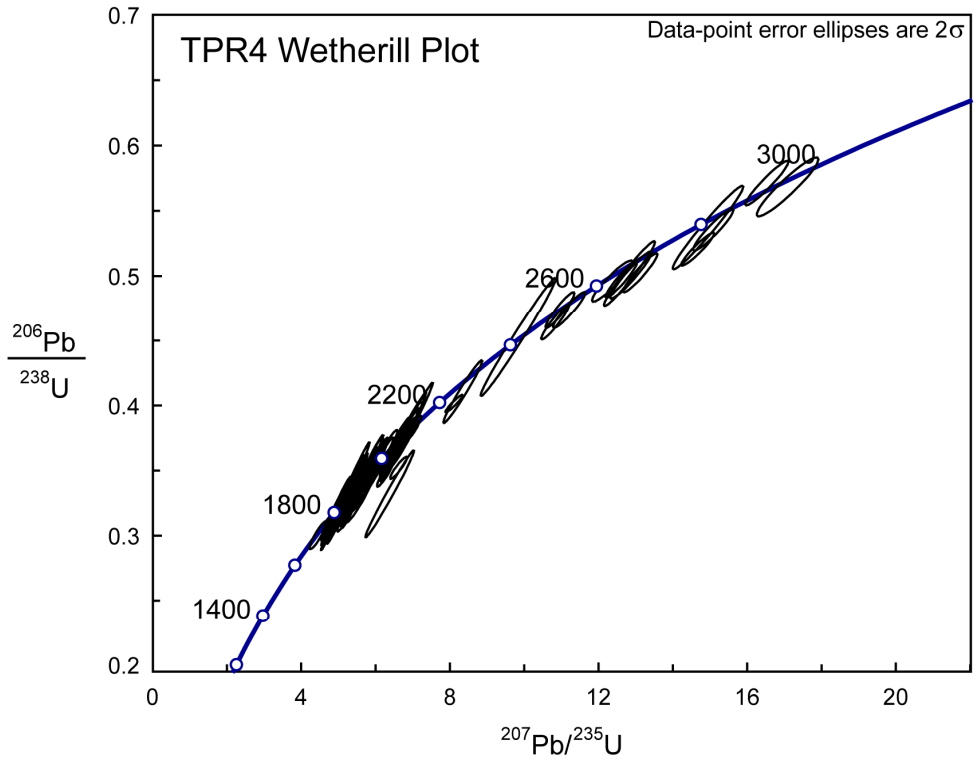
TPR4 Wetherill Plot
Data-point error ellipses are 2σ
0.7
0.6
0.5
0.4
0.3
0.2
206Pb/238U
3000
2600
2200
1800
1400
0
4
8
12
16
20
207Pb/235U

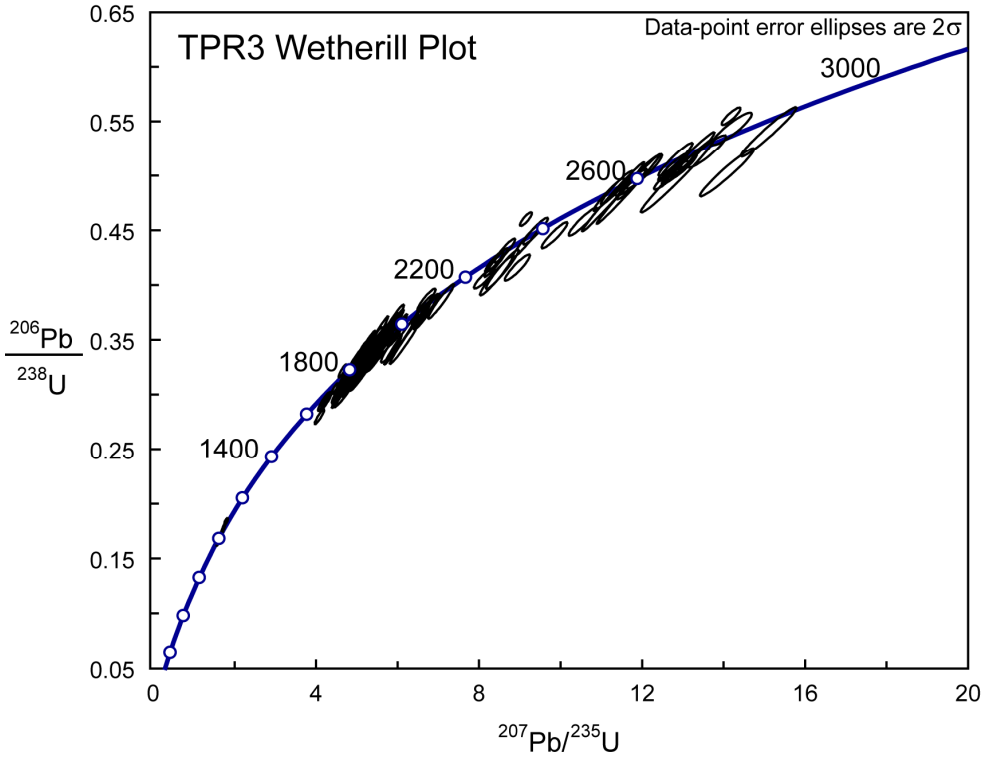
TPR3 Wetherill Plot
Data-point error ellipses are 2σ
0.65
0.55
0.45
0.35
0.25
0.15
0.05
206Pb/238U
3000
2600
2200
1800
1400
0
4
8
12
16
20
207Pb/235U

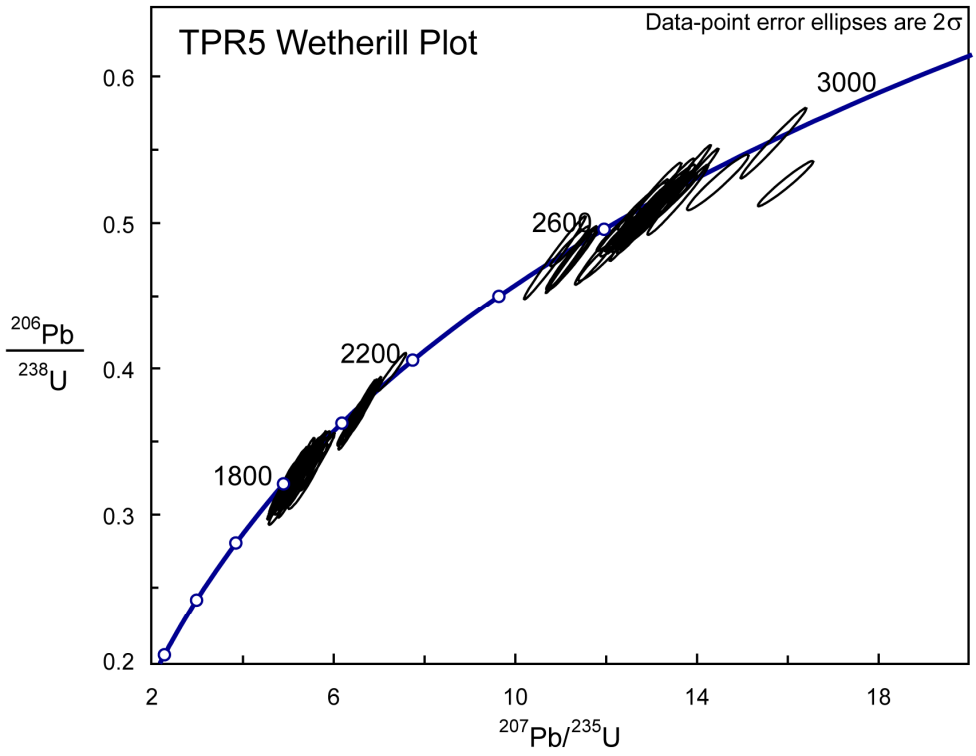
TPR5 Wetherill Plot
Data-point error ellipses are 2σ
0.6
0.5
0.4
0.3
0.2
206Pb/238U
3000
2600
2200
1800
2
6
10
14
18
207Pb/235U

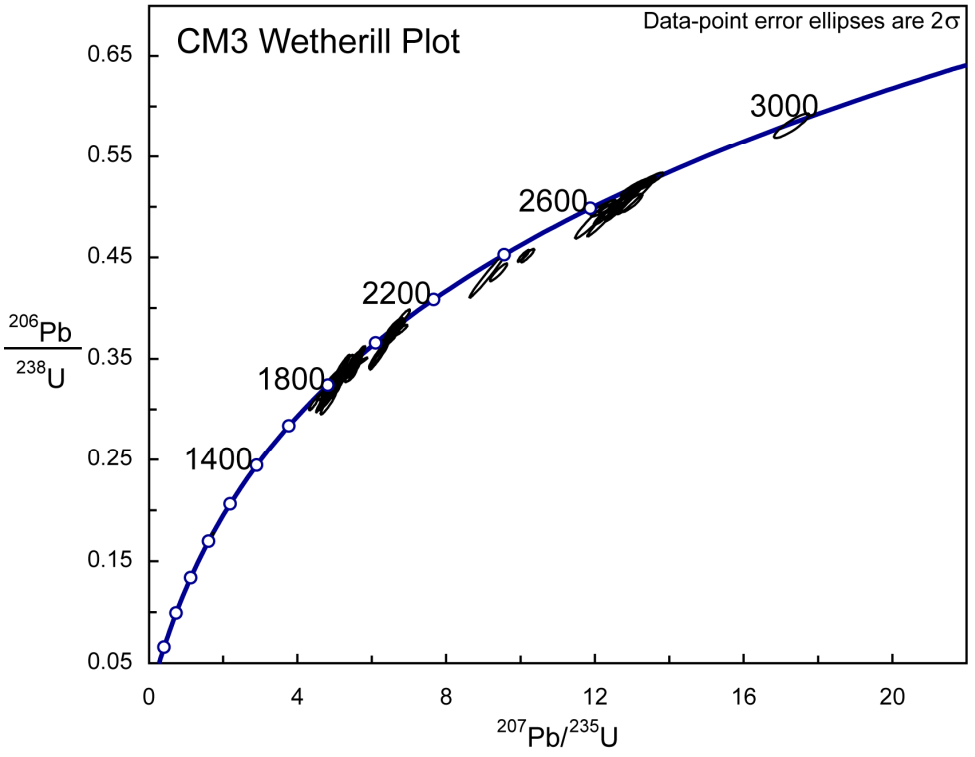
CM3 Wetherill Plot
Data-point error ellipses are 2σ
0.65
0.55
0.45
0.35
0.25
0.15
0.05
206Pb/238U
3000
2600
2200
1800
1400
0
4
8
12
16
20
207Pb/235U

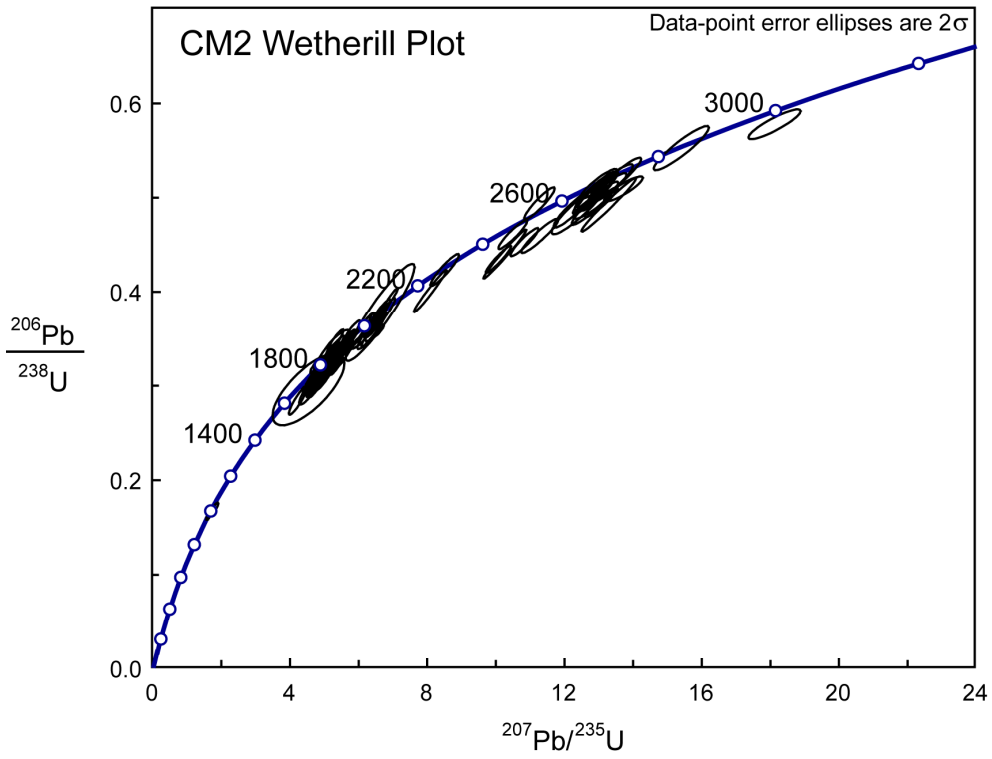
CM2 Wetherill Plot
Data-point error ellipses are 2σ
3000
2600
2200
1800
1400
0.6
0.4
0.2
0.0
0
4
8
12
16
20
24
206Pb/238U
207Pb/235U

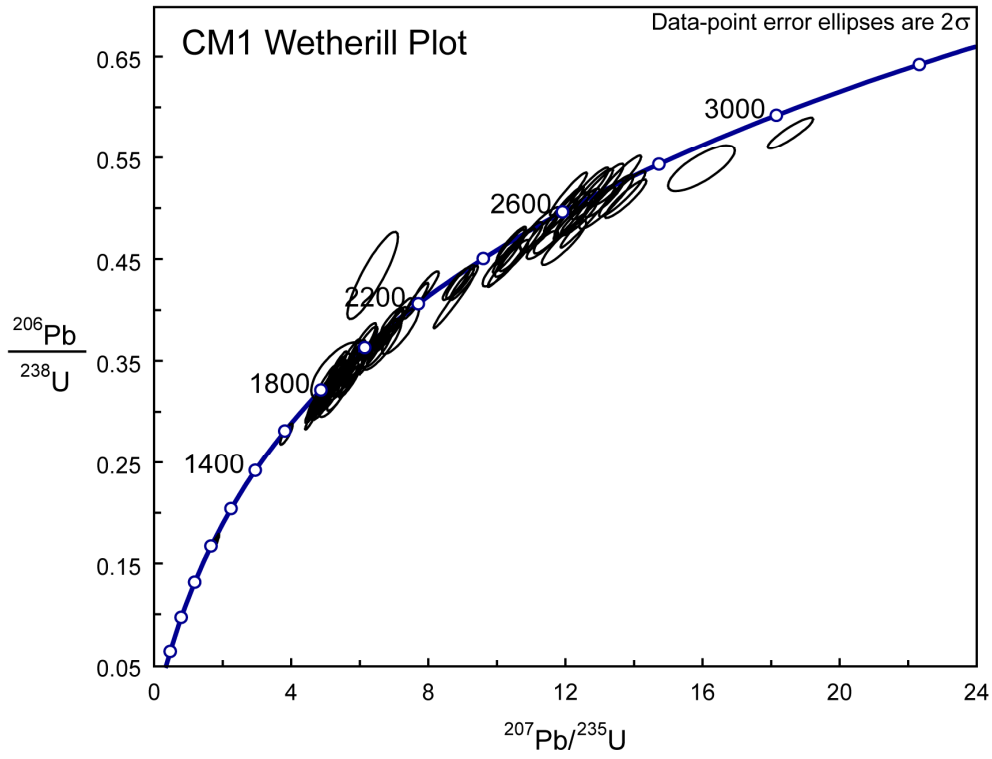
CM1 Wetherill Plot
Data-point error ellipses are 2σ
3000
2600
2200
1800
1400
0.65
0.55
0.45
0.35
0.25
0.15
0.05
0
4
8
12
16
20
24
206Pb/238U
207Pb/235U

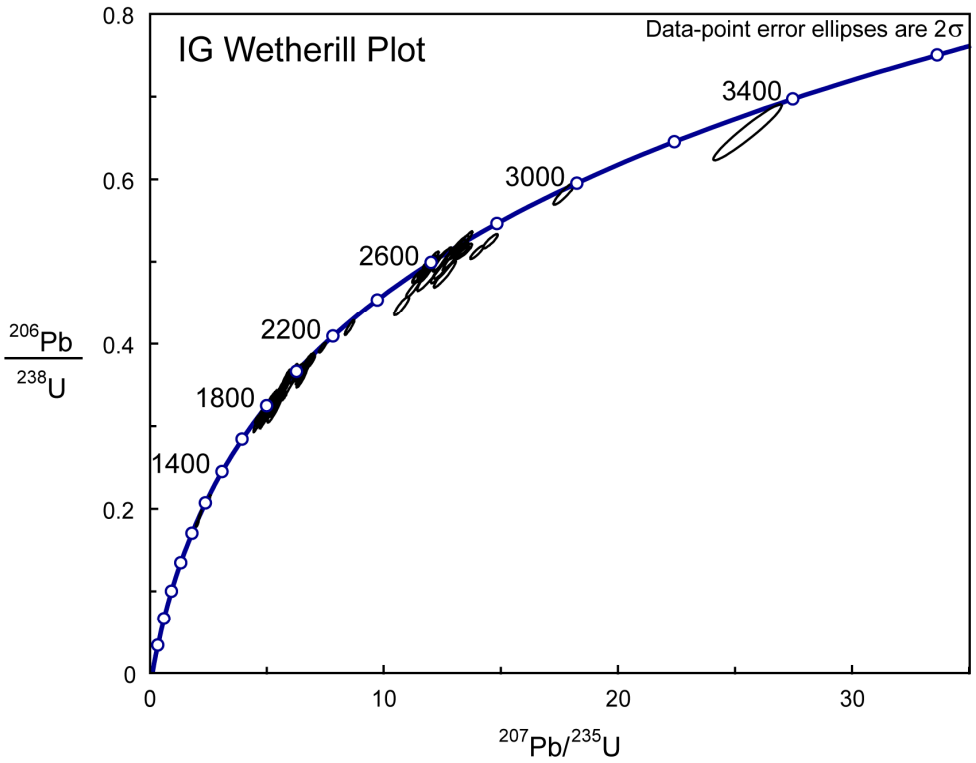
IG Wetherill Plot
Data-point error ellipses are 2σ
3400
3000
2600
2200
1800
1400
0.8
0.6
0.4
0.2
0
0
10
20
30
206Pb/238U
207Pb/235U

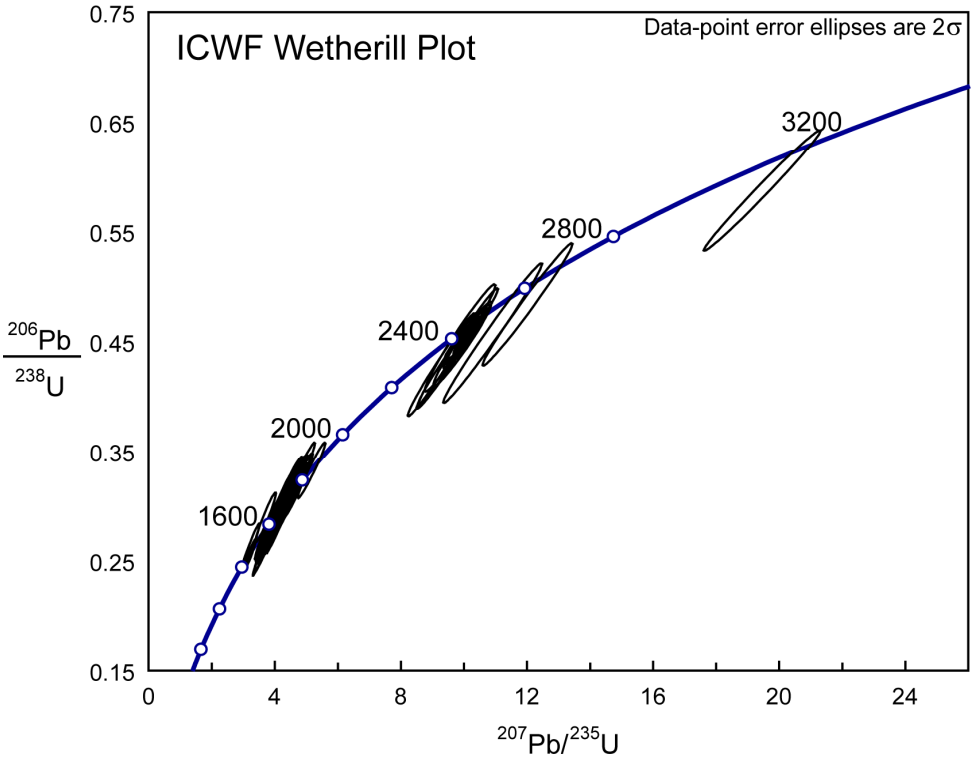
ICWF Wetherill Plot
Data-point error ellipses are 2σ
3200
2800
2400
2000
1600
0.75
0.65
0.55
0.45
0.35
0.25
0.15
0
4
8
12
16
20
24
206Pb/238U
207Pb/235U